

MAY 30 200



Digitized by the Internet Archive  
in 2017 with funding from  
University of Alberta Libraries

<https://archive.org/details/pelletier2006>





# University of Alberta

## Library Release Form

**Name of Author:** *Sarah Pelletier*

**Title of Thesis:** *Reducing Analysis Time in Liquid Chromatography*

**Degree:** *Doctor of Philosophy*

**Year this Degree Granted:** *2006*

Permission is hereby granted to the University of Alberta Library to reproduce single copies of this thesis and to lend or sell such copies for private, scholarly or scientific research purposes only.

The author reserves all other publication and other rights in association with the copyright in the thesis, and except as herein before provided, neither the thesis nor any substantial portions thereof may be printed or otherwise reproduced in any material form whatsoever without the author's prior written permission.

*Sarah Pelletier*  
signature

*Jan 31 2006*  
date





❀ ❀

*Si vous voulez construire un bateau, il est inutile de réunir des hommes, de leur donner des ordres et de répartir le travail. Donnez-leur simplement envie de partir à la découverte de mers lointaines.*

*-Antoine de Saint-Exupéry, Du vent, du sable et des étoiles*

❀ ❀

**University of Alberta**

*Reducing Analysis Time in Liquid Chromatography*

by

*Sarah Pelletier*



A thesis submitted to the Faculty of Graduate Studies and Research in partial fulfillment  
of the

requirements for the degree of *Doctor of Philosophy*

Department of *Chemistry*

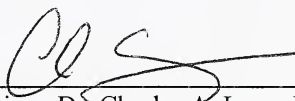
Edmonton, Alberta  
Spring 2006



University of Alberta

Faculty of Graduate Studies and Research

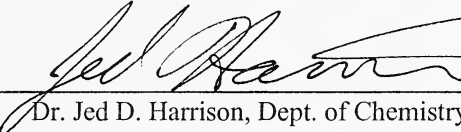
The undersigned certify that they have read, and recommended to the Faculty of Graduate Studies and Research for acceptance, a thesis entitled "Reducing Analysis Speed in Liquid Chromatography" by Sarah Pelletier in partial fulfillment of the requirements for the degree of Doctor of Philosophy.



Supervisor, Dr. Charles A. Lucy, Dept. of Chemistry



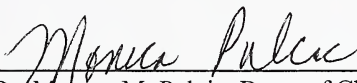
Dr. Christina G. Benishin, Dept. of Physiology



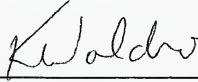
Dr. Jed D. Harrison, Dept. of Chemistry



Dr. Mark T. McDermott, Dept. of Chemistry



Dr. Monica M. Palcic, Dept. of Chemistry



External Examiner, Dr. Karen C. Waldron,  
Dept. de chimie, Université de Montréal

Jan 30/06  
Date



ଓঁ ষষ্ঠী

*This thesis is dedicated to my family*

ষষ্ঠী



## ABSTRACT

Over the past one hundred years high performance liquid chromatography (HPLC) has become one of the most important tools for determinations of numerous compounds. Today, the desire to increase productivity, especially in industry, inspires research to develop fast and easy HPLC methods. In this thesis two approaches are examined to meet such demands: elimination of sample preparation prior to the analysis and reduction of the separation columns dimensions.

Very often samples require time consuming chemical modifications before analysis. In the analysis of thiols and disulfides for instance, derivatisations are usually performed to enable detection using fluorescence or absorption spectrometry. This thesis presents a method involving detection of thiols and disulfides through indirect fluorescence. This reduces analysis time by three to one hundred-fold by eliminating the need for derivatisation. The molecules are separated in their native form by reverse phase liquid chromatography (RPLC). After separation the disulfides are reduced on-line to their thiol equivalent by reaction with the first post-column reactant: tris(2-carboxylethyl)phosphine (TCEP). The second post-column reactant is a highly fluorescent solution consisting of a cadmium and 8-hydroxyquinoline-5-sulfonic acid (CdHQS) complex. Thiols can quench the fluorescence of this complex thus decreasing the fluorescence background of the solution. Optimization of the separation and post-column conditions to maximise efficiency and sensitivity is presented.

Another way to reduce analysis time is to reduce the length of the separation column. Very short columns enable fast separations at the cost of less resolution. If



packed with very small particles, short columns (<2 cm) can achieve high resolution separations. To obtain efficient separations with such columns however, the extra-column band broadening effects have to be carefully minimized. Ion Chromatography (IC) is performed on 2 cm long columns packed with 1.8  $\mu\text{m}$  diameter particles resulting in up to 230,000 plates/meter. The IC columns are created from reverse phase column via coating with a hydrophobic surfactant (didodecyldimethylammonium bromide, DDAB). Also, IC is performed on 1 and 0.5 cm long monolithic columns. These columns have lower efficiency but possess unique internal structure that results in very low pressure drops. This facilitates the use of an inexpensive low pressure syringe pump.



## AKNOWLEDGEMENTS

I would like to thank my supervisor, Dr. Charles Lucy, for his support and guidance throughout the past five years. I have truly appreciated your patience and valuable advice. Life in the Lucy group has been very enjoyable. Thank you to present and past group members, especially Chris, Ebbing, Kim and Panos for motivating discussions, great ideas and precious friendships. I am also grateful to Jen Cook whose enthusiasm made my work as a supervisor effortless and pleasant.

Andy Szigety, whose dream of fast ion chromatography is now almost realized, has been a source of inspiration.

Research was funded by the University of Alberta, the Natural Sciences and Engineering Research Council of Canada and Dow chemicals.

Warm thanks go to my parents, my brother and Glen for their continuous love and encouragement. Your enthusiasm has helped me overcome all obstacles. Thank you for being there when I most need it.



## TABLE OF CONTENT

<b>CHAPTER ONE. Introduction.....</b>	1
1.1 Motivation and thesis overview .....	1
1.2 High Performance Liquid Chromatography (HPLC) .....	2
1.2.1 Chromatographic terms .....	3
1.2.2 Extra-column band broadening .....	10
1.2.3 Separation modes.....	11
1.2.3.1 Reverse-Phase (RPLC).....	11
1.2.3.2 Ion Chromatography (IC).....	15
1.2.4 Detection.....	18
1.2.4.1 Conductivity detection .....	18
1.2.4.2 Post-column reactions .....	22
1.2.4.3 Indirect detection.....	23
1.2.5 Columns.....	24
1.2.5.1 Particulate columns .....	24
1.2.5.2 Monolithic columns.....	26
1.2.5.2.1 IC on a silica-based C <sub>18</sub> monolithic column .....	28
1.3 References.....	31
<b>CHAPTER TWO. HPLC separation and indirect fluorescence detection of thiols .</b>	35
2.1 Introduction.....	35
2.2 Experimental .....	39
2.2.1 Reagents.....	39
2.2.2 Apparatus.....	40
2.2.3 Method.....	41
2.3 Results and discussion .....	42
2.3.1 Post-column reaction .....	42
2.3.1.1 HQS and Cd <sup>2+</sup> concentration.....	42
2.3.1.2 pH of the post-column solution.....	45
2.3.1.3 Buffers.....	47
2.3.1.4 Dynamic Reserve (DR) .....	48
2.3.1.5 Reaction rate and flow rates .....	49
2.3.1.6 Specificity of the reaction .....	49
2.3.2 Separation conditions, detection limits and determination of thiols in synthetic urine .....	50
2.4 Conclusions.....	54
2.5 References.....	56



<b>CHAPTER THREE. HPLC simultaneous analysis of thiols and disulfides: on-line reduction and indirect fluorescence detection without derivatisation .....</b>	59
3.1 Introduction .....	59
3.2 Experimental .....	61
3.2.1 Reagents.....	61
3.2.2 Apparatus.....	62
3.2.3 Method.....	63
3.2.3.1 Solution preparation .....	63
3.2.3.2 Optimization of post-column conditions.....	64
3.2.3.3 Calculations .....	64
3.3 Results and discussion .....	65
3.3.1 Optimization of the reduction reaction.....	65
3.3.2 Separation conditions and limits of detection.....	68
3.4 Conclusions.....	71
3.5 References.....	71
<b>CHAPTER FOUR. Rapid low pressure IC separations on short monolithic columns .....</b>	73
4.1. Introduction.....	73
4.2. Experimental .....	75
4.2.1 Apparatus .....	75
4.2.2 Reagents and solution preparation.....	78
4.2.3 DDAB Solubility .....	79
4.2.4 Column coating and removal of coating.....	79
4.3. Results and discussion .....	80
4.3.1 HPLC separations on short columns .....	80
4.3.1.1 Eluent conditions and selection.....	80
4.3.1.2 Coating conditions.....	85
4.3.1.3 Band broadening from extra-column effects.....	86
4.3.1.4 Improved stability and the removal of the DDAB coating .....	89
4.3.2 Multicomponent flow injection analysis .....	92
4.4. Conclusions.....	95
4.5 References.....	96



<b>CHAPTER FIVE. Small particle IC separations at high pH on a silica stationary phase.....</b>	98
5.1 Introduction.....	98
5.2 Experimental .....	99
5.2.1 Apparatus.....	99
5.2.2 Reagents and solution preparation.....	100
5.2.3 Column coating and removal of coating.....	101
5.3 Results and discussion .....	102
5.3.1 High pH eluent on a silica-based column.....	102
5.3.1.1 4-Hydroxybenzoic acid eluents .....	102
5.3.1.2 Carbonate eluents .....	106
5.3.2 Band broadening from extra-column effects.....	108
5.3.3 DDAB removal.....	110
5.4 Conclusions.....	112
5.5 References.....	113
<b>CHAPTER SIX. Conclusions and future work.....</b>	114
6.1 Conclusions and significance.....	114
6.2 Future work .....	116
6.2.1 Improvements in fast ion chromatography with small particles.....	116
6.2.1.1 Hybrid stationary phases .....	116
6.2.1.2 Improved suppressors.....	118
6.2.2 Increasing retention of weakly retained compounds in RPLC .....	118
6.3 References.....	120



## LIST OF TABLES

1.1	Effect of particle size and column length on efficiency, dead time and pressure drop .....	9
2.1	Response Factors for cys, hcys, gsh, serine, alanine and methionine.....	50
2.2	Detection limits, run to run %RSD and dynamic range for cys, hcys and gsh.....	53
3.1	Detection limits, run to run %RSD and dynamic ranges for cys, hcys, gsh, cyss, hcys and gssg.....	70
4.1	Detection limits and run to run %RSD for $\text{IO}_3^-$ , $\text{Cl}^-$ , $\text{NO}_3^-$ , $\text{HPO}_4^{2-}$ and $\text{SO}_4^{2-}$ .....	83
4.2	Column capacities according to coating solution .....	86
4.3	Peak efficiency in non-suppressed and suppressed modes .....	89
5.1	Peak efficiency in non-suppressed and suppressed modes .....	109



## LIST OF FIGURES

1.1	Typical HPLC instrumental scheme .....	3
1.2	Illustration of eddy diffusion .....	4
1.3	Illustration of zone spreading due to resistance to mass transfer.....	5
1.4	Determination of N using a) tangent method and b) the EMG method.....	7
1.5	Bonding of silica surface with chlorosilanes .....	13
1.6	Structure of a bidentate phase .....	14
1.7	Structure of a latex-based anion exchange particle.....	18
1.8	Suppressor for anion analysis and photo of a Dionex Self Regenerating Suppressor (SRS).....	21
1.9	Cross-section and photo of a Dionex Anion Atlas Electrolytic Suppressor (AAES) .....	22
1.10	Instrumental scheme of HPLC with post-column reaction.....	23
1.11	Hydrolysis of silica at high pH .....	25
1.12	Schematic illustration of the polystyrene/divinylbenzene skeleton.....	26
1.13	Flow paths of monolithic and packed bed columns.....	27
1.14	Macroporous and mesoporous structures of a monolith.....	27
1.15	Pressure vs. linear velocity for various columns .....	28
1.16	Coating and removal of DDAB on a C18 column .....	30
2.1	Chemical structures of thiol analytes.....	36
2.2	Structure of Cd(HQS) <sup>2-</sup> .....	37
2.3	Instrumental Scheme for indirect fluorescence post-column reaction detection.....	38
2.4	Fluorescence of Cd(HQS) <sub>2</sub> <sup>2-</sup> complex and Cd(HQS) <sub>2</sub> <sup>2-</sup> fraction as a function of increasing HQS concentration .....	43
2.5	Cys, gsh and hcys response as a function of increasing HQS concentration to a constant 40 $\mu$ M Cd <sup>2+</sup> .....	44
2.6	Fluorescence of the Cd(HQS) <sub>2</sub> <sup>2-</sup> complex and Cd(HQS) <sub>2</sub> <sup>2-</sup> fraction as a function of pH of post-column reagent.....	46
2.7	Cys, gsh and hcys response as a function of pH of post-column reactant .....	47
2.8	Cys, hcys and gsh chromatograms under different separation conditions.....	51
2.9	Calibration curves for cys, gsh and hcys .....	52
2.10	Separation of cys, hcys and gsh in urine matrix .....	54
3.1	Chemical structures of analytes .....	60
3.2	Instrumental scheme .....	61
3.3	Separation of cys, cyss, hcys, hcyss, gsh and gssg .....	70
4.1	a) High and b) low pressure IC systems .....	77
4.2	Life size pictures of the 0.5 and 1.0 cm long Chromolith guard cartridges and the column holder .....	78
4.3	Suppressed anion separations with 4-cyanophenol eluent.....	82
4.4	Suppressed anion separations with 4-hydroxybenzoic acid eluent.....	84
4.5	Variation of retention time of sulphate with column volumes.....	91
4.6	Low pressure separations with syringe pump .....	94



5.1	Variation of the retention factors with pH for a 4-hydroxybenzoic acid eluent ....	103
5.2	Suppressed anion separation with 4-hydroxybenzoic acid eluent at pH 10.0.....	105
5.3	Anion separations with carbonate/bicarbonate eluent at $t = 0$ , 36 and 36.3 hours	107
5.4	RPLC-UV chromatograms at 0 and 36 hours .....	107
5.5	Removal of DDAB using NaBr and 50% ACN.....	111
6.1	Structure of an ethylene bridged hybrid organic-inorganic particle .....	117



## LIST OF SYMBOLS AND ABBREVIATIONS

Symbol	Parameter
$[A]_m$	Analyte concentration in the mobile phase
$[A]_s$	Analyte concentration in the stationary phase
AAES	Anion Atlas Electrolytic Suppressor
ACN	Acetonitrile
ASRS	Anion Self Regenerated Suppressor
$A^{x-}$	Analyte anion
$(B/A)_{0.1}$	Ratio of the distances to and from $t_r$ at 10% height
$B_0$	Permeability
Caps	3-(cyclohexylamino)-1-propanesulfonic acid
Capso	3-(cyclohexylamino)-2-hydroxy-1-propanesulfonic acid
$C_{DDAB}$	DDAB concentration
$C_{lod}$	Limit of detection
$C_p$	Probe concentration
cys	Cysteine
cyss	Cystine
DDAB	Didodecyldimethylammonium bromide
$D_M$	Diffusion coefficient
$d_p$	Particle diameter
DR	Dynamic reserve
EMG	Exponentially Modified Gaussian
$E^{y-}$	Eluent anion



F	Flow rate
FIA	Flow Injection Analysis
gsh	Glutathione
gssg	Glutathione disulfide
H	Plate height
h	Reduced plate height
hcys	Homocysteine
hcyss	Homocystine
HPLC	High Pressure Liquid Chromatography
4-hb	4-Hydroxybenzoic acid
8-HQ	8-Hydroxyquinoline
HQS	8-Hydroxyquinoline-5-sulphonic acid
i	Inflection point
I.D.	Internal Diameter
IC	Ion Chromatography
inj.	Injection valve
k'	Retention factor
K <sub>IEX</sub>	Equilibrium constant in ion exchange
K <sub>p</sub>	Distribution constant
L	Column length
LC	Liquid Chromatography
LC/MS	Liquid Chromatography Mass Spectrometry
MeOH	Methanol



Mes	2-(N-Morpholino)-ethanesulfonic acid
Mopso	3-(N-Morpholino)-2-hydroxypropanesulfonic acid
MSM	Metrohm Suppressor Module
N	Number of plates/efficiency
PEEK	Poly ether ether ketone
ppb	Parts-per-billion
ppm	Part-per-million
psi	Pound per square inch
Q	Ion exchange capacity of the column
r	Column radius
RPLC	Reverse Phase Liquid Chromatography
R <sub>s</sub>	Resolution
RS	Thiol
RSD	Relative Standard Deviation
RSH	Thiol
RSSR	Disulfide
SB	StableBond
SB-Aq	StableBond-Aqueous
s <sub>BN</sub>	Relative standard deviation of the background noise
SolEq	Solution equilibria software
SRS	Self Regenerated Suppressor
SS	Disulfide
t <sub>b</sub>	Breakthrough time



TCEP	tris(2-carboxyethyl)phophine
TFA	Trifluoroacetic acid
$t_0$	Dead time
$t_r$	Retention time
$T_R$	Transfer ration
Tris	Tris(hydroxymethyl) aminomethane
$t_v$	Retention volume
$u$	Linear velocity
UPLC	Ultra-high Pressure Liquid Chromatography
US EPA	United-States Environmental Protection Agency
UV-VIS	Ultraviolet-Visible
$V_c$	Volume of the peak
$V_m$	Volume of the stationary phase
$V_o$	Void volume
$V_s$	Volume of sample loop
$w$	Weight of the stationary phase
$W_{0.1}$	Width of the peak at 10% height
$W_b$	Peak width at the base
$\Delta P$	Pressure drop
$\eta$	Viscosity
$\lambda$	Packing factor
$\lambda_{\text{emission}}$	Emission wavelength
$\lambda_{\text{excitation}}$	Excitation wavelength



$\mu_{\text{eq}}$	Micro equivalent
$\sigma$	Standard deviation of a peak
$\sigma^2$	Variance of a peak
$\sigma_{\text{col}}^2$	Variance from the column
$\sigma_{\text{fc}}^2$	Variance from the flow cell
$\sigma_{\text{inj}}^2$	Variance from the injector
$\sigma_{\text{rt}}^2$	Variance from the detector rise time
$\sigma_{\text{tu}}^2$	Variance from the tubing and connectors
$\Psi$	Obstruction factor



## CHAPTER ONE. Introduction

### 1.1 Motivation and thesis overview

High Performance Liquid Chromatography (HPLC) has become the premier analytical separation technique for many industries.<sup>1</sup> Numerous applications are developed and used in research, quality control and quality assurance laboratories. A key feature for analytical methods is speed. Very fast methods increase sample throughput and enable real-time monitoring of chemical processes. High speed analyses translate into increased operation efficiency, lower cost and ultimately larger profits.

To increase the speed of HPLC analysis one should focus on the overall method. Sample preparation is an integral part of the methods, and one which can consume a lot of time and resources.<sup>2-4</sup> From sample derivatisation to sample clean-up, a myriad of different techniques exist. If sample preparation cannot be avoided, it should be fast, simple, cheap and should not introduce error. However, this is rarely the case.

A second way to enhance sample throughput is to improve the apparatus, more specifically, the separation column. The column is the heart of an HPLC separation. In conjunction with the mobile phase, it ideally provides selectivity and resolution of all of the sample components. Nonetheless, superior resolution comes at a cost: low speed. Column design, namely its size and packing can be optimized for rapid and good quality separations.<sup>1</sup>

In Chapter 2 of this thesis, fast and simple analyses of thiols are achieved through elimination of the sample preparation steps. To achieve this, a post-column reaction is



used together with indirect fluorescence detection. Chapter 3 extends this method to the simultaneous analysis of both thiols and their associated disulfides without pre-derivatisation. In Chapters 4 and 5, the speed of ion chromatographic analyses is improved by optimizing the size of the column and the packing particles. More specifically, Chapter 4 explores the use of very short columns (<1 cm) for fast separations through optimization of the whole HPLC system. In Chapter 5, short columns packed with very small particles (1.8  $\mu\text{m}$ ) are used to achieve high efficiency separations at moderate pressures.

## 1.2 High Performance Liquid Chromatography (HPLC)

The Russian botanist Mikhail S. Tswett (1872-1919) is generally referred to as the father of chromatography for his work on the isolation of plant pigments.<sup>5,6</sup> He first presented his technique in 1903 at a meeting of the Warsaw Society of Natural Scientists<sup>7,8</sup>. He later named the method “chromatography”<sup>a</sup> and described it in detail in two papers<sup>8-10</sup> and a book<sup>11</sup>. His work led to a description of various aspects of liquid adsorption chromatography. Chromatography was however only barely used during Tswett’s lifetime, and was all but forgotten until its resurrection in the 1930’s by the German Edgar Lederer.<sup>6,12</sup> After the publication of Martin and Synge’s classic paper on partition chromatography in 1941<sup>13</sup>, modernization of the technique took place. Workers such as van Deemter and Giddings put forward rate and efficiency theories<sup>14,15</sup> which predicted that smaller particles would provide more efficient separations.<sup>16</sup> In the 1960’s, pumping systems that could accommodate the higher pressures generated by these small

---

<sup>a</sup> From the Greek roots *chroma* (color) and *graphein* (to write).



particles were developed by Horvath and co-workers, who coined the term “High Pressure Liquid Chromatography (HPLC)” for this new technique.<sup>17,18</sup> In the years since, HPLC has become the dominant separation technique in bioanalytical analysis.

Today, the HPLC instrumental setup consists of high pressure eluent pumps, injectors, separation columns, detectors and computers for data collection (Figure 1.1). The next sections will discuss some instrumental aspects of modern HPLC that are related to my work.

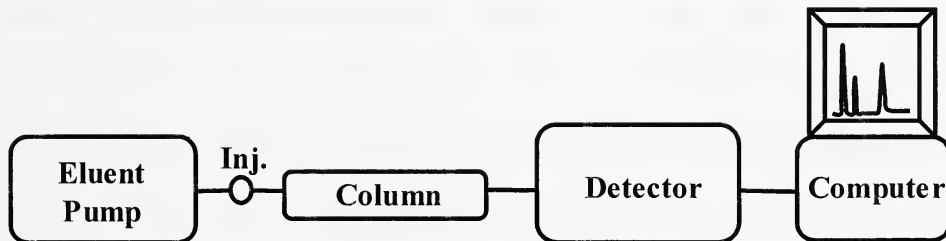


**Figure 1.1 Typical HPLC instrumental scheme.**

### 1.2.1 Chromatographic terms

In HPLC, samples are transported by a liquid mobile phase (eluent) through a column containing a solid stationary phase (tightly packed particles). If the sample components each interact differently with the stationary phase, separation occurs. The performance of a column and the speed of the separations are a function of various factors.

Ideally, analytes should separate and be detected as narrow peaks. However, molecules experience dispersion as they travel along the column which causes broadening of the peaks. Van Deemter's rate theory identifies three effects that



contribute to broadening: eddy diffusion (A), longitudinal molecular diffusion (B) and mass transfer in the stationary phase (C).

$$H = A + \frac{B}{u} + Cu \quad (1.1)$$

where  $u$  is the linear velocity of the mobile phase and  $H$  the plate height. A small value of  $H$  corresponds to a narrow peak and is proportional to A, B and C. Term A, the eddy diffusion, relates to the multi-path effect. During the separation, molecules find different paths through the stationary phase particles. Identical molecules injected at the same time should elute together since they have the same interactions with the stationary phase. However, the molecules that found the shortest path elute faster and vice versa (Figure 1.2). Eddy diffusion is proportional to the particle diameter ( $d_p$ ) and the packing factor ( $\lambda$ ):

$$A = 2 \lambda d_p \quad (1.2)$$

Small, tightly packed particles minimize eddy diffusion.

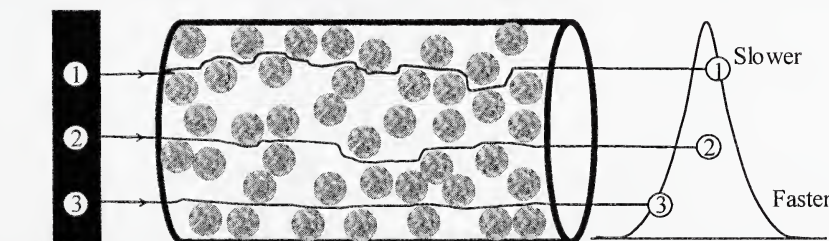


Figure 1.2 Illustration of eddy diffusion. Adapted from reference 1.

The B term refers to the contribution due to molecular diffusion. Zone broadening occurs when molecules diffuse from regions of high concentration to that of lower concentration with time. B is proportional to the diffusion coefficient ( $D_M$ ):

$$B = 2 \psi D_M \quad (1.3)$$



The obstruction factor,  $\psi$ , is function of the nature of the packed bed. The van Deemter equation (1.1) predicts that the contribution of B is minimized at high flow velocity. At high speed, a solute spends less time in the column thus has less time for molecular diffusion.

The C term of equation 1.1 concerns the transfer of molecules in and out of the stationary phase. At equilibrium, the molecules are distributed in the mobile and the stationary phases (Figure 1.3 a). When the molecules in the mobile phase move down stream, the ones in the stationary phase stay behind, thus broadening the zone (Figure 1.3 b). The molecules that moved ahead in the mobile phase must partition in the stationary phase and the molecules of the stationary phase must partition in the mobile phase (arrows on Figure 1.3 b). The C term is minimized by fast transfer in and out of the stationary phase (fast kinetics) and also is proportional to the particle diameter and average stationary phase film thickness.

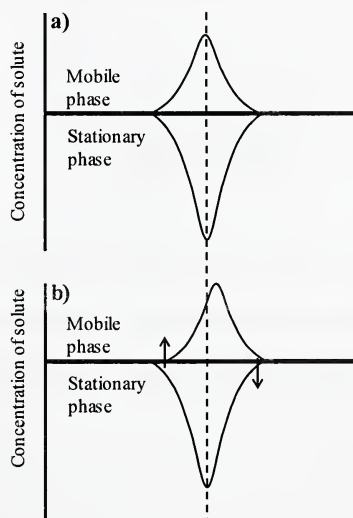


**Figure 1.3 Illustration of zone spreading due to resistance to mass transfer.**  
**Adapted from reference 1.**



The height equivalent to a theoretical plate (H, equation 1.1) is a measure of efficiency that is independent of the length of the column. It is usually expressed in  $\mu\text{m}$ .

$$H = L/N \quad (1.4)$$

The number of plates (N) or column efficiency is a measure of the broadening of a peak. It takes into account the dispersion that a peak undergoes during its travel through the chromatographic system. Assuming Gaussian peaks, N for each peak is commonly calculated using the tangent method (Figure 1.4 a). In this method, two tangents are drawn to the inflection points (i) of the peaks and their intersection with the baseline determines the peak width ( $W_b$ ) which is equal to four standard deviations ( $4\sigma$ ). However, when a peak is not Gaussian (tailed, for example), the tangent method overestimates the plate count.<sup>19</sup> In Chapters 4 and 5, N is calculated using the exponentially modified Gaussian (EMG) peak model developed by Foley and Dorsey (Figure 1.4 b):<sup>20</sup>

$$N = \frac{41.7(t_r / W_{0.1})^2}{(B/A)_{0.1} + 1.25} \quad (1.5)$$

where  $t_r$  is the retention time (min) of the peak maximum,  $W_{0.1}$  (min) is the width of the peak at 10% height,  $(B/A)_{0.1}$  is the ratio of the distances to and from  $t_r$  at 10% height

The resolution ( $R_s$ ) characterizes the separation between two peaks relative to the peak width:

$$R_s = \frac{t_{r2} - t_{r1}}{\frac{1}{2}(W_{b1} + W_{b2})} \quad (1.6)$$



where  $t_{r1}$  and  $t_{r2}$  are the retention times of the first and second peaks (min) and  $W_1$  and  $W_2$  their width at the baseline (min). (The width is obtained with the tangent method.) An  $R_s$  value of 1.0 represents about 90-94% resolution between two peaks and is usually considered adequate for a separation. Baseline resolution is achieved when  $R_s \geq 1.5$ .

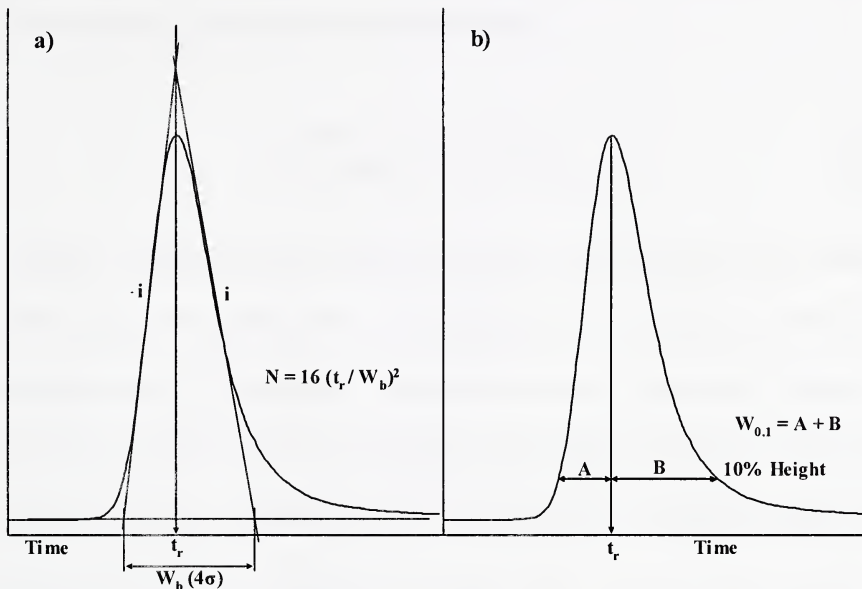


**Figure 1.4 Determination of N using a) tangent method and b) the EMG method.**  
Adapted from references 1 and 20.

$N$ ,  $H$ ,  $R_s$  as well as the speed of analysis and the column backpressure are all influenced by the column dimensions, the stationary phase and the experimental conditions. Long columns directly enhance the efficiency ( $N$ ) but also increase the analysis time and backpressure:

$$N = L/H \longrightarrow N \propto L \quad (1.7)$$

$$t_o = L/u \longrightarrow \text{Analysis time} \propto L \quad (1.8)$$

$$\Delta P = F\eta L / \pi r^2 B_o \longrightarrow \Delta P \propto L \quad (1.9)$$



were L is the column length,  $t_0$  the retention time of an unretained compound (dead time),  $u$  the flow velocity,  $\Delta P$  the pressure drop,  $F$  is the flow rate,  $\eta$  the viscosity,  $r$  the column radius and  $B_o$  the permeability (equation 1.12 below).

Also, columns packed with particles of small diameter ( $d_p$ ) are more efficient (small  $H$ ) but generate substantially more backpressure:

$$d_p \approx 3500H \longrightarrow H \propto d_p \quad (1.10)$$

$$d_p^2 = 1000B_o \longrightarrow \Delta P \propto 1/d_p^2 \quad (1.11)$$

Table 1.1 demonstrates the effects of  $d_p$  and  $L$  on  $N$ ,  $t_0$  and  $\Delta P$ . For example if 6,000-7,000 plates are needed to achieve a separation, this can be achieved with a 15 cm column packed with 10  $\mu\text{m}$  particles. However, the dead time of the column is 1.5 minutes and the retention time of a compound with a retention factor  $k'$  of 10 would be 16.5 minutes. The same separation could be achieved on a 5 cm column packed with 3  $\mu\text{m}$  particles, with a three-fold reduction in analysis time. Finally, a column packed with 1.8  $\mu\text{m}$  particles would only have to be 2.3 cm long to generate 6,000-7,000 plates and so would produce a separation in an eighth the time required versus using 10  $\mu\text{m}$  particles. However, while the time necessary for a separation decreases with particle size, the pressure increases (Table 1.1).



**Table 1.1 Effect of particle size and column length on efficiency, dead time and pressure drop.<sup>4</sup>**

dp (μm)	L (cm)	N	t <sub>0</sub> (min) <sup>a</sup>	ΔP (psi) <sup>b</sup>
<b>10</b>	<b>15</b>	<b>6,000-7,000</b>	<b>1.5</b>	<b>350</b>
10	25	8,000-10,000	2.5	590
5	10	7,000-9,000	1.0	940
5	15	10,000-12,000	1.5	1,410
5	25	17,000-20,000	2.5	2,360
<b>3</b>	<b>5</b>	<b>6,000-7,000</b>	<b>0.5</b>	<b>1,310</b>
3	7.5	9,000-11,000	0.8	1,960
3	10	12,000-14,000	1.0	2,620
3	15	17,000-20,000	1.5	3,930
1.8	2	5,000-6,000	0.2	1,450
<b>1.8</b>	<b>2.3</b>	<b>6,000-7,000</b>	<b>0.2</b>	<b>1,670</b>
1.8	10	27,000-30,000	1.0	7,270 <sup>c</sup>
1.8	15	41,000-43,000	1.5	10,910 <sup>c</sup>

<sup>a</sup> t<sub>0</sub> ≈ 0.1L/flow rate.<sup>4</sup> Flow rate = 1 mL/min.

<sup>b</sup> In a 50% methanol/water mobile phase. Calculated using equations 1.11 and 1.12.

<sup>c</sup> Standard HPLC systems have a maximum pressure limit of about 4,000 psi. Above this pressure, the recently developed Ultra-high Pressure Liquid Chromatography (UPLC) systems must be used.<sup>21</sup>

N, H and R<sub>s</sub> are useful parameters to assess the performance of a column and separation, but do not provide good comparison between diverse columns operated under different conditions. The reduced plate height (h=H/d<sub>p</sub>) is a dimensionless parameter which factors out many experimental conditions. A well packed column in an optimized system usually yields reduced plate heights of 1.5-3.<sup>22</sup>



Similarly, the permeability ( $B_o$ ) is a parameter which describes the ease of flow through a column, and corrects for viscosity, flow rate, column length and particle size.<sup>23</sup> It enables evaluation of the overall backpressure of a column.

$$B_o = \frac{F\eta L}{\pi r^2 \Delta P} \quad (1.12)$$

where  $B_o$  is in  $\text{cm}^2$ ,  $F$  is the flow rate ( $\text{cm}^3/\text{s}$ ),  $\eta$  the viscosity ( $\text{mPa}\cdot\text{s}$ ),  $L$  the column length (cm),  $r$  the column radius (cm) and  $\Delta P$  the pressure drop (Pa). The lower  $B_o$ , the easier it is to pump the mobile phase through the column.

### 1.2.2 Extra-column band broadening

The statistical variance of a peak is given by:<sup>1</sup>

$$\sigma^2 = (t_r F)^2 / N \quad (1.13)$$

where the retention time  $t_r$  is in min and the flow rate  $F$  in  $\mu\text{L}/\text{min}$ . This equation is used in Chapters 4 and 5. This variance or band spreading occurs in several parts of the separation system, in addition to the column. The contribution of the various components to the overall variance of the peak ( $\sigma^2$ ) is given by:<sup>1,4</sup>

$$\sigma^2 = \sigma_{\text{col}}^2 + \sigma_{\text{inj}}^2 + \sigma_{\text{tu}}^2 + \sigma_{\text{fc}}^2 + \sigma_{\text{rt}}^2 \quad (1.14)$$

where  $\sigma_{\text{col}}^2$  is the variance contribution from the column,  $\sigma_{\text{inj}}^2$  is from the injector,  $\sigma_{\text{tu}}^2$  from the tubing and connectors,  $\sigma_{\text{fc}}^2$  from the flow cell and  $\sigma_{\text{rt}}^2$  from the detector response (or rise) time. The column variance ( $\sigma^2$ ) represents the distribution of the analyte



molecules in the analyte zone and is related to the plate height by  $HL$ . In conventional HPLC systems, the extra-column effects have been minimized by the manufacturer such that  $\sigma_{col}^2$  is usually at least 60% larger than all of the other factors combined. However, when the column dead volume is small (e.g., for short columns and narrow diameters), the retention is low, and/or the number of plates is large (e.g., small particles), the extra-column effects become more significant.<sup>4</sup>

The presence of extra-column band broadening can be assessed by calculating and comparing the number of plates of each peak along the chromatogram.<sup>1,4,24</sup> Extra-column effects can be detected when the least retained peaks have a much lower efficiency than the late eluting peaks (early eluting peaks have a lower peak volume and so are more sensitive to extra-column effects). The various sources of extra-column band broadening and their elimination will be discussed in Chapters 4 and 5.

### 1.2.3 Separation modes

#### 1.2.3.1 Reverse Phase (RPLC)

Reverse phase chromatography is by far the most popular HPLC separation mode. Its applications encompass a wide range of compounds, including pharmaceuticals, proteins and environmental samples.<sup>4</sup> In reverse phase chromatography, the stationary phase is less polar than the mobile phase. A typical reverse phase consists of an 8 or 18 carbon long alkyl chain attached to a porous silica particle (silica- $(CH_2)_nCH_3$ ). The surface coverage of the bonded phase is usually around  $4 \mu\text{mol}/\text{m}^2$ . Usual mobile phases are mixtures of water, organic solvent (methanol, acetonitrile) and sometimes a buffer.



The retention of the analytes in RPLC is related to their equilibrium between the mobile phase and the stationary phase. The distribution constant,  $K_p$ , is the ratio of the analyte's concentration in the stationary phase  $[A]_s$  to the concentration in the mobile phase  $[A]_m$ :

$$K_p = \frac{[A]_s}{[A]_m} \quad (1.15)$$

The retention volume ( $t_v$ ) of an analyte that is not retained on the column (i.e.  $[A]_s=0$ ) corresponds to the void volume of the column ( $V_0$ ). On a chromatogram  $V_0$  corresponds to  $t_o$ ; the dead time or retention time of an unretained compound. For a retained compound,  $t_r$ , its retention time, minus  $t_o$  would then correspond to the time spent in the stationary phase. To express the relative retention of an analyte on a column, its retention factor ( $k'$ ) is calculated from  $t_r$  and  $t_o$ :

$$k' = \frac{\text{time spent in stat. phase}}{\text{time spent in the mobile phase}} = \frac{t_r - t_o}{t_o} \quad (1.16)$$

In most separations,  $k'$  is adjusted to be between 0.5 and 10 to achieve resolution of weakly retained analytes ( $k' \geq 0.5$ ), while maintaining the overall separation time relatively short ( $k' \leq 10$ ).

The driving force of the analyte equilibrium between stationary and mobile phase in RPLC is the degree of solubility of the analytes in the mobile phase. It is function of the polarities of the analytes, the mobile phase and the stationary phase. Analytes with greater polarity easily interact with the aqueous mobile phase through hydrogen bonding.



Conversely, less polar analytes contribute less to hydrogen bonding and adsorb onto the stationary phase through dispersion forces.

Changes in the polarity of the mobile phase control retention by altering the analytes equilibrium between the mobile and the stationary phases. A less polar mobile phase (less water in the mixture) is a stronger eluent since analytes adsorbed on the stationary phase become more soluble in the mobile phase and elute faster. Also, changes in the eluent pH can alter retention of acidic and basic molecules. Depending on the pH, these molecules can be charged or not. When charged, a molecule's ability to undergo hydrogen bonding is greater, which will increase its solubility in the mobile phase.

In general, reverse phase columns are composed of a silica-based bonded phase. The derivatisation of the silica involves a reaction with chlorosilanes, which carry the functional group ( $R_1$ ):

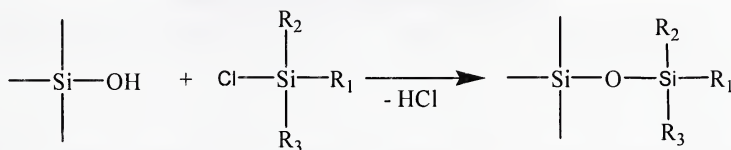


**Figure 1.5 Bonding of silica surface with chlorosilanes. Adapted from reference 23.**

$R_2$  and  $R_3$  can be additional functional groups or protecting methyl, isopropyl or *t*-butyl groups. It is usually recommended that siloxane bonded phases such as this one be used only from pH 2-8. In acidic eluent conditions, hydrolysis of the siloxane bond (Si-O) attaching the bonded phase to the silica particle compromises the chemical stability. Sterically protected phases where  $R_2$  and  $R_3$  are bulky groups such as isopropyl or isobutyl instead of the conventional methyl groups improve the stability with regard to



hydrolysis.<sup>25</sup> Alternately, low-pH stable phases can be made using bidentate stationary phases (Figure 1.6), where the bonded phase is linked to the silica surface through dual siloxane bonds. The bridging group Q is  $-(CH_2)_n-$  with  $-(CH_2)_3-$  being optimum when R is an additional octadecyl group.<sup>26</sup> In addition, bidentate phases have been found to protect the silica structure and enhance stability at elevated pH. Normally, at high pH the stability of the silica particle (not the bonded phase) is low, hence the limitation of use at  $pH > 8$ . This will be discussed in Section 1.2.5.1. In Chapter 5, a bidentate column, the Zorbax Extend-C18, is used at elevated pH.

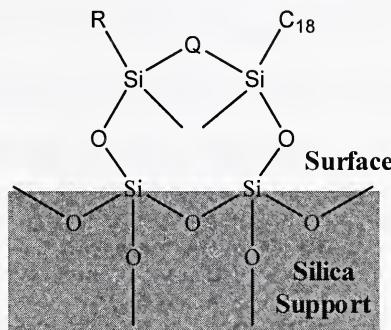


**Figure 1.6 Structure of a bidentate phase. Adapted from reference 26.**

Highly polar analytes are weakly retained on reverse phase columns. To maximize their retention they are separated using weak eluents containing 95-100% water. This high water content however, may result in *phase collapse* or *dewetting* of the bonded phase.<sup>27</sup> This phenomenon refers to the expulsion of water from the pores and results in low retention, peak tailing and non reproducible retention times. Partially hydrophilic phases where polar groups are added within the silica surface or bonded phase are available for highly aqueous conditions.<sup>28,29</sup> These phases greatly reduce phase collapsing and enable separations in 100% water. They can be classed as: polar



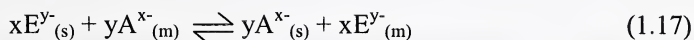
embedded, polar/hydrophilic encapped or phases with enhanced-polar selectivity. Polar embedded phases have a polar functionality such as an amide, ether or carbamate inserted into the alkyl ligand ( $R_1$  in Figure 1.5) close to the silica surface. Examples are the Supelco Discovery Amide, the Waters SymmetryShield RP18 (carbamate) and the Agilent Zorbax Bonus-RP (amide). Phases with enhanced-polar selectivity have methoxy ( $CH_3O-$ ) or ethoxy ( $CH_3CH_2O-$ ) groups as  $R_2$  and  $R_3$ . After bonding, these groups are hydrolyzed to non-acidic Si-OH which interact through hydrogen bonding with water. The Agilent Zorbax SB-Aq column is an example of such a phase and will be used in Chapter 3. Finally, polar/hydrophilic endcapped phases are obtained by reacting trimethoxy or triethoxysilanes ( $(CH_3O)_3SiH$  or  $(CH_3CH_2O)_3SiH$ ) with the silica free silanols (Figure 1.11 in Section 1.2.5.1). After hydrolysis, they also provide non-acidic silanol functional groups. Examples are Alltech Altima AQ or Thermo Aquasil C18 columns.

### 1.2.3.2 Ion Chromatography (IC)<sup>30-32</sup>

Ion chromatography evolved from the pioneer work of Hamish Small in 1975.<sup>33</sup> It is used for the separation of ions and ionizable compounds. Retention is achieved by the exchange of analytes (cations or anions) between the stationary and the mobile phases. For simplicity, I will only discuss anion exchange IC since the work presented in Chapters 4 and 5 involves anion analysis. In anion exchange IC, the stationary phase carries a fixed positive charge and the eluting ion is negatively charged ( $E^y-$ ). The



equilibrium of the stoichiometric exchange of the anions between stationary (s) and mobile (m) phases is expressed as follow:



where  $A^{x-}$  is the analyte ion. The equilibrium constant ( $K_{IEX}$ ) determines the relative retention of each analytes. Strongly retained analytes (spending most time in the stationary phase) have a larger  $K_{IEX}$  thus, a larger retention factor ( $k'$ ). For instance, doubly charged analyte ions ( $A^{-2}$ ) are more retained because they have a stronger electrostatic attraction on the column than singly charged analytes ( $A^{-1}$ ). Similarly, increased eluent charge (y) reduces retention factors by decreasing  $K_{IEX}$  since the eluent becomes more attracted to the stationary phase.

Retention is controlled by  $K_{IEX}$ , the ion exchange capacity of the column (Q), the weight and volume of stationary phase (w and  $V_m$  respectively) and by the nature and concentration of the eluent anion,  $E^{y-}$ :<sup>32</sup>

$$\log k' = \frac{1}{y} \log K_{IEX} + \frac{x}{y} \log \left( \frac{Q}{y} \right) + \log \left( \frac{w}{V_m} \right) - \frac{x}{y} \log [E^{y-}_{(m)}] \quad (1.18)$$

where x and y are the charges of the analyte and the eluent respectively. This equation suggests that increases in  $K_{IEX}$ , Q or  $w/V_m$  lead to increased retention factors and that increasing  $[E^{y-}_{(m)}]$  results in decreased retention. Plots of  $\log k'$  vs  $\log (Q/y)$  or vs  $\log [E^{y-}_{(m)}]$  have slopes of  $x/y$  and  $-x/y$  respectively. In both cases, the slope of a graph for doubly charged analyte is then double the slope of a graph for singly charged analyte when eluted with the same eluent. The retention of doubly charged analytes is thus more



affected by changes of column capacity and eluent concentration than the retention of singly charged analytes.

Preferred eluents are salts of weak acids ( $\text{pH} > 7$ ) such as (in order of increasing strength): hydroxide ( $\text{OH}^-$ ), bicarbonate ( $\text{HCO}_3^-$ ) and carbonate ( $\text{CO}_3^{2-}$ ). The mixture of bicarbonate and carbonate ions is often used as a powerful eluent for the separation of both singly and doubly charged analytes in a single chromatogram.

Due to the alkaline nature of IC eluents, the stationary phases in IC are normally high pH stable polymer-based ion exchangers (Section 1.2.5.1). As will be explained in Section 1.2.5.1, polymeric phases do not usually enable high efficiency separations because of the poor mass transfer into porous particles. However, polymeric phases with high efficiencies ( $N=4,000-7,000$ ) can be obtained using particles where the ion exchange sites are only located on the outer surface of the particle. Such *agglomerated particles* are synthesized by Dionex by electrostatically attaching small latex particles on the surface of solid nonporous particles. In anion exchange IC, the  $0.1 \mu\text{m}$  aminated latex particles (Particle- $(\text{NR}_3^+)_n$ ) are agglomerated onto a surface-sulfonated (Particle- $(\text{SO}_3^-)_n$ ) solid polymeric particle of  $5-10 \mu\text{m}$  diameter (Figure 1.7).

Anion exchange separations are typically performed on strong base (quaternary ammonium) stationary phases and only rarely on weak base (tertiary amine) phases. The ion-exchange capacity of a resin, expressed in  $\mu\text{eq/g}$ , is defined as the number of ion-exchange sites per weight equivalent of the column packing. Typical IC columns have capacities of  $6-60 \mu\text{eq/g}$ . In contrast, classic polystyrene-divinyl benzene anion exchange resins such as Dowex A1 have much higher capacity ( $0.8-2.4 \text{ meq/mL}$ ).<sup>31</sup>



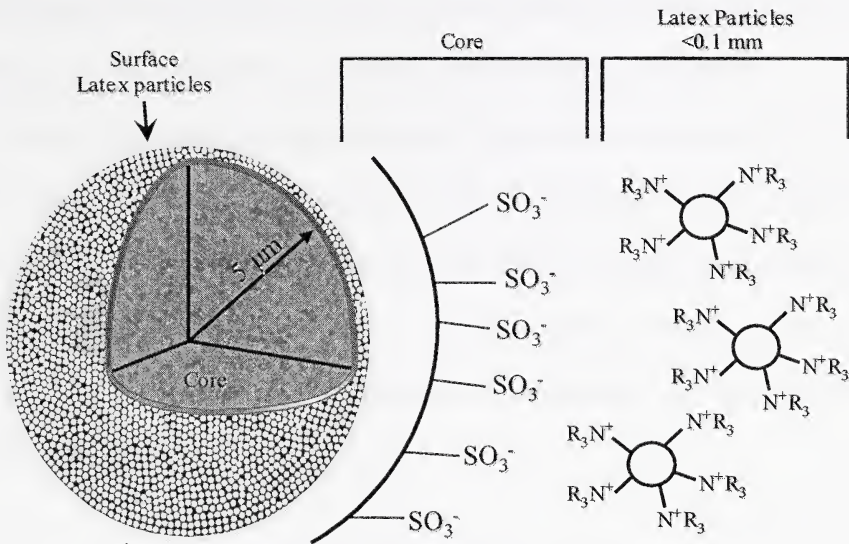


**Figure 1.7 Structure of a latex-based anion exchange particle.** Adapted from reference 35 with permission.

### 1.2.4 Detection

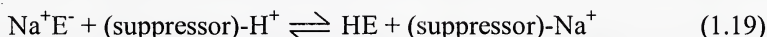
#### 1.2.4.1 Conductivity detection

Conductivity detection is very important in IC as it is a universal detection mode for ionic species. A conductivity detector consists of a cell with two electrodes through which an electric potential is applied. When ions enter the cell, they move towards the anode or the cathode and generate an electrical current. This current is measured and depends of the concentration and conductance of the ions. However, since the eluent in IC is conductive itself, it causes a large conductivity background, worsening limits of detection. To reduce this background, either low concentrations of weakly conductive



eluent are used with low capacity columns (non-suppressed IC) or an eluent suppressor is added to the system between the column and the detector (suppressed IC).

Eluent suppression in anion exchange IC improves the detection limits of anions from the parts-per-million (ppm,  $\mu\text{g/mL}$ ) to the parts-per-billion (ppb,  $\text{ng/mL}$ ) level through two processes. First, the eluent is converted to a lower conductive form to decrease the conductivity background. In anion analysis, the suppressor is a cation exchanger. When the eluent ( $\text{Na}^+\text{E}^-$ , salt of a weak acid) passes through the suppressor, the following equilibrium occurs:



The resulting conductivity background is reduced. After suppression, this residual conductivity background depends on the strength of the acid HE. Weak acids such as  $\text{H}_2\text{O}$ , which is obtained from the suppression of a  $\text{NaOH}$  eluent, only very slightly dissociate, generating background conductivity as low as  $0.06 \mu\text{S/cm}$ . Stronger acids such as  $\text{H}_2\text{CO}_3$  ( $\text{pK}_a$  6.6) obtained from suppression of a carbonate eluent generate backgrounds of  $12\text{-}15 \mu\text{S/cm}$ .

Second, suppression increases the conductivity of the analytes. As with the eluent, the analyte anions ( $\text{A}^-$ ) are converted to their acid form:



Common anions ( $\text{F}^-$ ,  $\text{Cl}^-$ ,  $\text{NO}_2^-$ ,  $\text{Br}^-$ ,  $\text{NO}_3^-$ ,  $\text{HPO}_4^{2-}$ ,  $\text{SO}_4^{2-}$ ) are the salts of strong and relatively strong acids. Therefore, they will mostly or fully dissociate yielding  $\text{H}^+$  and  $\text{A}^-$  which is more conductive than  $\text{Na}^+\text{A}^-$ , hence a sensitivity improvement.



Since the mid-1990s, many types and designs of suppressors have been commercially available.<sup>34</sup> The suppressors used in my work are based on cation exchange membranes or monolithic beds, with the regenerant ( $H^+$ ) generated electrochemically. The operation of a suppressor is illustrated in Figure 1.8.<sup>35</sup> The eluent and sample components flow through the center of the suppressor between the two cation exchange membranes. On the outside of the membrane flows the regenerant (water) in the opposite direction. Finally, two electrodes sandwich the membranes and flow paths. When a current is applied, hydronium ions are formed at the anode and cross the membrane to form HE with the eluent's anions ( $E^-$ ) and acids ( $H^+A^-$ ) with the sample anions ( $A^-$ ). At the same time, sodium ions are attracted towards the cathode and cross the opposite membrane to form NaOH before going to the waste.

More recently a new type of suppressor (Dionex, Atlas) based on a monolithic (Section 1.2.5.2) suppression bed was released. The suppression process is identical to the one described above. However, here, the suppression bed is made of cation exchange monolith disks through which the eluent flows (Figure 1.9). A water regenerant flows in the opposite direction and a current is applied across the suppressor to enable neutralization.



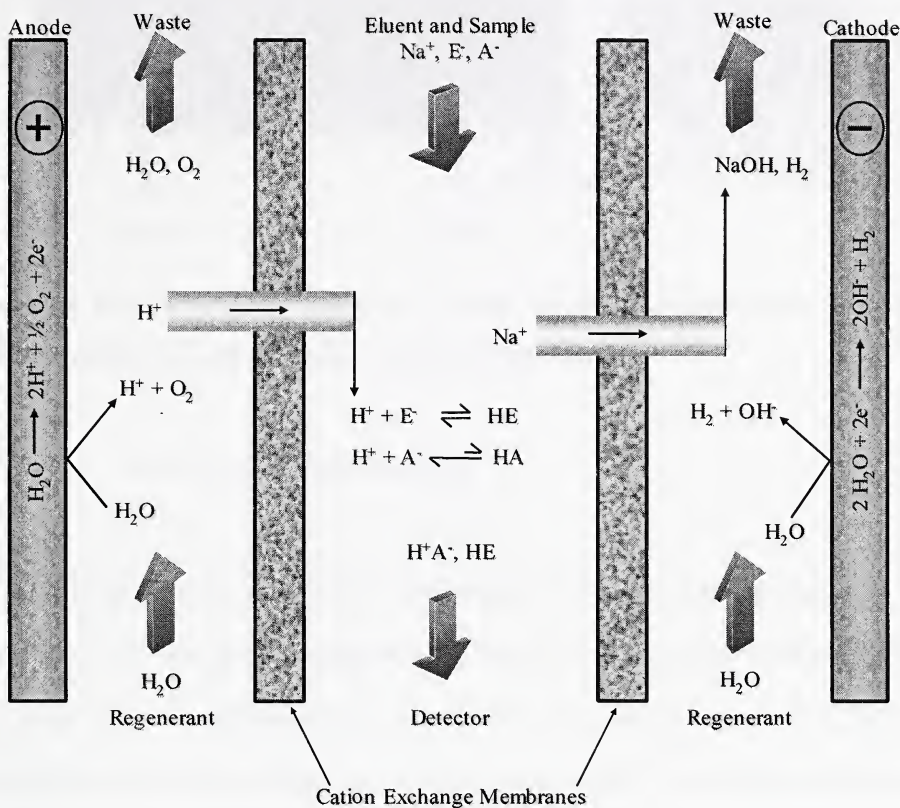


**Figure 1.8 Suppressor for anion analysis and photo of a Dionex Self Regenerating Suppressor (SRS). Adapted from reference 35 with permission.**



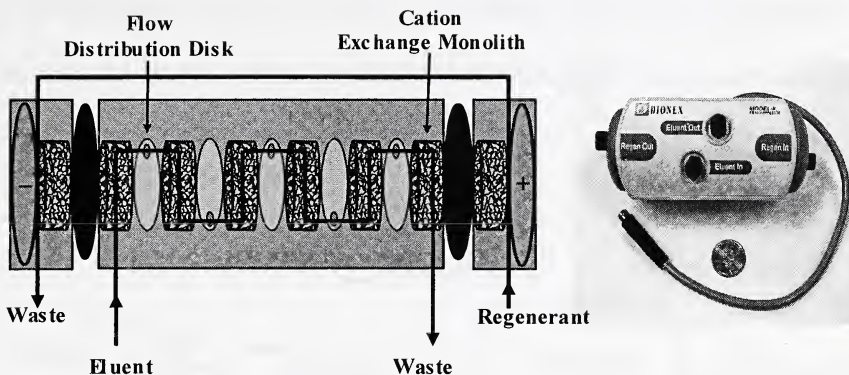


**Figure 1.9 Cross-section and photo of a Dionex Anion Atlas Electrolytic Suppressor (AAES). Adapted from reference 35 with permission.**

#### 1.2.4.2 Post-column reactions

Post-column reactions involve the on-line modification of analytes after their separation.<sup>36</sup> To the cost of complexity and band spreading, these reactions increase selectivity or facilitate detection of analytes with weak detector response. They also present the possibility to separate the analytes in their native form, before derivatisation. Eluent suppression in IC is an example of a post-column reaction.<sup>37</sup> Very commonly chromophores or fluorophores are reacted with the analyte to enable UV/VIS absorbance or fluorescence detection. In Chapters 2 and 3, analytes are detected through quenching of the fluorescence of a post-column reactant.

The most simple apparatus design (Figure 1.10) involves the continuous addition of one reagent through a T-piece just after the separation.<sup>22,36</sup> Even though the on-line derivatisation reaction does not have to go to completion, it must be reproducible and reasonably fast. Depending on the needs of the reaction, on-line mixing, incubation or a



change of temperature might be necessary. In addition, the reaction solution(s) must be miscible with the eluent. When possible, the introduction of the post-column reactant must be pulse-less to reduce excessive baseline noise.

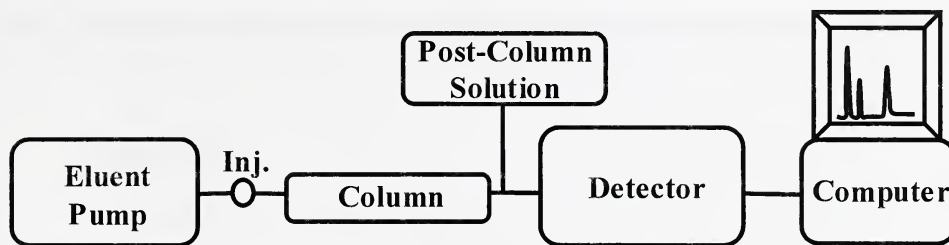


**Figure 1.10 Instrumental scheme of HPLC with post-column reaction.**

#### 1.2.4.3 Indirect detection

Indirect detection is used for detection of analytes having a weak detector response. In this method, the eluent or eluent additives give a strong and constant signal background. During elution, the analytes displace the eluent molecules and decrease the detector signal when passing through the detector, resulting in a dip in the baseline.<sup>22,38</sup> The method presented in Chapters 2 and 3 is based on indirect fluorescence detection coupled with a post-column reactant.

The theoretical limit of detection for indirect fluorescence detection is given by:<sup>38,39</sup>

$$C_{\text{lod}} = \frac{C_p s_{\text{BN}}}{T_R} = \frac{C_p}{T_R \times DR} \quad (1.21)$$

where  $C_p$  is the concentration of the detectable probe in the eluent,  $s_{\text{BN}}$  is the relative standard deviation of the background signal fluctuations (noise),  $T_R$  is the transfer ratio



(the number of probe molecules displaced by one analyte molecule), and DR is the dynamic reserve (ratio of the background signal intensity to the noise; =  $s_{BN}^{-1}$ ). To maximize the sensitivity for indirect detection it is desirable to maximize the signal due to the probe so as to maximize DR or to allow reduction in the probe concentration ( $C_p$ ).

## 1.2.5 Columns

### 1.2.5.1 Particulate columns

Most commonly, the stationary phase in HPLC is based on small, spherical, porous silica particles. Silica has high mechanical strength (resists high pressures), does not swell in the presence of organic solvents and can be easily modified to offer different surface chemistries (Section 1.2.3.1).<sup>22</sup> However, the chemical stability of silica at pH>8 is poor. Figure 1.11 illustrates the dissolution mechanism of silica in alkaline condition. Nucleophilic attack of the Si-O bonds by hydroxide results in the formation of  $Si(OH)_4$  and erosion of the silica surface.<sup>22,40</sup> When a silica-based column is exposed to elevated pH, its efficiency decreases, its backpressure increases and eventually the bonded phase collapses.<sup>25</sup> The speed of particle degradation at high pH depends on many factors, but principally on the nature of the stationary phase, the buffer used in the mobile phase, the nature and content of the organic modifier and the temperature.<sup>22,25</sup> In addition, free ionized silanol groups (at pH>3)<sup>23</sup> on the silica surface (Figure 1.11) interact with basic compounds and negatively affect peak shape.



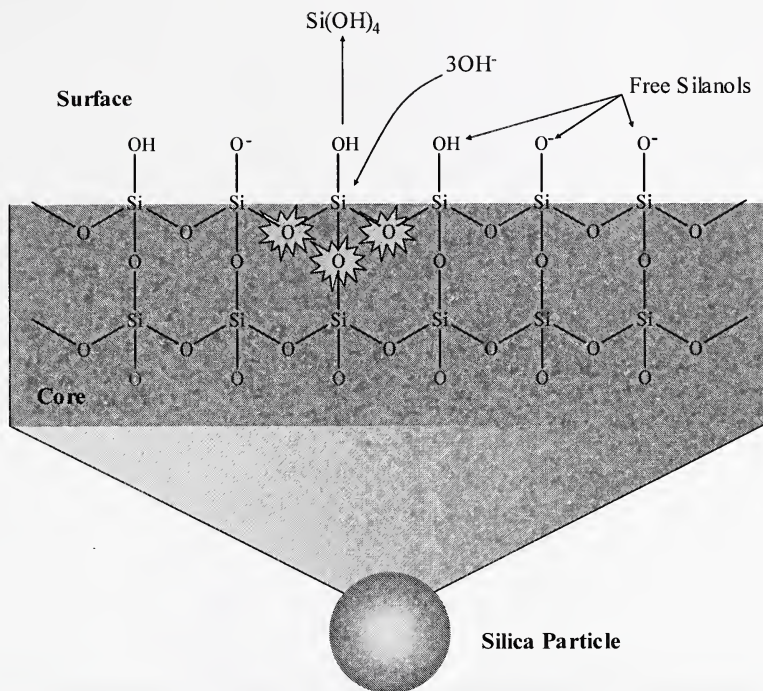


**Figure 1.11** Hydrolysis of silica at high pH. Adapted from reference 40, courtesy of Waters Corporation.

Organic polymeric materials such as styrene/divinylbenzene copolymer (Figure 1.12), polymethacrylate or polyvinyl resins can be used as an alternate support to silica.<sup>23</sup> These stationary phases are stable from pH 1-14 and have no silanol interaction problem since none are present. However, polymeric packings are mechanically soft and susceptible to shrinking or swelling in the presence of organic solvents. More importantly, they exhibit significantly lower efficiency than silica packing because of poor mass transfer properties into the stationary phase.<sup>41</sup>



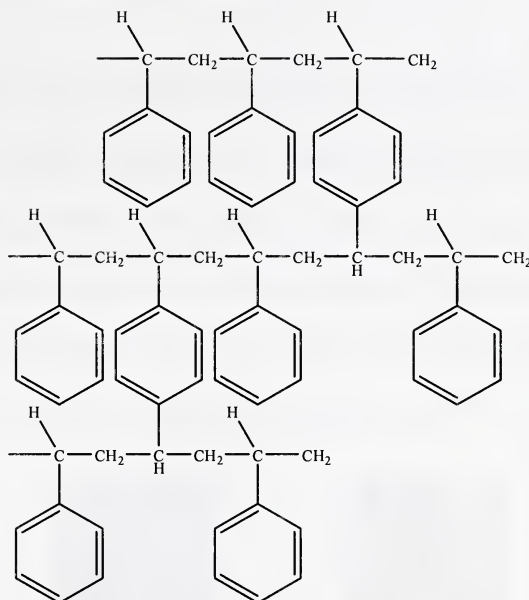


**Figure 1.12 Schematic illustration of the polystyrene/divinylbenzene skeleton.**  
**Adapted from reference 30.**

Silica-based stationary phases are known to be more stable at high pH when eluents are buffered with organic molecules or with borates.<sup>25,26,42</sup> It is believed that organic molecules, especially nitrogen containing compounds, are sorbed on the silica surface and act as a shield to protect the silica from the nucleophilic attack by the hydroxide ions.<sup>43</sup> Inorganic buffers, however, would not be as effective in protecting the silica.<sup>43</sup> They may even complex with the silica surface at pH>7, weakening the silicasiloxane bonds.<sup>44</sup> The use of carbonates and phosphates is therefore not recommended with silica based stationary phases.



### 1.2.5.2 Monolithic columns

In the recent years, monolithic columns (or continuous bed columns) have been increasingly used in HPLC separations.<sup>45</sup> These columns exhibit a different internal geometry than columns packed with particles, as illustrated in Figure 1.13.<sup>46,47</sup> Monoliths are obtained through a sol-gel process and enclosed in a PEEK sheath.<sup>48</sup> In essence, they consist of a rod of stationary phase (e.g. silica) with mesopores for retention and macropores (larger channels) for through-flow (Figure 1.14).<sup>48-50</sup>

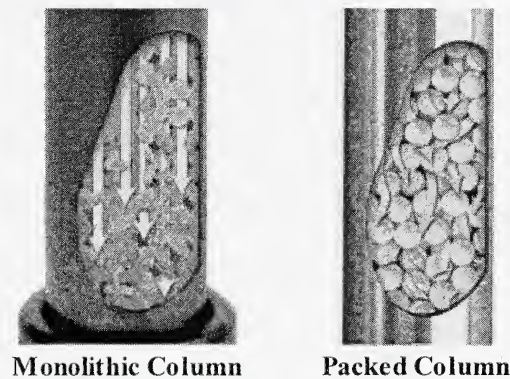


Figure 1.13 Flow paths of monolithic and packed bed columns. From reference 46, with permission.

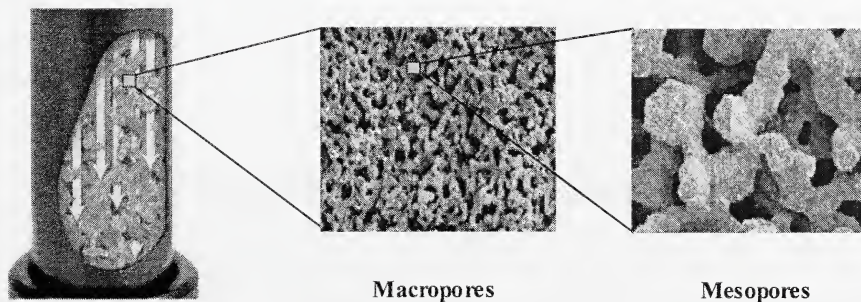
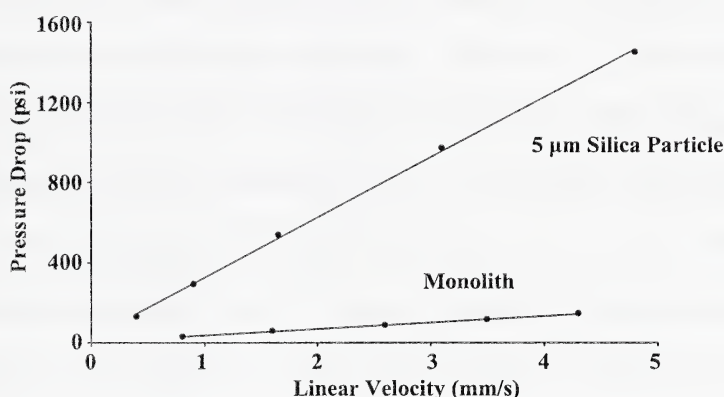


Figure 1.14 Macroporous and mesoporous structures of a monolith. Adapted from references 46 and 47 with permission.



For HPLC applications monolithic columns are usually silica-based, with mesopores typically around 10-25 nm and macropores around 1-3  $\mu\text{m}$ . Tallarek and co-workers<sup>51</sup> demonstrated that monolithic columns are equivalent to 3  $\mu\text{m}$  particulate columns in terms of band broadening and to 15  $\mu\text{m}$  particles with regard to permeability. In other words, these columns exhibit high efficiency while generating minimal pressure drops (Figure 1.15). Thus, these characteristics enable the use of very high flow rates (as high as 16 mL/min) for ultra-fast separations.<sup>45,52</sup> Polymeric monolith columns exist for HPLC but for the same reason as stated in Sections 1.2.3.2 and 1.2.5.1., they are seldom used because of low efficiencies generated.



**Figure 1.15 Pressure vs. linear velocity for various columns.** Adapted from reference 48.

### 1.2.5.2.1 IC on a silica-based C<sub>18</sub> monolithic column

Speed of analysis is an important factor, as it leads to improvements in sample throughput and productivity. Anion analysis is an important application in industry and



up to a few years ago was not a very fast process. Separations were performed on anion exchange polymer-based columns (10-25 cm) and would take 10-20 minutes for the analysis of the common anions.<sup>30</sup> Our group developed a high-speed IC method for anions using 5 cm long monolithic columns.<sup>53</sup> In this method, ion chromatography is performed by converting a silica-based reverse phase (C<sub>18</sub>) monolithic column into an ion exchanger.<sup>53,54</sup> To do so, a long chain cationic surfactant solution (1 mM Didodecyl-dimethylammonium bromide, DDAB), is flushed onto the RPLC column until complete breakthrough of DDAB is observed (Figure 1.16). The hydrophobic alkyl chains of DDAB adsorb strongly onto the C<sub>18</sub> column leaving the charged ammonium group of the surfactant available for anion exchange. After coating and washing with water, the column is equilibrated with the eluent and is then ready for IC. To remove the DDAB coating, 100% acetonitrile (ACN) is flushed through the column. This coating procedure was first designed for particulate columns.<sup>54</sup> The use of monolithic columns enable flow rates of 10 mL/min, resulting in 30 second separations of 7 analytes.<sup>53</sup> The column capacity is varied by adjusting the ACN content in the DDAB coating solution.<sup>53,55</sup> A higher content of ACN results in a lower capacity since less surfactant coats on the column.

Since the monolith column is silica-based, the usual alkaline IC eluents cannot be used (Section 1.2.5.1). Instead, a solution of 2-cyanophenol (pK<sub>a</sub>=6.9) at pH 7 is used as the eluent. 2-Cyanophenol can be suppressed and also used in non-suppressed mode because of its low conductivity.



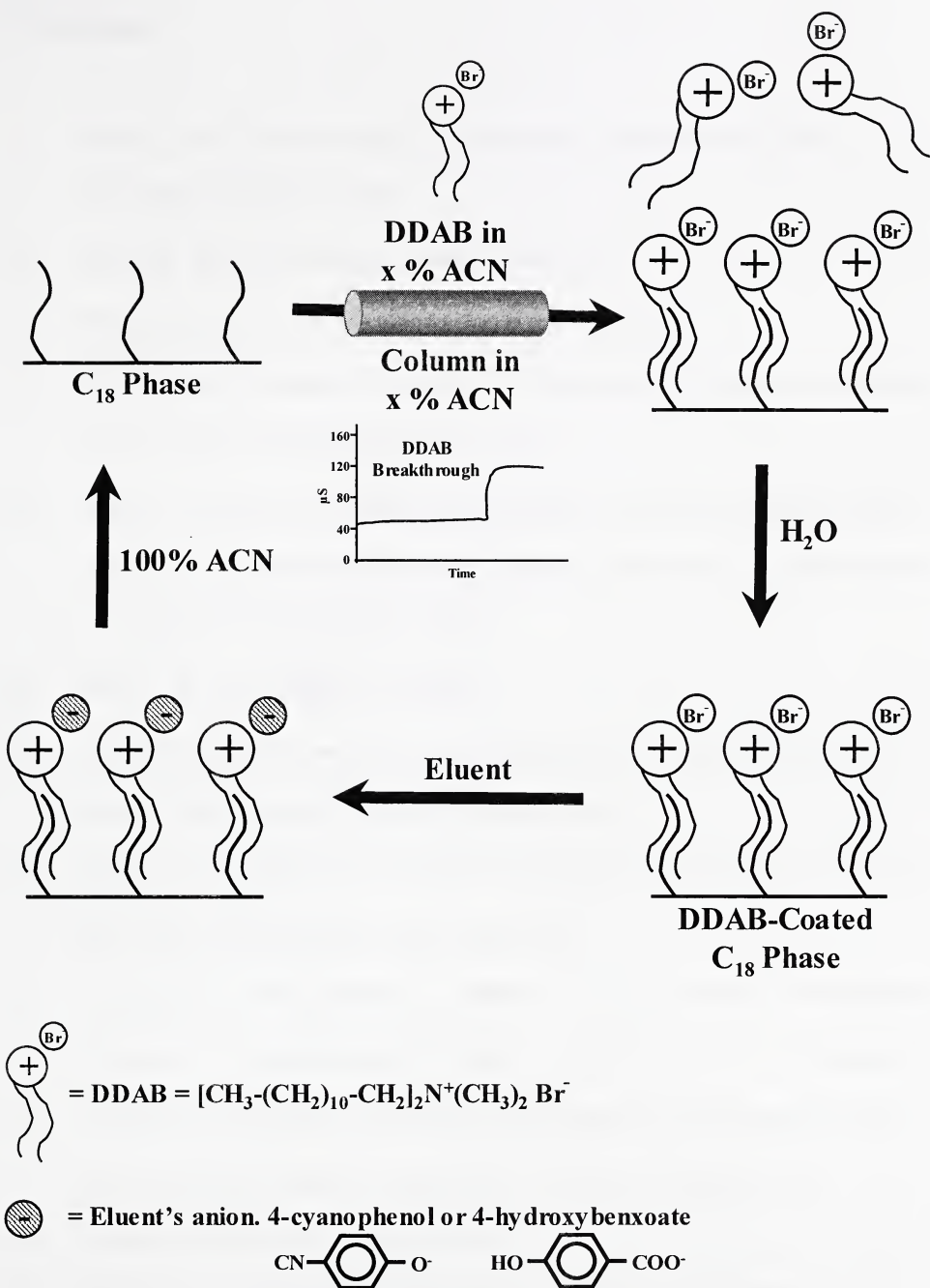


Figure 1.16 Coating and removal of DDAB on a  $C_{18}$  column.



### 1.3 References

- (1) Miller, J. M. *Chromatography, Concepts and Contrasts*, 2nd ed.; Wiley Interscience: Hoboken, 2005.
- (2) Smith, R. M. *J. Chromatogr. A* **2003**, *1000*, 3-27.
- (3) Moldoveanu, S. C. *J. Chromatogr. Sci.* **2004**, *42*, 1-14.
- (4) Snyder, L. R.; Kirkland, J. J.; Glajch, J. L. *Practical HPLC method development*, 2nd ed.; Wiley Interscience: Hoboken, 1997.
- (5) Ettre, L. S. *Evolution of liquid chromatography: a historical overview in High Performance Liquid Chromatography Advances and Perspectives*; Ed. Horvath C.; Academic Press: New York, 1980.
- (6) Ettre, L. S. *LCGC* **2003**, *21*, 458-467.
- (7) Tswett, M. S. *Trudy varshavskogo obshchestva estestvoispytatelei* *otdelenie biologii* **1905**, *14*, 20-39, (see ref. 8 for translation).
- (8) Berezkin, V. G., Ed. *Chromatographic adsorption analysis: selected works of M.S. Tswett*; Ellis Horwood: New York, 1990.
- (9) Tswett, M. *Ber. Dtsch. Botan. Ges.* **1906**, *24*, 316-323, (see ref. 8 for translation).
- (10) Tswett, M. *Ber. Dtsch. Botan. Ges.* **1906**, *24*, 384-393, (see ref. 8 for translation).
- (11) Tswett, M. *Khromofilly v rastitel'nom i zhivotnom mire (Chromophylls in the plant and animal kingdom)*; Karbasnikov Publishers: Warsaw, 1910.
- (12) Kuhn, R.; Lederer, E. *Naturwiss.* **1931**, *19*, 306.
- (13) Martin, A. J. P.; Synge, R. L. M. *Biochem. J.* **1941**, *35*, 1358-1368.
- (14) van Deemter, J. J.; Zuiderweg, F. J.; Klinkenberg, A. *Chem. Eng. Sci.* **1956**, *5*, 271-289.



(15) James, A. T.; Martin, A. J. P. *Int. Congr. Anal. Chem.* **1952**, *77*, 915-932.

(16) Giddings, J. C. *Anal. Chem.* **1963**, *35*, 2215-2216.

(17) Horvath, C.; Lipsky, S. R. *J. Chromatogr. Sci.* **1969**, *7*, 109-116.

(18) Horvath, C. G.; Preiss, B. A.; Lipsky, S. R. *Anal. Chem.* **1967**, *39*, 1422-1428.

(19) Bidlingmeyer, B. A.; Warren, F. V. *Anal. Chem.* **1984**, *56*, 1583A-1596A.

(20) Foley, J. P.; Dorsey, J. G. *Anal. Chem.* **1983**, *55*, 730-737.

(21) Swartz, M. E. *J. Liq. Chromatogr. Relat. Technol.* **2005**, *28*, 1253-1263.

(22) Pool, C. F. *The essence of chromatography*; Elsevier Science B.V.: Amsterdam, 2003.

(23) Neue, U. D. *HPLC columns, theory, technology and practice*; Wiley-VCH: New York, 1997.

(24) Dolan, J. W. *LCGC* **2004**, *22*, 26-30.

(25) Claessens, H. A.; van Straten, M. A. *J. Chromatogr. A* **2004**, *1060*, 23-41.

(26) Kirkland, J. J.; Adams, J. B. J.; van Straten, M. A.; Claessens, H. A. *Anal. Chem.* **1998**, *70*, 4344-4352.

(27) Przybyciel, M.; Majors, R. E. *LCGC* **2002**, *20*, 516-523.

(28) Majors, R. E.; Przybyciel, M. *LCGC* **2002**, *20*, 584-593.

(29) Euerby, M. R.; Petersson, P. *994* **2003**, 13-36.

(30) Weiss, J. *Handbook of Ion Chromatography*, 3rd ed.; Wiley-VCH: Darmstadt, 2004.

(31) Lucy, C. A.; Hatsis, P. In *Chromatography, part A: fundamentals and techniques*, 6<sup>th</sup> ed.; Heftmann, E., Ed.; Elsevier B.V.: Amsterdam, 2004; Vol. 69A, Journal of Chromatography Library.



(32) Haddad, P. R.; Jackson, P. E. *Ion Chromatography: Principles and Applications*; Elsevier: New York, 1990.

(33) Small, H.; Stevens, T. S.; Bauman, W. C. *Anal. Chem.* **1975**, *47*, 1801-1809.

(34) Haddad, P. R.; Jackson, P. E.; Shaw, M. J. *J. Chromatogr. A* **2003**, *1000*, 725-742.

(35) Later, D.; Adams, B.; Chapeau, O.; Pelletier, S.; Fitchet, A. *Short Course: Introduction to modern ion chromatography* International Ion Chromatography Symposium (IICS), Montreal, Canada, September 18 2005.

(36) Krull, I. S., Ed. *Reaction detection in liquid chromatography*; Marcel Dekker, Inc.: New York, 1986.

(37) Dasgupta, P. K. *J. Chromatogr. Sci.* **1989**, *27*, 422-448.

(38) Yeung, E. S.; Kuhr, W. G. *Anal. Chem.* **1991**, *63*, 275A.

(39) Kuhr, W. G.; Yeung, E. S. *Anal. Chem.* **1988**, *60*, 2642.

(40) *XBridge<sup>TM</sup> HPLC Columns*; Waters Corporation, 2005.

(41) Dawkins, J. V.; Lloyd, L. L.; Warner, F. P. *J. Chromatogr.* **1986**, *352*, 157-167.

(42) Kirkland, J. J.; Henderson, J. W.; SeStefano, J. J.; van Straten, M. A.; Claessens, H. A. *J. Chromatogr. A* **1997**, *762*, 97-112.

(43) Kirkland, J. J.; van Straten, M. A.; Claessens, H. A. *J. Chromatogr. A* **1998**, *797*, 111-120.

(44) Claessens, H. A.; van Straten, M. A.; Kirkland, J. J. *J. Chromatogr. A* **1996**, *728*, 259-270.

(45) Cabrera, K. *J. Sep. Sci.* **2004**, *27*, 843-852.

(46) [www.merck.de/servlet/PB/menu/1209750/](http://www.merck.de/servlet/PB/menu/1209750/).



(47) [www.phenomenex.com](http://www.phenomenex.com).

(48) Tanaka, N.; Kobayashi, H.; Nakanishi, K.; Minakuchi, H.; Ishizuka, N. *Anal. Chem.* **2001**, 73, 420A-429A.

(49) Ikegami, T.; Tanaka, N. *Curr. Opin. Chem. Biol.* **2004**, 8, 527-533.

(50) Miyabe, K.; Guiochon, G. *J. Sep. Sci.* **2004**, 27, 853-873.

(51) Leinweber, F. C.; Lubda, D.; Cabrera, K.; Tallarek, U. *Anal. Chem.* **2002**, 74, 2470-2477.

(52) Mistry, K.; Grinberg, N. *J. Liq. Chromatogr. Relat. Technol.* **2005**, 28, 1055-1074.

(53) Hatsis, P.; Lucy, C. A. *Anal. Chem.* **2003**, 75, 995-1001.

(54) Connolly, D.; Paull, B. *J. Chromatogr. A* **2002**, 953, 299-303.

(55) Cassidy, R. M.; Elchuk, S. *J. Chromatogr. Sci.* **1983**, 21, 454-459.



## CHAPTER TWO. HPLC separation and indirect fluorescence detection of thiols<sup>a</sup>

### 2.1 Introduction

Organosulfur compounds include a large variety of molecules and among them, the thiols group is very important. Widely distributed in living cells, as part of proteins or as independent molecules, thiols are involved in numerous biological reactions. Interest in their determination has been growing in recent years as their role in biological processes has become more evident.<sup>1-5</sup> Variations in the concentration of certain thiols have been related to many illnesses. For example, high levels of cysteine (cys) or homocysteine (hcys) in physiological fluids result from metabolic disorders, and have been related to coronary heart disease, renal disease, Alzheimer's disease, Parkinson's disease and mental retardation.<sup>3,4,6,7</sup> Glutathione (gsh) is a cellular antioxidant and its level in cells is indicative of oxidative stress. Analysis of thiols is extremely important for the biochemical and clinical domains of research in order to understand many physiological and metabolism processes.

A number of recent reviews detail the many methods (mainly HPLC) that have been reported for the analysis of thiols.<sup>1,7-10</sup> The compounds in Figure 2.1 are the most studied due to their biological importance and structural simplicity. Since thiols lack strong chromophores or fluorophores, the analysis methods require pre-, post- or on-column derivatisation for UV-VIS, fluorescence, chemiluminescence or electrochemical detection. The most popular and sensitive detection reagents are the fluorimetric

---

<sup>a</sup> A version of this chapter has been published as Pelletier, S; Lucy C. A. *J. Chromatogr. A* 2002, 972, 221-229.



bimanes, maleimides and halogenosulphonylbenzofurazans. Unfortunately, these reagents often require drastic, complex and time consuming reaction conditions.<sup>11-14</sup>

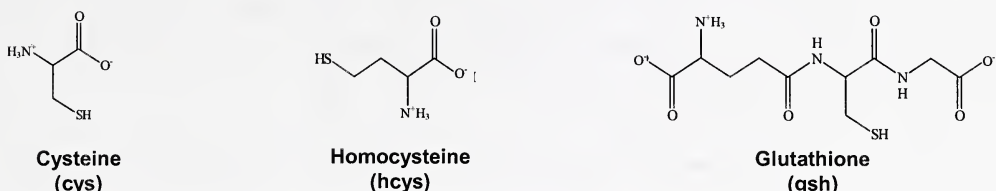


**Figure 2.1 Chemical structures of thiol analytes.**

In this Chapter, thiols are separated by RPLC and detected using a post-column indirect fluorescence system (Section 1.2.4.2 and 1.2.4.3). The thiol separation is based on that published by Manna et al.<sup>15</sup> A C<sub>18</sub> column is used to separate cys, hcys and gsh using a mobile phase of 0.01 M trifluoroacetic acid (TFA) in water containing 0.5% methanol. This yields baseline resolution separation of the three analytes in 5 minutes.

The post-column reactant is a fluorescent complex of cadmium and 8-hydroxyquinoline-5-sulphonic acid (HQS) (Figure 2.2).<sup>16</sup> HQS, like its parent compound (8-hydroxyquinoline; oxine; 8-HQ), forms stable complexes with a wide variety of metals.<sup>16,17</sup> However, only those metals which have stable electron configurations (i.e. either completely full or empty electron shells) yield fluorescent complexes.<sup>17</sup> Thus HQS can provide sensitive fluorescence detection only for Cd<sup>2+</sup>, Zn<sup>2+</sup>, Mg<sup>2+</sup>, Al<sup>3+</sup> and La<sup>3+</sup>.<sup>18-23</sup> The detection limits for these metals, and particularly for Cd<sup>2+</sup> are very good. For instance, Paull et al. achieved detection limits as low as 0.02 µM (2 µg/L) using an ion-interaction reverse phase liquid chromatographic method with on-column complexation with HQS.<sup>22</sup> Alternatively, Soroka et al. reported that detection limits well below 10<sup>-8</sup> M



and approaching  $10^{-9}$  M could be achieved for  $\text{Cd}^{2+}$  using post-column reaction detection.<sup>17</sup>

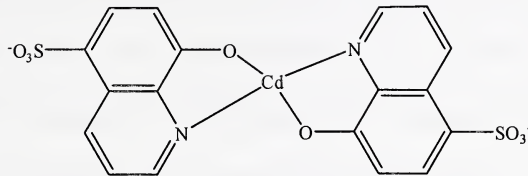
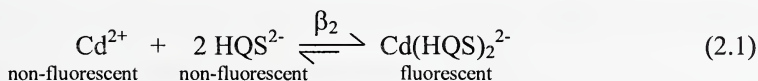


**Figure 2.2 Structure of  $\text{Cd}(\text{HQS})^{2-}$ . Adapted from reference 16.**

In addition to direct fluorescence detection of  $\text{Cd}^{2+}$ ,  $\text{Zn}^{2+}$ ,  $\text{Mg}^{2+}$ ,  $\text{Al}^{3+}$  and  $\text{La}^{3+}$ , HQS can be used for indirect detection of other species if they perturb the fluorescent metal-HQS complex. For instance, Soroka et al. and Dasgupta et al. demonstrated that  $\text{Fe}^{3+}$ ,  $\text{Cu}^{2+}$ ,  $\text{Ni}^{2+}$  and  $\text{Co}^{2+}$  could be detected based on their quenching of the fluorescent Al-HQS complex.<sup>17,18</sup> The post-column detection of thiols used in this chapter is based on the quenching of the strongly fluorescent  $\text{Cd}(\text{HQS})_2^{2-}$  complex. Competitive complexation of the cadmium by thiols forms non-fluorescent Cd-thiols complexes as observed by Wang et al. in their spectrofluorimetric studies of the complex with cysteine.<sup>24</sup> Alternatively, the weaker fluorescent  $\text{Zn}(\text{HQS})_2^{2-}$  also provides indirect detection of thiols.<sup>25</sup> However, as the detection limits for  $\text{Zn}(\text{HQS})_2^{2-}$  are comparable to that for  $\text{Cd}(\text{HQS})_2^{2-}$ , only  $\text{Cd}(\text{HQS})_2^{2-}$  is studied herein.<sup>25</sup>

After the RPLC separation, the column effluent is mixed with the post-column reagent containing  $\text{Cd}^{2+}$  and HQS (Figure 2.3). When mixed together,  $\text{Cd}^{2+}$  and HQS form 1:1 and 1:2 complexes. Stability constants for the Cd/HQS system are  $\log K_1=7.7$ ,  $\log \beta_2=14.2$  (equation 2.1), and HQS  $\text{pK}_{a2}=8.23$ .<sup>26,27</sup> As shown by Bishop, only the 1:2 complex fluoresces.<sup>28</sup>





Stability constants for complexation of  $\text{Cd}^{2+}$  with thiols such as cys ( $\log\beta_2=19.6$ )<sup>29</sup> are much greater than that for the complexation of  $\text{Cd}^{2+}$  with HQS ( $\log\beta_2=14.2$ ). Thus, when the thiols ( $\text{RS}^-$ ) eluting from the chromatographic column mix with the  $\text{Cd}(\text{HQS})_2^{2-}$ , the thiols complex the cadmium. This leaves HQS uncomplexed.



Since neither  $\text{HQS}^{2-}$  nor the new complex thiol-cadmium is fluorescent,<sup>24,30</sup> the decomposition of the  $\text{Cd}(\text{HQS})_2^{2-}$  complex results in a decrease in the fluorescence background. Presumably, mixed thiol/HQS complexes would also be formed and would be non-fluorescent. However, stability constants are available only for the 1:2 complexes. Therefore, for simplicity, equation 2.2 does not include such mixed complexes.

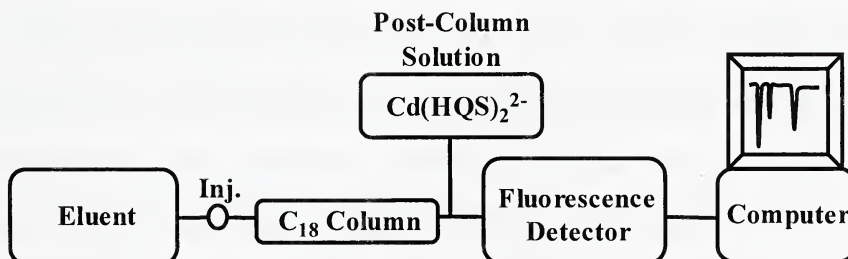


**Figure 2.3 Instrumental Scheme for indirect fluorescence post-column reaction detection.**

In this chapter, the HPLC conditions, the concentrations of HQS and Cd, the pH of the post-column solution and the flow rates are optimized. The specificity of the reaction is studied and the linearity and sensitivity of the method are determined. Artificial urine samples are also analyzed for cys, hcys and gsh.



## 2.2 Experimental

### 2.2.1 Reagents

All solutions and eluents were prepared in deionised 18 MΩ water (Nanopure Water System, Barnstead, Chicago, IL, USA). L-cysteine, L-alanine, L-methionine, L-serine,  $\gamma$ -Glu-Cys-Gly (Glutathione reduced form; gsh), 2-Amino-4-mercaptoputyric acid (DL-homocysteine), 3-[cyclohexylamino]-1-propanesulfonic acid (Caps), 3-[cyclohexylamino]-2-hydroxy-1-propanesulfonic acid (Capso), 2-[N-Morpholino]-ethanesulfonic acid (Mes) and 3-[N-Morpholino]-2-hydroxypropanesulfonic acid (Mopso) were purchased from Sigma (St. Louis, MO, USA). Disodium hydrogen orthophosphate was from BDH (Toronto, Canada). 8-Hydroxyquinoline-5-sulfonic acid monohydrate (HQS) was obtained from Janssen Chimica (Beerse, Belgium), cadmium sulfate from Matheson Coleman & Bell (Norwood, OH, USA), Tris ultra pure buffer from Schwarz/Mann Biotech (Cleveland, OH, USA), sodium hydroxide analytical reagent from BDH, trifluoroacetic acid 99% (TFA) from Aldrich (Milwaukee, WI, USA), hydrochloric acid reagent grade from Anachemia (Montreal, Canada) and HPLC grade methanol and acetonitrile were purchased from Fisher (Fair Lawn, NJ, USA). Artificial urine matrix<sup>31</sup> was made of 55 mM sodium chloride (Fisher), 67 mM potassium chloride (EM Science, Gibbstown, NJ, USA), 2.6 mM calcium sulfate dihydrate (Sigma), 3.2 mM magnesium sulfate (Caledon, Georgetown, Canada), 29.6 mM sodium sulfate (BDH), 19.8 mM sodium dihydrogen orthophosphate (BDH), 310 mM urea (BDH) and 9.8 mM creatinine (Sigma).



## 2.2.2 Apparatus

The HPLC system consisted of a Beckman System Gold Model 125 dual piston pump (Beckman, Fullerton, CA, USA) operated at 1.0 mL/min, a Rheodyne 7120 sampling valve (Rheodyne, Berkeley, CA, USA) fit with a 20  $\mu$ L loop and a fluorimetric detector (Model 470, Waters Associates, Milford, MA, USA;  $\lambda_{\text{excitation}}$ : 365 nm;  $\lambda_{\text{emission}}$ : 510 nm;<sup>24</sup> bandwidth, emission: 30 nm, excitation: 18 nm; rise time: 4 sec). Data was collected at 5 Hz with PeakNet 5.2 data software (Dionex, Sunnyvale, CA, USA) interfaced to a 100 MHz microcomputer. Initial optimization studies of the Cd-HQS post-column reagent were performed in the flow injection analysis (FIA) mode (i.e., no separation column was present). All separations were performed on a C<sub>18</sub> analytical column (150 mm long x 4.6 mm I.D., 5  $\mu$ m) (Phenomenex, Torrance, CA, USA).

The post-column reagent was delivered by a LC-600 Shimadzu solvent delivery module (Shimadzu, Kyoto, Japan) at a flow rate of 1.0 mL/min and using an Upchurch (Oak Harbor, WA, USA) U-609 500 psi backpressure device. For dynamic reserve, linearity, specificity and sensitivity studies, a constant pressure reagent delivery module<sup>32,33</sup> was used to deliver the post-column reagent at 1.0 mL/min. This system was used to minimise background noise. An Upchurch P-727 tee was used to connect the post-column solution to the column effluent. Connecting tubing was 0.005" I.D. polyether ether ketone (PEEK, Upchurch). The post-column reactor was ~5 cm of 0.005" I.D. PEEK tubing.

A Corning 445 pH-meter (Corning, NY, USA) with a Corning electrode (3 in 1 Combo P/N 476436) was used in all pH measurements. The software *Solution Equilibra*:



*principles and application (SolEq)* (1999) from Academic Software (Otley, UK) was used for the construction of theoretical speciation curves for the different equilibria.

### **2.2.3 Method**

The MeOH/TFA/Water mobile phase, the Cd/HQS/Buffer post-column as well as all thiols and urine solutions were prepared daily. Thiols solutions were stored at 4°C. Post-column solutions were prepared by first dissolving the buffer in water on a stirring plate and then by adding HQS and cadmium sulfate. The solution was sonicated for 10 to 20 minutes to dissolve the HQS. The pH was adjusted with NaOH or HCl depending on the buffer.

The HPLC eluent and Tris, Mes and Mopso buffered post-column solutions were degassed by sparging with helium. Since Caps and Capso solutions generate foams, the post-column reagent was not degassed when using these buffers. For background measurements, water was used as the post-column reactant to set the zero fluorescence on the detector.

In the post-column pH study, after equilibration and before injection, about 5 mL of the effluent was collected and  $\text{pH}_{\text{effluent}}$  was determined using the pH-meter.



## 2.3 Results and discussion

### 2.3.1 Post-column reaction

Initial studies focused on optimizing the fluorescence signal from  $\text{Cd}(\text{HQS})_2^{2-}$  with the objectives of minimizing the concentration of the probe ( $C_p$ ) while maintaining a high transfer ratio ( $T_R$ ) and dynamic reserve (DR) (Section 1.2.4.3).

#### 2.3.1.1 HQS and $\text{Cd}^{2+}$ concentration

The concentration ratio of cadmium and HQS in the post-column solution is a key factor when considering the background fluorescence intensity. As shown in Figure 2.4, for a post-column reagent containing a constant concentration of  $\text{Cd}^{2+}$  (40  $\mu\text{M}$ ), the background (fluorescence signal of  $\text{Cd}(\text{HQS})_2^{2-}$ ) increases as the concentration of HQS is increased. The signal then levels off at HQS concentrations greater than about 140  $\mu\text{M}$  (ratios of HQS/Cd higher than 3.5). This behaviour is consistent with that predicted based on literature stability constants. The solid curve in Figure 2.4 is the fraction of cadmium in the  $\text{Cd}(\text{HQS})_2^{2-}$  form calculated using *SolEq* based on literature stability constants for  $\text{Cd}^{2+}$  and HQS (Cd-HQS, Cd-Hydroxide species,  $\text{H}_2\text{O}$ )<sup>29,34</sup> and HQS  $\text{pK}_{\text{a}2}^{27}$  under the concentration conditions used in Figure 2.4. Increasing the HQS concentration increases the fluorescence signal by forming more of the fluorescent  $\text{Cd}(\text{HQS})_2^{2-}$ . At high concentrations of HQS all cadmium is in the  $\text{Cd}(\text{HQS})_2^{2-}$  form, and so no further increase in background intensity is observed. Thus, on the basis of maximizing the



dynamic reserve it would seem reasonable to use HQS concentrations of 140  $\mu\text{M}$  or greater with 40  $\mu\text{M}$   $\text{Cd}^{2+}$ .

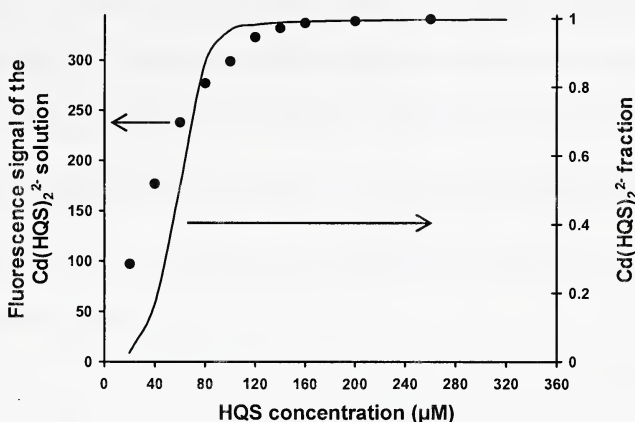


**Figure 2.4 Fluorescence of  $\text{Cd}(\text{HQS})_2^{2-}$  complex and  $\text{Cd}(\text{HQS})_2^{2-}$  fraction as a function of increasing HQS concentration.** Experimental conditions: post-column reagent is  $\text{Cd}^{2+}=40 \mu\text{M}$ , Tris 100 mM,  $\text{pH}_{\text{effluent}}=9.1$ .

However, as shown in Figure 2.5, the signal observed for cys, hcys and gsh increases as the concentration of HQS increases up to only 80  $\mu\text{M}$  HQS for hcys and gsh and to 140  $\mu\text{M}$  for cys. At higher concentrations of HQS, the signals gradually decrease. This behaviour can be understood on the basis of the fundamental equilibria governing this post-column reagent (equations 2.1 and 2.2). Firstly, at low concentrations of HQS ( $<80 \mu\text{M}$ ), only a portion of the cadmium is present as  $\text{Cd}(\text{HQS})_2^{2-}$  (curve in Figure 2.4 based on equation 2.1). Under these conditions thiols eluting from the HPLC column can complex free  $\text{Cd}^{2+}$ . Thus the thiols will not directly affect the  $\text{Cd}(\text{HQS})_2^{2-}$  fluorescence. Therefore, under these conditions the transference ratio ( $T_R$ ) is low, resulting in lower sensitivity. As the concentration of HQS increases above 80  $\mu\text{M}$ , essentially all cadmium



is present as  $\text{Cd}(\text{HQS})_2^{2-}$  (curve in Figure 2.4). Under these conditions, the thiol will disrupt the  $\text{Cd}(\text{HQS})_2^{2-}$  complex, as shown in equation 2.2, with a resultant higher transference ratio. As the concentration of HQS is increased beyond that needed for formation of  $\text{Cd}(\text{HQS})_2^{2-}$ , the excess HQS competes with the thiol for complexation of the cadmium. As a consequence, we observe a decrease in the sensitivity when HQS concentrations are higher than 100  $\mu\text{M}$  (ratio of 2.5) for hcys and gsh and higher than 180  $\mu\text{M}$  (ratio of 4.5) for cys. Such decreases in sensitivity at high HQS concentrations were also observed by Wang et al.<sup>24</sup>

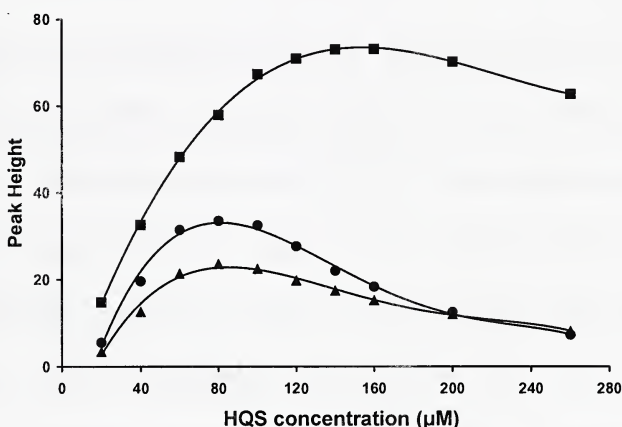


**Figure 2.5** Cys; ■, gsh; ● and hcys; ▲ response as a function of increasing HQS concentration to a constant 40  $\mu\text{M}$   $\text{Cd}^{2+}$ . The curves are simply a guide to the eye. Experimental conditions as in Figure 2.4. Analyte concentration is 200  $\mu\text{M}$ .

The conditional cumulative formation constant for  $\text{Cd}(\text{cys})_2$  ( $\log\beta'_2=19.6$ , based on  $\log\beta_2=19.6$ ,  $\text{pK}_a=8.33^{27,29}$  and  $\text{pH}=9.1$ ) is substantially higher than that of  $\text{Cd}(\text{gsh})_2$  ( $\log\beta'_2=15.2$  based on  $\log\beta_2=15.4$ ,  $\text{pK}_a=8.66^{26,27}$  and  $\text{pH}=9.1$ )<sup>29</sup>. Cys can then more effectively compete with HQS for cadmium complexation (equation 2.2) than can gsh.



Thus, the optimum fluorescence response occurs at a higher concentration of HQS for cys than gsh. Unfortunately, no literature formation constants are available for Cd-hcys.

### 2.3.1.2 pH of the post-column solution

The pH of the post-column solution is also an important variable which must be optimized. The fluorescence signal for the  $\text{Cd}(\text{HQS})_2^{2-}$  complex is pH dependent with maximum intensity at pH 7 according to Soroka et al.<sup>17</sup> and from pH 8-9 based on Wang et al.<sup>24</sup>

Speciation curves are generated using the *SolEq* software for the cadmium-HQS system using literature stability constants (see Section 2.3.1.1). The curve in Figure 2.6 shows the fraction of cadmium present as  $\text{Cd}(\text{HQS})_2^{2-}$  in a solution containing 40  $\mu\text{M}$  cadmium and 100  $\mu\text{M}$  HQS over a variety of pH. Based on these calculations the background  $\text{Cd}(\text{HQS})_2^{2-}$  would be expected to exhibit a broad optimum from pH 8-12. Below pH 8 the HQS is incompletely ionized ( $\text{pK}_{\text{a}2} = 8.23$ ). Thus, the conditional formation constant decreases dramatically as the pH decreases. At high pH, formation of cadmium-hydroxide species competes with the HQS for complexation of cadmium.<sup>35</sup> Under these same solution conditions, the intensity of the  $\text{Cd}(\text{HQS})_2^{2-}$  fluorescence (background) is experimentally observed (data points in Figure 2.6) to increase with pH to a maximum signal between pH 9-11 and then decreased at higher pH. This behaviour is in agreement with that expected (curve in Figure 2.6).



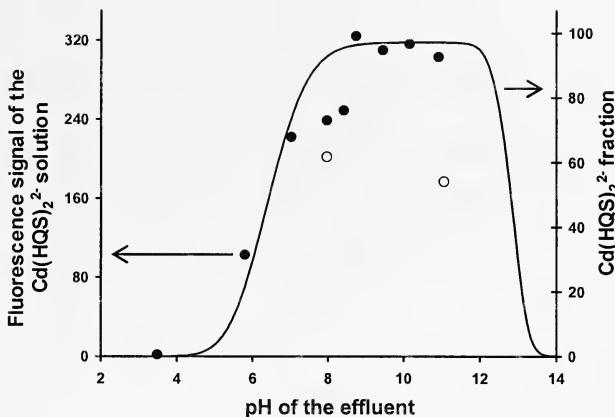


**Figure 2.6 Fluorescence of the  $\text{Cd}(\text{HQS})_2^{2-}$  complex and  $\text{Cd}(\text{HQS})_2^{2-}$  fraction as a function of pH of post-column reagent.** Experimental conditions: analyte concentration is 200  $\mu\text{M}$ , post-column solution is 100  $\mu\text{M}$  HQS, 40  $\mu\text{M}$   $\text{Cd}^{2+}$  (ratio HQS/Cd=2.5), buffered in ●  $\text{pH}_{\text{effluent}}=3.5=100$  mM Tris,  $\text{pH}_{\text{effluent}}=5.8=100$  mM Mes,  $\text{pH}_{\text{effluent}}=7.0=100$  mM Mopso,  $\text{pH}_{\text{effluent}}=7.8-8.5=100$  mM Tris,  $\text{pH}_{\text{effluent}}=8.7-9.8=200$  mM Caps,  $\text{pH}_{\text{effluent}}=10.0-11.0=100$  mM Caps or buffered in ○  $\text{pH}_{\text{effluent}}=7.9$  and  $11.1=100$  mM Phosphate.

The effect of pH on the indirect response observed for thiol analytes is shown in Figure 2.7. For all of the analytes, optimal signal is observed at about pH 10.3. This is consistent with the results above. To achieve optimal sensitivity, the formation of  $\text{Cd}(\text{HQS})_2^{2-}$  has to be maximized. For this, the pH has to be higher than 8 (Figure 2.6). In addition, the thiols have to be ionized. Thus pH has to be higher than their S-H group  $\text{pK}_a$ . In this case, the highest  $\text{pK}_a$  is 8.87 (hcys). Therefore, the most favourable pH of the post-column solution should be above 8.87. Figure 2.7 illustrates this very well.

Also, above pH 10.5 the thiol response decreases. This too is consistent with the studies above (Figure 2.6) and results from the formation of cadmium-hydroxides species limiting the amount of  $\text{Cd}(\text{HQS})_2^{2-}$  in solution, and hence the sensitivity.



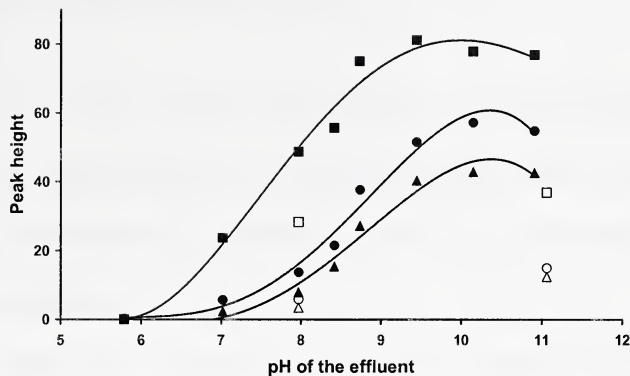


**Figure 2.7 Cys; ■ □, gsh; ● ○ and hcys; ▲ △ response as a function of pH of post-column reactant.** The curves are simply a guide to the eye. Experimental conditions as in Figure 2.6.

### 2.3.1.3 Buffers

To obtain the wide range of pH in the studies in Section 2.3.1.2, a number of buffers are used in the post-column solutions. Special care is taken to choose non-complexing buffers<sup>18</sup> such as Tris, Mes, Mopso, Caps and Capso. This is done to ensure that the formation of  $\text{Cd}(\text{HQS})_2^{2-}$  is not compromised by competitive complexation of the  $\text{Cd}^{2+}$  by the buffer anion. To illustrate the potential detrimental effects of  $\text{Cd}^{2+}$  complexation by the buffer, data for a 100 mM phosphate buffer is included in Figures 2.6 and 2.7 (stability constant for phosphate and cadmium is  $\log \beta_2 = 5.1$ )<sup>34</sup>. The use of a phosphate buffer considerably lowers both the  $\text{Cd}(\text{HQS})_2^{2-}$  background (open symbols in Figure 2.6), and as a consequence the sensitivity (open symbols, Figure 2.7).



#### 2.3.1.4 Dynamic Reserve (DR)

Equation 1.21 shows that the dynamic reserve (background/noise) is inversely proportional to the limit of detection. To maximize dynamic reserve in order to improve detection limits, the background of the fluorescent probe has to be as high as possible and the noise in the baseline low.

Firstly, instrumental conditions are adjusted to minimize the baseline noise. Using a dual piston HPLC pump (LC-600 Shimadzu) along with a 500 psi backpressure device, a periodic oscillation of about 1 mV is evident in the background of an HQS/Cd 100/40  $\mu$ M post-column reagent. Addition of pulse dampers yield essentially no improvement. The use of a constant pressure delivery system to deliver the post-column solution reduces the noise to 0.2 mV for the same reagent solution. By reducing the overall noise, dynamic reserves are improved by factors of 5 to 6, which has a direct impact on decreasing detection limits.

The concentrations of HQS and cadmium in the post-column reactant are varied to determine the optimum conditions as defined as maximum ratio background to noise (maximum DR). The HQS/Cd ratio in the post-column solution is kept constant at 2.5 at a pH of 10.0 with Caps at 100 mM. The responses for cys, hcys and gsh are monitored at concentrations ( $\mu$ M) of 50/20, 100/40 and 200/80 for HQS and Cd<sup>2+</sup> respectively. As the concentration of Cd-HQS increases, the background increases by an overall factor of 4. However, simultaneously the noise increases by a factor of 3. Thus the overall dynamic reserve increases slightly: 900, 1400 and 1300 for the 50/20, 100/40 and 200/80 solutions. About a 21% sensitivity is thus achieved by varying the probe concentration



(Cd-HQS concentration). In all further studies, the concentration of HQS and Cd are at 100  $\mu\text{M}$  and 40  $\mu\text{M}$  respectively.

### 2.3.1.5 Reaction rate and flow rates

The reaction between  $\text{Cd}(\text{HQS})_2^{2-}$  and the thiols (equation 2.2) is very fast.<sup>18</sup> The sensitivity observed using a 5 cm segment of straight 0.005" I.D. PEEK is comparable to that for a 1000 cm 0.018" I.D. knitted reaction coil (*RXN 1000 Coil*, P/N 030805 Waters Associates, Milford, MA, USA). Further, significant band broadening is observed with the longer reaction coil. Thus 5 cm of tubing is used as the reaction coil in all studies reported herein.

The flow rate of the post-column solution is varied from 0.5 to 1.5 mL/min while keeping the eluent flow constant at 1.0 mL/min. The best resolution between cys and hcys is obtained at a post-column flow rate between 0.9 and 1.1 mL/min. Therefore, a flow rate of 1 mL/min is selected for the post-column solution.

### 2.3.1.6 Specificity of the reaction

Stability constants for  $\text{Cd}^{2+}$  with carboxylate, amine and thioether ( $\text{RSCH}_3$ ) groups are small ( $\log \beta_2 < 5.5$ )<sup>26,34,36</sup> relative to the complexation of  $\text{Cd}^{2+}$  by thiols (e.g.,  $\log \beta_2 = 19.6$  for cysteine). Thus it is expected that Cd-HQS should show good specificity for thiols relative to other biomolecules. To confirm this, high concentration solutions (5 mM) of serine, alanine and methionine are injected. The post-column



solution is HQS/Cd at 100/40  $\mu\text{M}$  in a 100 mM Caps buffer with  $\text{pH}_{\text{effluent}}=10.1$ . When comparing the sensitivity with an almost 27 times lower concentration of cys, hcys and gsh (188  $\mu\text{M}$ ), response factors (signal/concentration) of serine, alanine and methionine are found to be on average about 300 times lower than those of the thiols (Table 2.1). This demonstrates that the reaction with  $\text{Cd}(\text{HQS})_2^{2-}$  is governed by  $\text{RS}^-$  groups (equation 2.2).

**Table 2.1 Response Factors (signal/concentration) for cys, hcys, gsh, serine, alanine and methionine.**

Compound	Concentration ( $\mu\text{M}$ )	Response Factor ( $\text{mV}/\mu\text{M}$ )
Cysteine	188	414 000
Homocysteine	188	207 000
Glutathione	188	313 000
Serine	5 000	1 670
Alanine	5 000	1 300
Methionine	5 000	604

### 2.3.2 Separation conditions, detection limits and determination of thiols in synthetic urine

The separation mode in RPLC with TFA is a concerted mechanism involving both ionic and hydrophobic interactions.<sup>37-39</sup> TFA acts as a small ion-pairing agent by adsorbing onto the stationary phase and interacting with positively charged analytes. Thiols are therefore retained on the stationary phase through both ionic and hydrophobic interactions. This system is tuneable by adjusting the concentration of organic modifier



(i.e., interaction of the ion-pair with  $C_{18}$ ), the concentration of TFA (i.e., amount of TFA for ionic interaction with analytes) and the pH of the mobile phase (i.e., ionization of the analytes). Manna et al.<sup>15</sup> separated gsh and gssg (oxidized form of gsh) using 0.1% TFA (0.01 M) in a water-acetonitrile (98:2) mobile phase. However, under these conditions cys and hcys are too weakly retained ( $k' < 1$ ) to achieve separation. Decreasing the organic modifier concentration results in greater retention of all analytes, and  $\leq 1\%$  acetonitrile or methanol gives adequate separations (Figure 2.8). An eluent of 0.5% MeOH v/v with 0.01 M TFA is used in all further studies as it provides a baseline resolution between cys and hcys ( $R_S = 1.7$ ). A mobile phase containing 0.5% acetonitrile gives similar retention times as methanol 0.5% but with an inferior cys-hcys resolution ( $R_S = 1.5$ ).

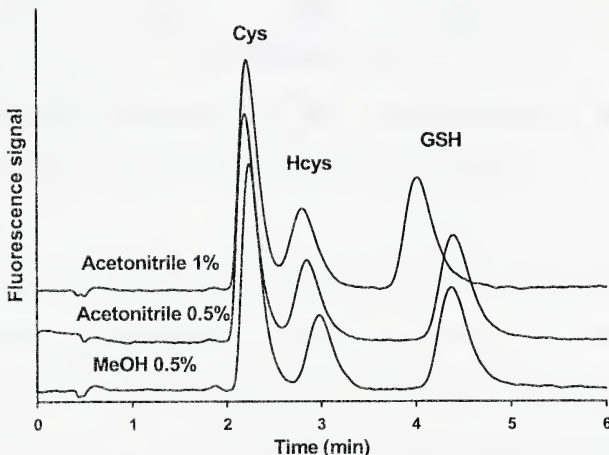


**Figure 2.8 Cys, hcys and gsh chromatograms under different separation conditions.** Experimental conditions: mobile phase: TFA 0.01M/ACN 1%, TFA 0.01M/ACN 0.5% and TFA 0.01M/MeOH 0.5%, post-column is HQS/Cd<sup>2+</sup> 80/40  $\mu$ M, Tris 100 mM, pH<sub>solution</sub> 8.5, analyte concentration is 200  $\mu$ M.



Calibration curves for cys and hcys are linear ( $R^2=0.9993$  and  $0.9987$ ) up to 370  $\mu\text{M}$  with intercepts equal to zero at the 95% confidence limit (Figure 2.9). Calibrations for gsh however show a small negative deviation from linearity. The gsh response is well fit by a quadratic expression ( $R^2=0.9994$ ) up to 370  $\mu\text{M}$  with an intercept equal to zero at the 95% confidence limit.

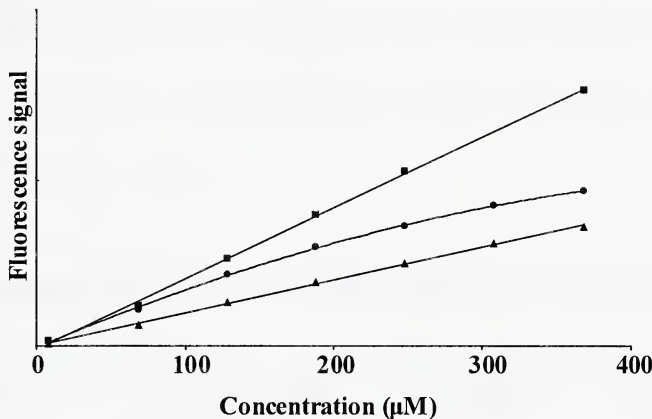


**Figure 2.9 Calibration curves for cys; ■, gsh; ● and hcys; ▲.** Experimental conditions as in Figure 2.8 with TFA 0.01M/MeOH 0.5% eluent.

Table 2.2 shows the detection limits we determined using the detection limit evaluation procedure recommended by the US Environmental Protection Agency (EPA).<sup>40</sup> This method gives the minimum concentration of an analyte that can be reported with 99% confidence to be greater than the noise (equivalent to the  $3\sigma$  method). Analytes with a concentration of 4-10 times the estimated limit of detection are injected 7 to 10 times in the system. The standard deviation of the peak area between the runs is multiplied by the Student's  $t$  (at the 95% confidence level) to obtain the limit of detection. The detection limits range from 0.1 to 0.2  $\mu\text{M}$  for cys, hcys and gsh. This is



an improvement in comparison with Wang's et al. indirect fluorescence method where the cysteine detection limit is 0.4  $\mu\text{M}$  with a narrow dynamic range of 0-18  $\mu\text{M}$ .<sup>24</sup> In contrast, Tang et al. achieve 23 nM and 35 nM detection limits for gsh and cys, respectively using a pre-column derivatisation method with SBD-F.<sup>11</sup> However, the derivatisation procedure is complex and time consuming (>5 steps over 1.5 hour including incubation at high temperature). Another derivatisation method using dansyl chloride give detection limits of 1 pM (signal-to-noise ratio 2) for gsh and gssg.<sup>41</sup> Pre-column derivatisation (over 2 hours including incubation in the dark) and a 30 minute gradient separation are necessary.

**Table 2.2 Detection limits, run to run %RSD and dynamic range for cys, hcys and gsh.**

Thiol	Detection limit	% RSD	Dynamic Range
Cysteine	0.1 $\mu\text{M}$ , 0.02 ppm	2.7	0.1-430 $\mu\text{M}$
Homocysteine	0.1 $\mu\text{M}$ , 0.02 ppm	5.5	0.1-370 $\mu\text{M}$
Glutathione	0.2 $\mu\text{M}$ , 0.05 ppm	3.4	0.2-430 $\mu\text{M}^a$

<sup>a</sup> Quadratic fit

b. Experimental conditions: as in Figure 2.8 with TFA 0.01M/MeOH 0.5% eluent.

Calibration curves are equivalent whether standards are prepared in water or synthetic urine. Synthetic urine samples are spiked with 200  $\mu\text{M}$  of cys, hcys and gsh. Recoveries vary between 87% and 120%. Figure 2.9 shows a chromatogram of cys, hcys and gsh at 200  $\mu\text{M}$  in synthetic urine. The large negative peak at the dead volume is due to the urine matrix. The cys peak is expected to show poor recovery due to being so close



to the negative peak but actually recoveries are near quantitative (95.6% to 99.7%). Similar quantitative recoveries are observed by Wang et al.<sup>25</sup> for cys in protein hydrosylate and gsh in human blood serum using Zn-HQS.

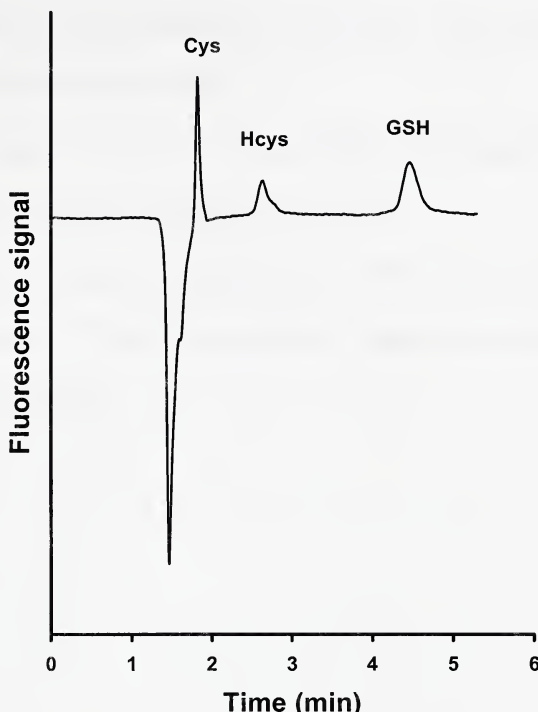


**Figure 2.10 Separation of cys, hcys and gsh (200  $\mu$ M) in urine matrix.** Experimental conditions as in Figure 2.8, mobile phase: TFA 0.01 M, methanol 0.2%. Analyte concentration is 200  $\mu$ M. Fluorescence detector rise time at 0.5 sec.

## 2.4 Conclusions

Cys, hcys and gsh are separated by reverse phase HPLC in their native form and simply detected by the quenching of a fluorescent  $\text{Cd}(\text{HQS}_2)^{2-}$  complex added as a post-column reactant. No derivatization or sample preparations of the analytes prior to



injection are needed. Detection limits as low as 0.1  $\mu\text{M}$  are achieved and a broad dynamic range of 0.1-370  $\mu\text{M}$  is obtained in the calibrations. This dynamic range is suited for the analysis of urine or blood samples (normal and abnormal) in which a typical concentration of thiols ranges from 1 to 200  $\mu\text{M}$ .<sup>42</sup> The method is applied to the analysis of spiked artificial urine samples.

In the next chapter, I will show how this method can be applied to the analysis of both thiols (RSH) and disulfides (RSSR) simultaneously.

Finally, the low retention of the thiols on the RPLC column made the separation challenging. In Chapter 6, I will discuss possible strategies to increase the retention of hydrophilic analytes in RPLC.



## 2.5 References

- (1) Pastore, A.; Federici, G.; Bertini, E.; Piemonte, F. *Clin. Chim. Acta* **2003**, *333*, 19-39.
- (2) Jacobsen, D. W. *Arterioscler., Thromb., Vasc. Biol.* **2000**, *20*, 1182-1184.
- (3) Carmel, R.; Jacobsen, D. W., Eds. *Homocysteine in health and disease*; Cambridge University Press: Cambridge, 2001.
- (4) Stamler, J. S.; Slivka, A. *Nutr. Rev.* **1996**, *54*, 1-30.
- (5) Locigno, R.; Castronovo, V. *Int. J. Oncol.* **2001**, *19*, 221-236.
- (6) Lock, J.; Davis, J. *TrAC, Trends Anal. Chem.* **2002**, *21*, 807-815.
- (7) Ducros, V.; Demuth, K.; Sauvant, M.-P.; Quillard, M.; Caussé, E.; Candito, M.; Read, M.-H.; Drai, J.; Garcia, I.; Gerhardt, M.-F. *J. Chromatogr., B: Biomed. Appl.* **2002**, *781*, 207-226.
- (8) Amores-Sanchez, M. I.; Medina, M. A. *Clin. Chem. Lab Med* **2000**, *38*, 199-204.
- (9) Shimada, K.; Mitamura, K. *J. Chromatogr., B: Biomed. Appl.* **1994**, *659*, 227-241.
- (10) Nekrassova, O.; Lawrence, N. S.; Compton, R. G. *Talanta* **2003**, *60*, 1085-1095.
- (11) Tang, D.; Wen, L.-S.; Santschi, P. H. *Anal. Chim. Acta* **2000**, *408*, 299-307.
- (12) Fermo, I.; Arcelloni, C.; Mazzola, G.; D'Angelo, A.; Paroni, R. *J. Chromatogr., B: Biomed. Appl.* **1998**, *719*, 31-36.
- (13) Ivanov, A. R.; Nazimov, I. V.; Baratova, L.; Lobazov, A. P.; Popkovich, G. B. *J. Chromatogr., A* **2001**, *913*, 315-318.



(14) Accinni, R.; Campolo, J.; Parolini, M.; Maria, R. D.; Caruso, R.; Maiorana, A.; Galluzzo, C.; Bartesaghi, S.; Melotti, D.; Parodi, O. *J. Chromatogr., B: Biomed. Appl.* **2003**, *785*, 219-226.

(15) Manna, L.; Valvo, L.; Betto, P. *J. Chromatogr., A* **1999**, *846*, 59-64.

(16) Phillips, J. P. *Chemical Reviews* **1956**, *56*, 271-297.

(17) Soroka, K.; Vithanage, R. S.; Phillips, D. A.; Walker, B.; Dasgupta, P. K. *Anal. Chem.* **1987**, *59*, 629.

(18) Dasgupta, P. K.; Soroka, K.; Vithanage, R. S. *J. Liq. Chromatogr.* **1987**, *10*, 3287-3319.

(19) Jones, P.; Ebdon, L.; Williams, T. *Analyst* **1988**, *113*, 641.

(20) Lucy, C. A.; Ye, L. *Anal. Chem.* **1995**, *67*, 79.

(21) Williams, T.; Barnett, N. W. *Anal. Chim. Acta* **1992**, *259*, 19.

(22) Paull, B.; Twohill, E.; Bashir, W. *J. Chromatogr., A* **2000**, *877*, 123.

(23) Vos, C. J.; Melanson, J. E.; Lucy, C. A. *Anal. Sci.* **2001**, *17*, 225.

(24) Wang, H.; Wang, W.-S.; Zhang, H.-S. *Talanta* **2001**, *53*, 1015-1019.

(25) Wang, H.; Wang, W.-S.; Zhang, H.-S. *Spectrochim. Acta, Part A* **2001**, *57*, 2403-2407.

(26) Smith, R. M.; Martell, A. E. *Critical stability constants*; Plenum Press: New York, 1975.

(27) Budavari, S.; O'Neil, M. J.; Smith, A.; Heckelman, P. E., Eds. *The Merck Index*; Merck & Co. Inc.: Rahway, NJ, 1989.

(28) Bishop, J. A. *Anal. Chim. Acta* **1963**, *29*, 172.



(29) Smith, R. M.; Martell, A. E. *Critical stability constants*; Plenum Press: New York, 1975.

(30) Bardez, E.; Devol, I.; Larrey, B.; Valeur, B. *J. Phys. Chem. B* **1997**, *101*, 7786-7793.

(31) Wang, J.; Hansen, E. H.; Gammelgaard, B. *Talanta* **2001**, *55*, 117-126.

(32) Stewart, K. K.; Beecher, G. R.; Hare, P. E. *Anal. Biochem.* **1976**, *70*, 167-173.

(33) Fossey, L.; Cantwell, F. F. *Anal. Chem.* **1982**, *54*, 1693-1697.

(34) Power, K. J.; Academic Software: Otley, 1999.

(35) Porter, N.; Hart, B. T.; Morrison, R.; Hamilton, I. C. *Anal. Chim. Acta* **1995**, *308*, 313.

(36) Smith, R. M.; Martell, A. E. *Critical stability constants, Vol. 3*; Plenum Press: New York, 1975.

(37) Patthy, M. *J. Chromatogr., A* **1994**, *660*, 17-23.

(38) Guo, D.; Mant, C. T.; Hodges, R. S. *J. Chromatogr.* **1987**, *386*, 205-222.

(39) Inchauspe, G.; Delrieu, P.; Dupin, P.; Laurent, M.; Samain, D. *J. Chromatogr.* **1987**, *404*, 53-66.

(40) Grant, C. L.; Hewitt, A. D.; Jenkins, T. F. *Am. Lab. (Shelton, Conn.)* **1991**, *23*, 15-32.

(41) Martin, J.; White, I. N. H. *J. Chromatogr.* **1991**, *568*, 219-225.

(42) Pastore, A.; Massoud, R.; Moti, C.; Russo, A. L.; Fucci, G.; Cortese, C.; Federici, G. *Clin. Chem.* **1998**, *44*, 825-832.



## CHAPTER THREE. HPLC simultaneous analysis of thiols and disulfides: on-line reduction and indirect fluorescence detection without derivatisation<sup>a</sup>

### 3.1 Introduction

In this chapter, the method for thiols described in Chapter 2 is extended to the analysis of both thiols and disulfides. Disulfides, which consist of two thiol molecules joined by a sulfur-sulfur bond (examples include cyss, hcyss and gssg in Figure 3.1), are neither naturally fluorescent nor UV active. Therefore, as for thiols, their determination also requires chemical modification. Lock and Davis have recently published a review on disulfide analysis.<sup>1</sup> Essentially all procedures for disulfides first reduce the sulfur-sulfur link and then derivatize the resultant thiols. The reduction is usually performed using strong reductants (e.g., sodium borohydride), reduced thiols (dithiothreitol, 2-mercaptoethanol) or phosphine derivatives (tris(2-carboxyethyl)phosphine (TCEP), tri-*n*-butylphosphine (TBP), triphenylphosphine). Phosphine derivatives present many advantages over strong reductants and reduced thiols: they do not interfere with thiol-reactive labels and therefore do not need to be removed after reaction; they do not produce gas while reacting; and they are stable for longer periods of time and over a wider pH range (1.5-8.5).<sup>2,3</sup> Among phosphines, TCEP has the advantages of being water soluble, odourless, non-volatile, non-flammable, non-corrosive, and not sensitive to air or humidity.<sup>4</sup> Thus, TCEP has been extensively utilised, and will be used for on-line reduction of the disulfides herein.

---

<sup>a</sup> A version of this chapter has been published as Pelletier, S; Lucy C.A. *Analyst* 2004, 129, 710-713.



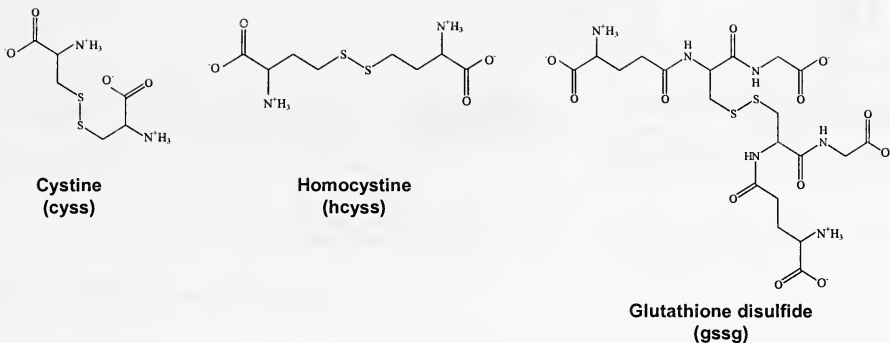


**Figure 3.1 Chemical structures of analytes.**

Often, it is necessary to determine the independent concentrations of disulfides and thiols, such as in the gssg /gsh assessment of health.<sup>5</sup> However, such determinations must normally be done sequentially. For example, for the gssg-gsh ratios, direct determination yields a concentration of only the thiol gsh. Reduction of the sample prior to a second analysis then yields a signal corresponding to the combined concentrations of gssg and gsh. The gssg concentration is determined as the difference between these determinations. Only a few reports of simultaneous detection of thiols and disulfides using mass spectrometry<sup>6,7</sup> or electrochemical detection<sup>8-10</sup> have been reported.

This chapter presents a simple method to simultaneously detect underivatized thiols and disulfides by indirect fluorescence. As in Chapter 2, thiols and disulfides are separated in their native form and detected using a post-column reagent based on the highly fluorescent Cd(HQS)<sub>2</sub><sup>2-</sup> complex. Disulfides do not complex cadmium and as such do not affect the Cd(HQS)<sub>2</sub><sup>2-</sup> fluorescence. Thus, to use this post-column reaction system for disulfides, the TCEP reagent is added on-line immediately after the separation and before addition of the Cd(HQS)<sub>2</sub><sup>2-</sup> solution (Figure 3.2).



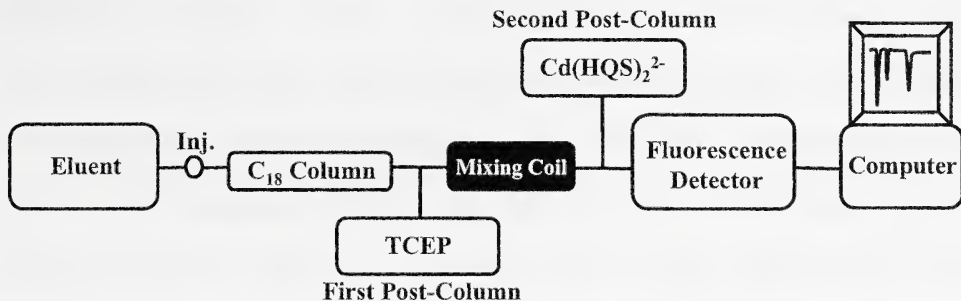
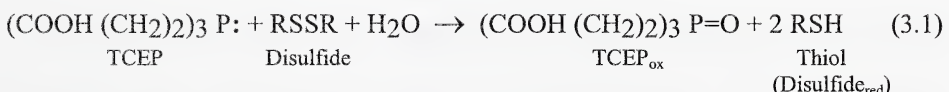


**Figure 3.2 Instrumental scheme.**

This on-line reduction of disulfides to their corresponding thiol allows for simultaneous detection of thiols and disulfides in the same determination. For the reasons mentioned above, TCEP is used as the reductant:



In this work, the separation conditions, TCEP reduction and  $\text{Cd}(\text{HQS})_2^{2-}$  indirect fluorescence detection are all optimized. The linearity and sensitivity of the method are determined

### 3.2 Experimental

### 3.2.1 Reagents

All solutions and eluents were prepared in deionised 18 MΩ water (Nanopure Water System, Barnstead, Chicago, IL, USA). L-cysteine (cys), L-cystine (cyss), DL-homocysteine (hcys), DL-homocystine (hcyss), L-glutathione (gsh, γ-Glu-Cys-Gly), L-



glutathione disulfide (gssg, ( $\gamma$ -Glu-Cys-Gly)<sub>2</sub>), tris(carboxyethyl)phosphine hydrochloride salt (TCEP) and tris 3-[cyclohexylamino]-2-hydroxy-1-propanesulfonic acid (Capso) were purchased from Sigma (St. Louis, MO, USA). 8-Hydroxyquinoline-5-sulfonic acid monohydrate (HQS) was obtained from Janssen Chimica (Beerse, Belgium), cadmium sulfate from Matheson Coleman & Bell (Norwood, OH, USA), sodium hydroxide 10M certified solution from Fisher (Fair Lawn, NJ, USA), trifluoroacetic acid 99% (TFA) from Aldrich (Milwaukee, WI, USA), and HPLC grade methanol was purchased from Fisher.

### 3.2.2 Apparatus

The eluent pump, fluorimeter, sample loop and data handling were as in Section 2.2.2 (except for data collection which was 10 Hz in this chapter). Initial optimization studies of the TCEP post-column reagent were performed in the flow injection analysis (FIA) mode (i.e., no separation column was present) or with a C<sub>18</sub> analytical column (150 mm long X 4.6 mm I.D., 5  $\mu$ m) (Phenomenex, Torrance, CA, USA). All other separations were performed on a C<sub>18</sub> Zorbax SB-Aq analytical column (150 mm long X 4.6 mm I.D., 5  $\mu$ m) (Agilent Technologies, Palo Alto, CA, USA).

The first post-column reagent (TCEP) in Figure 3.2 was pumped using a Waters 625 LC system and mixed with the effluent in an Upchurch P-727 tee (Oak Harbor, WA, USA). The TCEP plus effluent then passed through a mixing coil (knitted PTFA tubing, 0.018" I.D., 1000 cm long) (*RXN 1000 Coil*, P/N 030805, Waters). After the mixing coil, a constant pressure reagent delivery module<sup>11,12</sup> was used to deliver the second post-



column reagent ( $\text{Cd}(\text{HQS}_2)^{2-}$ ) at 1.0 mL/min through a second Upchurch P-727 tee. The second tee was connected to the detector via a 5 cm segment of 0.005" I.D. PEEK tubing (Upchurch). The total length of tubing between the injection valve and the detector was about 10 cm (excluding mixing coil).

A Corning 445 pH-meter (Corning, NY, USA) with a Corning electrode (3 in 1 Combo P/N 476436) was used for solution pH measurements. To measure  $\text{pH}_{\text{eff}}$  (i.e. pH of the solution coming out of the detector) and  $\text{pH}_{\text{coil}}$  (i.e. pH of the solution coming out of the mixing coil), pH indicator strips (EM Science, Gibbstown, NJ, USA) with resolution from 0.2-0.5 pH units were used.

### 3.2.3 Method

#### 3.2.3.1 Solution preparation

All solutions were prepared daily. The eluent was made by adding the proper amount of TFA and MeOH to water, adjusting the pH with NaOH and diluting to volume with water. The first post-column solution (TCEP) was prepared by dissolving the appropriate amount of solid in water, adjusting the pH with NaOH and diluting with water to the desired volume. The second post-column solution ( $\text{Cd}(\text{HQS}_2)^{2-}$ ) was prepared with Capso as in Section 2.2.3. The pH was adjusted with NaOH. Samples containing thiols (cys, hcys, gsh) and disulfides (cyss, hcyss, gssg) were dissolved in the eluent, sonicated 10-15 minutes and diluted with the eluent. The eluent and the first post-column solution (TCEP) were degassed by sparging with helium.



### 3.2.3.2 Optimization of post-column conditions

Factorial experiments<sup>13,14</sup> (analysis of multiple variables) were used to optimize the post-column conditions. Three concentrations (32, 64 and 80 mM), two pH values (5, 8) for the TCEP solution and three cadmium concentrations (20, 40 and 64  $\mu$ M) for the  $\text{Cd}(\text{HQS})_2^{2-}$  post-column solution were used. Optimization of the post-column reagents was performed using flow injection analysis.

Mixing of eluent and the first post-column reagent (TCEP) resulted in slight changes in the pH within the reaction coil. The pH of the effluent from the TCEP reaction coil was measured using pH strips and was 5.0 when a TCEP solution of pH 5.0 was used and 7.5 when the pH 8.0 solution was used. The use of 300 mM (pH 9.6) Capso in the second post column reagent resulted in a constant pH for the effluent (9.5) regardless of the TCEP solution. The eluent and the  $\text{Cd}(\text{HQS})_2^{2-}$  flow rates were 1.0 mL/min, the TCEP was 0.5 mL/min and the HQS concentration 100  $\mu$ M unless otherwise stated.

### 3.2.3.3 Calculations

As shown in equation 3.1, reducing one mole of disulfide (SS) produces two moles of thiol (SH). Based on the 2:1 stoichiometry of the disulfide to the thiol, complete disulfide reduction would result in a signal double that obtained from an equimolar concentration of thiol (SS/SH=2). For a given thiol/disulfide pair (cys/cyss for example), the percent of disulfide reduction was obtained by comparing the experimental peak area



SS/SH ratios with the calculated SS/SH ratio, the latter being equal to twice the disulfide concentration divided by the thiol concentration.

### 3.3 Results and discussion

#### 3.3.1 Optimization of the reduction reaction

The pH of TCEP, its concentration and the concentration of cadmium in the post-column solution were optimized in a series of FIA experiments as described in Section 3.2.3.2. When increasing the pH of the TCEP solution from 5 to 8, sensitivity was, on average, 60% higher for the disulfides. This improved sensitivity at pH 8 is the result of more complete reduction - increasing from ~ 50% at pH 5 to ~ 90% at pH 8. This is consistent with the work of Han and Han where increasing the pH of a TCEP solution from 6 to 8 doubled the reduction of the disulfide 5,5'-dithiobis(2-nitrobenzoic acid (DTNB).<sup>2</sup> Increasing the TCEP concentration from 32 to 80 mM did not significantly affect either the thiol or disulfide sensitivity (<10% change). Finally, the sensitivity of thiols and disulfides increased by 40% when the cadmium concentration in the post-column solutions was increased from 20  $\mu$ M to 40  $\mu$ M. However, a 20% loss in sensitivity was observed when the cadmium concentration was further increased to 64  $\mu$ M. This is consistent with the observations in Section 2.3.1.1. A TCEP concentration of 32 mM at pH 8 and 40  $\mu$ M cadmium were used in all further experiments.

The flow rate of the eluent and the TCEP solution also affect both the disulfide reduction and the general sensitivity by regulating the reaction time and the reagent-to-analyte concentration ratio. Flow rates were optimized in the FIA mode. At a TCEP



flow rate of 0.3 mL/min, the reduction of disulfides was low (10-30%) due to the low concentration of TCEP in the effluent. From 0.5 to 1.5 mL/min TCEP, the disulfide reduction rapidly increased to 70-100%. However, at flow rates higher than 0.5 mL/min, the sensitivity linearly decreased (at 0.8 mL/min 20% decrease, 1.5 mL/min 88% decrease) due to the combined effects of effluent pH and detector response. At these high flow rates, the large amount of TCEP solution (pH 8) overwhelmed the buffering capacity of the Cd(HQS)<sub>2</sub><sup>2-</sup> solution, causing the pH of the effluent to fall below the optimal value of pH 8.5 (Section 2.3.1.2). This could have been avoided by increasing the amount of Capso buffer in the Cd(HQS)<sub>2</sub><sup>2-</sup> solution, but was judged unnecessary since the peak area would still show a reciprocal relationship with flow rate through the detector, reducing sensitivity.<sup>15</sup> As well, high TCEP flow rates degraded the resolution between cys and cyss in the separation. A TCEP flow rate of 0.5 mL/min was the best compromise for optimal sensitivity and disulfide reduction, and was used in further experiments.

Varying the eluent flow rate from 0.5-1.4 mL/min did not significantly (<10%) change the disulfide reduction. However, increasing the eluent flow did cause a 53% average overall reduction in sensitivity. A compromise eluent flow rate of 0.8 mL/min was used. This resulted in a 17% decrease in sensitivity relative to 0.5 mL/min but reduced the separation time from 35 to 20 minutes.

In preliminary experiments a 17 cm long x 0.005" I.D. PEEK tubing was used as the reaction coil (i.e., in place of the mixing coil in Figure 3.2). This provided a reaction time of ~ 0.1 s for the TCEP reduction. Under these conditions (eluent 1.0 mL/min, TCEP 0.5 mL/min, cyss and cys injected independently) the level of disulfides reduction



was low: 22% for cyss; 51% for hcyss; and 13% for gssg. Installing the mixing coil described in Section 3.2.2 increased the reduction time to ~38 s, and increased the disulfide reduction to 45% for cyss; 76% for hcyss; and 19% for gssg. This is consistent with Han and Han's experiments where increasing the reaction time from 1 to 40 s increased the disulfide reduction from 8 to 100% in the presence of TCEP (pH 8)<sup>2</sup>. Longer reaction times were not explored as over 80% reduction was obtained after full optimization as described below. Upon addition of the mixing coil, extra-column band broadening (Section 1.2.2) was observed since values of N (number of plates) increased from 1500 to 4500 from the least retained compound (cyss) to the more retained (gssg). However, the resolution between the less retained analytes remained satisfactory (Section 3.3.2).

Finally, separations in triplicate of all six analytes with mixing coil and under optimized conditions (eluent 0.8 mL/min; TCEP 0.5 mL/min 32 mM pH 8; Cd(HQS)<sub>2</sub><sup>2-</sup> 1.0 mL/min 40  $\mu$ M Cd 100  $\mu$ M HQS 200 mM CAPSO pH 9.7) resulted in disulfide reduction efficiency of 98% for cyss/cys, 82% for gssg/gsh and 208% for hcyss/hcys.

The unexpectedly high signal for hcyss relative to hcys was investigated. The injection of hcys alone (freshly opened new bottle) resulted into two peaks: one, which corresponded to hcys (4.0 min) and a second about 70% smaller corresponding to hcyss (8.5 min). This was possibly caused by the partial oxidation of hcys to hcyss in the acidic sample<sup>16</sup> (dissolved and diluted in eluent) and explained the high percent reduction since the ratio SS/SH increased due to the underestimate of hcys and overestimate of hcyss. This occurrence can be minimized by keeping the solutions at 0 °C or by blocking the thiol group with N-ethylmaleimide (NEM).<sup>16,17</sup> However, a blocking agent cannot be



used in our procedure since the thiols must be free to be detected. When hcys solutions were prepared at room temperature and immediately injected, the oxidation product was observed, indicating that the oxidation of hcys to hcyss is rapid. The amount of hcyss measured in a sample kept at room temperature was constant throughout the day. The addition of TCEP 40 mM to an hcys sample prevented the formation of hcyss.

### 3.3.2 Separation conditions and limits of detection

The separation on a C<sub>18</sub> column (Figure 3.3) was adapted from Chapter 2 by decreasing the pH from 2.6 to 2.0 and increasing the TFA concentration from 0.01 M to 0.2 M. The lower pH increased the overall charge of the analytes and resulted in stronger interaction with TFA. A higher concentration of TFA increased retention of the sample enabling a better separation. A resolution of 0.8 between cys and cyss, a baseline separation between all other analytes and a retention factor of about 9 for the most retained compounds was obtained. The typical cys to cyss concentration ratio in blood samples is around 6.<sup>18</sup> This would generate a peak height for cyss much smaller than showed on Figure 3.3 where the cys/cyss concentration ratio is about 1. In a real biological sample, the resolution between cys and cyss would then be improved since the cyss peak would be much smaller.<sup>15</sup> Improved peak shape compared to Figure 2.8 was obtained since the separation column used was new.

The separations were performed using a Zorbax StableBond-Aq column (SB-Aq). In StableBond (SB) columns, the bonded phase is sterically protected with isobutyl groups to improve low pH stability (Section 1.2.3.1) resulting in a phase that is stable



from pH 1-8.<sup>19</sup> The SB-Aq is a modified SB column which incorporates a hydrophilic group to improve compatibility in highly aqueous phases (Section 1.2.3.1).

Calibration curves were linear ( $R^2 = 0.9964-0.9995$ ) with intercepts equal to zero at the 95% confidence limit. TCEP 40 mM was added to the hcys calibration solutions to prevent the formation of hcyss during calibration of hcys. Table 3.1 shows the detection limits determined as in Section 2.3.2. The detection limits were 0.3-4.3  $\mu\text{M}$  for all analytes, which are comparable in range to those observed for the thiols in Chapter 2. Dynamic ranges were up to 200  $\mu\text{M}$  (75  $\mu\text{M}$  for cyss due to its low solubility) and %RSD typically between 3 and 5%. As showed in Section 2.4, these dynamic ranges and limits of detection are suitable for the analysis of biological samples. An LC/MS method capable of simultaneous analysis of thiols and disulfides developed for the same analytes by Guan et al.<sup>6</sup> showed similar detection limits and standard deviations, but required labour-intensive pre-derivatization steps. In contrast, electrochemical methods for gsh and gssg have yielded detection limits on the order of 2 nM.<sup>8,20</sup>



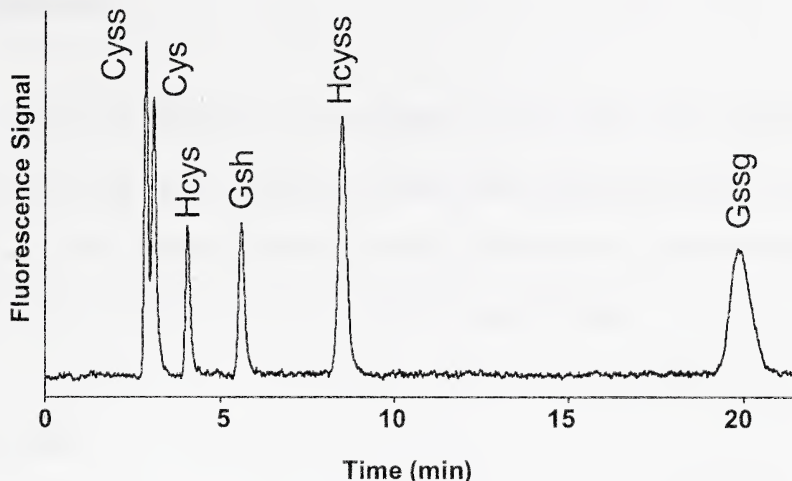


**Figure 3.3 Separation of cys, cyss, heys, hcyss, gsh and gssg.** Experimental conditions: Eluent is TFA 0.2 M, Methanol 0.5%, pH 2.1, 0.8 mL/min First post-column is TCEP 32 mM, pH 8.3, 0.5 mL/min Second post-column is HQS 100  $\mu$ M, Cd<sup>2+</sup> 40  $\mu$ M, Capso 200 mM, pH 9.7, 1.0 mL/min Analyte concentrations is cys 79  $\mu$ M, cyss 55  $\mu$ M, heys 98  $\mu$ M, hcyss 72  $\mu$ M, gsh 103  $\mu$ M, gssg 174  $\mu$ M Column is Zorbax SB-Aq, 150X4.6 mm., 5  $\mu$ m.

**Table 3.1 Detection limits, run to run %RSD and dynamic ranges for cys, heys, gsh, cyss, hcyss and gssg.<sup>a</sup>**

Analyte	Detection limit		% RSD	Dynamic Range ( $\mu$ M)
	$\mu$ M	ppm		
Cys	0.3	0.04	4.0	0.3-200
Cyss	0.9	0.2	3.6	0.9-75
Heys	0.6	0.1	4.5	0.6-150
Hcyss	0.6	0.2	3.4	0.6-100
Gsh	0.3	0.1	3.4	0.3-150
Gssg	4.3	2.6	2.5	4.3-200

<sup>a</sup> Conditions as in Figure 3.3



### 3.4 Conclusions

Thiols and disulfides were separated in their native form and detected by quenching of a fluorescent Cd(HQS)<sub>2</sub><sup>2+</sup> complex after on-line reduction of the disulfides with TCEP. The method is simple and rapid, as it requires no sample preparation and only one single injection to determine both thiols and disulfides.

### 3.5 References

- (1) Lock, J.; Davis, J. *TrAC, Trends Anal. Chem.* **2002**, *21*, 807-815.
- (2) Han, J. C.; Han, G. Y. *Anal. Biochem.* **1994**, *220*, 5-10.
- (3) Getz, E. B.; Xiao, M.; Chakrabarty, T.; Cooke, R.; Selvin, P. R. *Anal. Biochem.* **1999**, *273*, 73-80.
- (4) Krijt, J.; Vackova, M.; Kozich, V. *Clin. Chem. (Washington, D.C.)* **2001**, *47*, 1821-1828.
- (5) Camera, E.; Picardo, M. *J. Chromatogr., B: Biomed. Appl.* **2002**, *781*, 181-206.
- (6) Guan, X. M.; Hoffman, B.; Dwivedi, C.; Matthees, D. P. *J. Phar. Biomed. Anal.* **2003**, *31*, 251-261.
- (7) Loughlin, A. F.; Skiles, G. L.; Alberts, D. W.; Schaefer, W. H. *J. Phar. Biomed. Anal.* **2001**, *26*, 131-142.
- (8) Terashima, C.; Rao, T. N.; Sarada, B. V.; Kubota, Y.; Fujishima, A. *Anal. Chem.* **2003**, *75*, 1564-1572.
- (9) Jandik, P.; Cheng, J.; Evrovski, J.; Avdalovic, N. *J. Chromatogr., B: Biomed. Appl.* **2001**, *759*, 145-151.



- (10) Manna, L.; Valvo, L.; Betto, P. *J. Chromatogr., A* **1999**, *846*, 59-64.
- (11) Fossey, L.; Cantwell, F. F. *Anal. Chem.* **1982**, *54*, 1693-1697.
- (12) Stewart, K. K.; Beecher, G. R.; Hare, P. E. *Anal. Biochem.* **1976**, *70*, 167-173.
- (13) Neter, J.; Kutner, M. H.; Nachtsheim, C. J.; Wasserman, W. *Applied linear statistical models*, fourth ed.; Irwin: Chicago, 1996.
- (14) Mason, R. L.; Gunst, R. F.; Hess, J. L. *Statistical design and analysis of experiments with applications to engineering and science*, second ed.; John Wiley and Sons, Inc.: Hoboken, 2003.
- (15) Miller, J. M. *Chromatography, Concepts and Contrasts*, 2nd ed.; Wiley Interscience: Hoboken, 2005.
- (16) Rossi, R.; Milzani, A.; Dalle-Donne, I.; Giustarini, D.; Lusini, L.; Colombo, R.; Di Simplicio, P. *Clin. Chem. (Washington, D.C.)* **2002**, *48*, 742-753.
- (17) Steghens, J. P.; Flourie, F.; Arab, K.; Collombel, C. *J. Chromatogr., B: Biomed. Appl.* **2003**, *798*, 343-349.
- (18) Melnyk, S.; Pogribna, M.; Pogribny, I.; Hine, R. J.; James, S. J. *J. Nutr. Biochem.* **1999**, *10*, 490-497.
- (19) *Zorbax SB-C18 Datasheet*; Agilent Technologies, 2003.
- (20) Lakritz, J.; Plopper, C. G.; Buckpitt, A. R. *Anal. Biochem.* **1997**, *247*, 63-68.



#### 4.1. Introduction

Over the past few years, ion chromatography has developed into a significant chromatographic technique for ion analysis within the field of separation sciences. Small organic and inorganic ions, proteins, peptides, carbohydrates and amines are the main compounds determined.<sup>1</sup> Applications are numerous within the fields of environmental and clinical analysis as well as in the industries of semiconductors, food and beverage, and pharmaceutical. Most of the time, matrices are relatively simple and require easy cleaning steps such as filtration, extraction or centrifugation. The method presented in this chapter can be applied to water samples for analysis of small inorganic anions.

As mentioned in Section 1.2.1, ultra-high pressure HPLC (UPLC) is used to generate very large number of theoretical plates using small particles and long columns.<sup>2</sup> Such separation power is not always essential. For instance, most ion chromatography determinations involve just a few common anions ( $\text{Cl}^-$ ,  $\text{NO}_3^-$ ,  $\text{HPO}_4^{2-}$ ,  $\text{SO}_4^{2-}$ ). Thus, the wish to perform cheaper, faster and easier analyses is pushing researchers to explore the use of short columns for separations. Fast separations have been performed using short ( $\leq 5$  cm) and wide columns (up to 120 mm).<sup>3-6</sup> However, these examples used large particles (30-200  $\mu\text{m}$ ) to minimize the pressure drop across the columns so that inexpensive peristaltic pumps could be used for elution. The use of such large particles results in low resolution separations of only 2-4 compounds.

---

<sup>a</sup> A version of this chapter has been accepted in Jan 2005 for publication in a special issue of the *Journal of Chromatography A* devoted to the International Ion Chromatography Symposium 2005 (IICS05).



Monolithic columns offer new opportunities for high-resolution analytical separations at low pressure (Section 1.2.5.2). Very high flow rates (as high as 16 mL/min) can be used for ultra-fast separations.<sup>7,8</sup> However, typical HPLC pumps are not designed for these flow rates, and such a method would have excessive solvent consumption. In this Chapter the use of short monolithic columns at lower flow velocities is explored to overcome these difficulties. Efficient separations are achieved because of the high efficiencies inherent to the monolithic phases and the low flow velocities used (equation 1.1). In addition, the short length and high permeability make possible fast separations at reduced pressure. One advantage of such low back pressure is the possibility of using low pressure pumps in what is essentially a flow injection analysis (FIA) manifold that includes a separation component.

The use of peristaltic pumps for IC on monolithic columns has recently been demonstrated for inorganic anion separations.<sup>9,10</sup> Using a 1.0 cm long x 0.4 cm I.D. silica monolith, Paull and co-workers observed a 50 psi pressure drop at 0.3 mL/min. Unfortunately, this back pressure (mainly due to a 10 cm long packed bed suppressor) was sufficiently high that they had to simultaneously use two peristaltic pumps in parallel to achieve this flow rate. The low flow rates resulted in long separations - 6 anions in 30 minutes using gradient elution. This method showed that peristaltic pumps could be used for low pressure IC separations, but does not compare with the actual state of the art in anion analysis where up to 8 anions are separated in 10-15 minutes with superior resolution.<sup>1</sup> This method also suffered from extra-column band broadening due to large void volumes originating mainly in the long suppressor and the large injection loop (25  $\mu$ L).



Satinsky's group also reported the use of a low pressure syringe pump to drive separations on a monolithic column (2.5 cm and 5 cm long x 0.46 cm I.D.).<sup>11,12</sup> Four organic drugs were analysed using a commercial FIA system fitted with a 5 or 10 mL syringe for eluent delivery. The pressure limitations of the pump (360 psi) permitted separations at 0.6 mL/min. The system also suffered from extra-column band broadening since very wide connecting tubing was used (0.030" I.D. compared to the usual 0.005" I.D.).

In the present Chapter, the use of 0.5 and 1 cm long monolithic columns for the separation of inorganic anions is discussed. Ion chromatography is performed by coating the reverse phase silica monolithic columns with a long chained cationic surfactant as described in Section 1.2.5.2.1. Rapid, high resolution and low pressure separations on monoliths are achieved at low flow rates using isocratic elution. It is also demonstrated that the separations can be performed using a low pressure syringe pump at a constant flow rate of 0.9 mL/min.

## 4.2. Experimental

### 4.2.1 Apparatus

The equipment used for high and low pressure IC is illustrated in Figure 4.1. In high pressure IC (Figure 4.1 a) a model 625LC Waters (Milford, MA, USA) HPLC pump was used to deliver the eluent. A Chromolith RP-18e column (25 mm long x 4.6 mm I.D., Merck KGaA, Darmstadt, Germany) was used as a pre-column and coated with didodecyldimethylammonium bromide (DDAB). A Rheodyne (Berkeley, CA, USA)



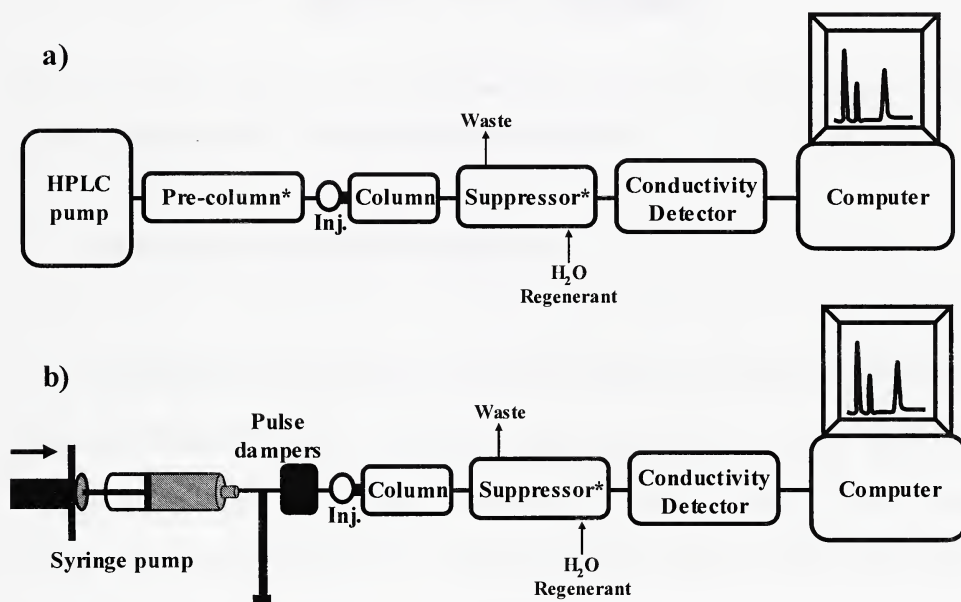
injection valve (model 7520) was fitted with a 0.5  $\mu\text{L}$  loop for low dead volume experiment or a 1  $\mu\text{L}$  loop for quantitative studies. Chromolith guard cartridges RP-18e (5 mm and 10 mm long x 4.6 mm I.D.) with cartridge holder (Figure 4.2) were used as the columns and connected directly to the injection valve through the 10-32 female port of the column holder. In eluent suppression mode, a Dionex (Sunnyvale, CA, USA) Anion Atlas Electrolytic Suppressor (AAES) was connected to the column with 5 cm of PEEK tubing (0.005" I.D, Upchurch, Oak Harbor, WA, USA). The suppressor operated in external water mode with a regenerant flow rate of ~2 mL/min. (The suppressor was removed when coating or uncoating the columns.) A Dionex ED-50A electrochemical detector and a DS3 Detection Stabilizer (Dionex, model DS3-1) were used for detection. A 10 cm 0.005" I.D. PEEK tubing (Upchurch) connected the column or suppressor directly to the cell which was within the DS3-1 stabilizer. The conductivity cell was 1  $\mu\text{L}$ , the rise time 0.05 s and data was collected with the PeakNet 5.2 software (Dionex) at 20 Hz.

Low pressure separations (Figure 4.1 b) were performed with a Sage Multi-Range Syringe pump, model M365 (Thermo Electron Corporation, Beverly, MA, USA) fitted with a 5 mL glass gastight syringe (model #1005, Hamilton Corporation, Reno, NV, USA). To insure smooth flow, the syringe and piston were periodically cleaned with an ethanolic 5% wt KOH solution. The tubing from the syringe to the injection port was 1/16" I.D. Teflon PFA (Upchurch). To reduce noise from the syringe pump, 2 pulse dampers were introduced before the injector.<sup>13</sup> The first one consisted of a 40 cm long piece of 1/8" I.D. Teflon tubing partially filled with eluent and introduced perpendicularly in the flow line with a micro-splitter valve (Upchurch, P/N P-460S). The



splitter valve was used as a T-junction. The second pulse damper was model Lo-Pulse 21 (Scientific Systems Inc., State College PA, USA). The injection valve, columns, suppressor and detector were as described in the previous paragraph.

A Corning 445 pH-meter (Corning, New York, NY, USA) with a Corning electrode (3 in 1 Combo P/N 476436) was used for pH measurements.



\* Optional

Figure 4.1 a) High and b) low pressure IC systems.



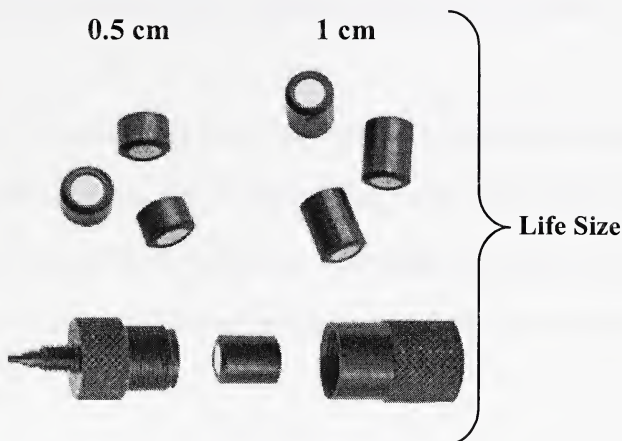


**Figure 4.2** Life size pictures of the 0.5 and 1.0 cm long Chromolith guard cartridges and the column holder.<sup>14</sup> Adapted from reference 14.

#### 4.2.2 Reagents and solution preparation

All solutions were prepared in deionised 18 MΩ water (Nanopure Water System, Barnstead, Chicago, IL, USA). Chemicals were reagent grade or better. The sodium salts of chloride (EMD Chemicals, Gibbstown, NJ, USA), nitrite (BDH, Toronto, Canada), nitrate (ACP Chemicals Inc. Montreal, Canada), sulphate (BDH) and phosphate ( $\text{NaH}_2\text{PO}_4 \cdot \text{H}_2\text{O}$ , EMD) were used. Potassium salts of bromide (Fisher, Fair Lawn, NJ, USA) and iodate (ACP Chemicals Inc.) were used.

The eluents were freshly prepared by dissolving the appropriate amount of 4-cyanophenol (95%, Aldrich, St-Louis, MI, USA) or 4-hydroxybenzoic acid (99%, Aldrich, St-Louis, MI, USA) in water, adjusting the pH with a 2.5 M sodium hydroxide (Fisher) solution and diluting with water to the desired volume. The solutions were



filtered through 0.22  $\mu\text{m}$  Magna nylon membrane filters (GE Osmonic, Trevose, PA, USA) prior to use.

The column coating solution was 1 mM didodecyldimethylammonium bromide (DDAB 98%, Aldrich) in 1% or 5% v/v acetonitrile (ACN, HPLC grade, Fisher). The appropriate amount of DDAB was dissolved in water using a sonicator, acetonitrile was added, the solution was diluted to the desired volume and finally it was filtered through a 0.22  $\mu\text{m}$  nylon filter.<sup>15</sup>

#### **4.2.3 DDAB Solubility**

The solubility of DDAB in 50% ACN/water and 100% acetonitrile was measured by adding small amounts (between 0.01 and 0.05 mL) of the ACN solution to a known mass of DDAB (~0.1 g) under constant stirring until the DDAB visibly dissolved.

#### **4.2.4 Column coating and removal of coating**

The monolithic guard columns were coated using the procedure illustrated in Figure 1.16 where a column is equilibrated with 1% or 5% acetonitrile and then flushed with a DDAB/ACN solution at 1 mL/min until complete breakthrough of DDAB is observed ( $\leq 25$  mL), as determined by a rapid increase in the conductivity. Then, the columns were washed with water to remove any unretained DDAB for 10 min at 1 mL/min. Finally the columns were equilibrated with the 4-cyanophenol or 4-hydroxybenzoic acid eluents at 1 mL/min.



The ion exchange capacity of the coated columns (Q in  $\mu\text{eq}/\text{column}$ ) is estimated according to this equation:<sup>15-17</sup>

$$Q = C_{\text{DDAB}}F(t_b - t_0) \quad (4.1)$$

where  $C_{\text{DDAB}}$  is the concentration of the DDAB coating solution ( $\mu\text{eq}/\text{mL}$  or  $\mu\text{mol}/\text{mL}$ ), F is the flow rate ( $\text{mL}/\text{min}$ ),  $t_b$  the breakthrough time of DDAB (min) and  $t_0$  the dead time of the column (min). The column capacity is varied by adjusting the ACN content in the coating solution.<sup>15,18</sup>

The DDAB coating was stable for up to 3 weeks (Section 4.3.1.4). However, to insure reproducible retention behaviour, the columns were typically recoated every 3-5 days using the following procedure. The column was first flushed with water at 1  $\text{mL}/\text{min}$  for 3 minutes to remove the eluent. The %ACN was gradually increased to 50% over 1 min and the column was flushed at 1  $\text{mL}/\text{min}$  for 7 min to remove the DDAB. Finally the %ACN was reduced to 1% or 5% and held for 2 minutes to equilibrate the column prior to the next coating.

## 4.3. Results and discussion

### 4.3.1 HPLC separations on short columns

#### 4.3.1.1 Eluent conditions and selection

Traditional eluents for IC are hydroxide and bicarbonate/carbonate (Section 1.2.3.2). Such alkaline eluents cannot be used with silica stationary phases, which experience dissolution at pH greater than 8 (Section 1.2.5.1). Cyanophenols have been



demonstrated to be a good alternative to basic eluents for suppressed conductivity ion chromatography on silica columns.<sup>15</sup> Initially, the use of 2-cyanophenol at pH 7.0 appeared to be an ideal choice. However, it causes pressure increase problems possibly by forming a precipitate in the column.<sup>15,19</sup> In these experiments, 4-cyanophenol was used instead.

The strength of weak acid eluents in IC is tuneable by adjusting their concentration (Section 1.2.3.2) and pH. Using a pH near the pKa of the eluent ( $\pm 1$  pH unit) provides both good buffering capacity and insures that the amount of deprotonated acid (the actual eluent) stays constant. The pH of the 4-cyanophenol ( $pK_a$  7.7)<sup>20</sup> eluent was adjusted at 7.3 or 7.4, to be close to the pKa without exceeding the column pH limitations.

The separation of chloride, nitrate, phosphate and sulphate on a 0.5 cm column in less than 2 min at 2 mL/min is presented in Figure 4.3 a. The 9 mM 4-cyanophenol (pH 7.3) provides a resolution of 1.8 between chloride and nitrate (minimum resolution of the separation). The same anions along with iodate are separated on a 1 cm column using 9 mM 4-cyanophenol, pH 7.4 in 3 min at 2 mL/min (Figure 4.3 b). Chloride and nitrate are now baseline resolved and a resolution of 1.4 is obtained between iodate and chloride. A slightly lower eluent concentration of 6 mM 4-cyanophenol enables the separation of five singly charged analytes in 1 min with a resolution of 1.1 between the critical pairs (Figure 4.3 c). Phosphate and sulphate elute in 4 and 8 minutes respectively using this eluent.



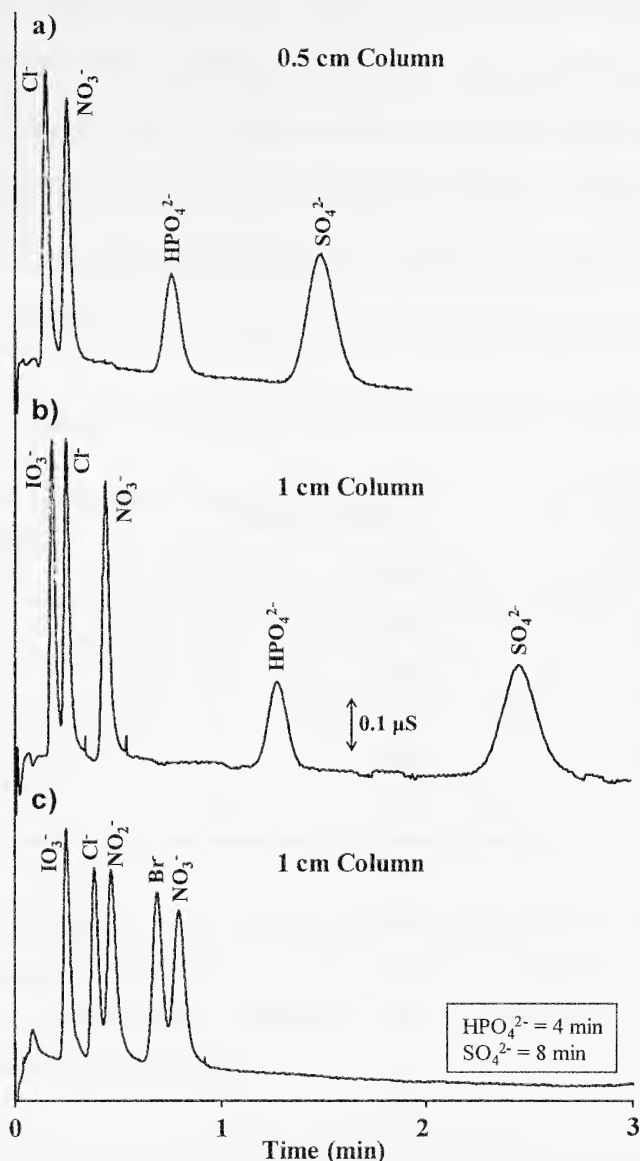


**Figure 4.3 Suppressed anion separations with 4-cyanophenol eluent.** Experimental conditions: flow rate is 2.0 mL/min, injection is 0.5  $\mu$ L, analyte concentration is 250  $\mu$ M.

a) 0.5 cm column, eluent is 4-cyanophenol 9 mM pH 7.3, coating solution is DDAB 1 mM in 1% ACN, column capacity is 12  $\mu$ eq/column, suppression at 60 mA.

b) 1 cm column, eluent is 4-cyanophenol 9 mM pH 7.4, coating solution is DDAB 1 mM in 5% ACN, column capacity is 20  $\mu$ eq/column, suppression at 80 mA, pre-column is 2.5 cm column coated with DDAB 1 mM in 5% ACN.

c) 1 cm column, eluent is 4-cyanophenol 6 mM pH 7.3, coating solution is DDAB 1 mM in 5%ACN, column capacity is 21  $\mu$ eq/column, suppression at 70 mA.



Calibration plots are linear up to 350  $\mu\text{M}$  ( $R^2 = 0.9985\text{-}0.9999$ ) with intercepts equal to zero at the 95% confidence limit. Table 4.1 shows the detection limits determined as in Section 2.3.2.<sup>21</sup> The detection limits are from 0.3 to 0.5  $\mu\text{M}$  (0.02 to 0.06 ppm) for all analytes. These limits of detection are higher than previously reported for suppressed IC (usually in the ppb range<sup>1,22</sup>) because of the use of a small (1  $\mu\text{L}$ ) injection loop to minimize extra-column band broadening (Section 4.3.1.3).

**Table 4.1 Detection limits and run to run %RSD for  $\text{IO}_3^-$ ,  $\text{Cl}^-$ ,  $\text{NO}_3^-$ ,  $\text{HPO}_4^{2-}$  and  $\text{SO}_4^{2-}$**

Analyte	Detection limits		% RSD
	$\mu\text{M}$	ppm	
$\text{IO}_3^-$	0.3	0.06	1.5
$\text{Cl}^-$	0.5	0.02	3.7
$\text{NO}_3^-$	0.3	0.02	1.6
$\text{HPO}_4^{2-}$	0.3	0.03	0.8
$\text{SO}_4^{2-}$	0.4	0.04	1.0

a. Experimental conditions: 1 cm column, flow rate is 1.0 mL/min, injection is 1  $\mu\text{L}$ , eluent is 4-cyanophenol 9 mM pH 7.3, coating solution is DDAB 1 mM in 5%ACN, column capacity is 20  $\mu\text{eq}/\text{column}$ , suppression at 40 mA, pre-column is 2.5 cm column coated with DDAB 1 mM in 5% ACN.

As suggested by Paull and co-workers 4-hydroxybenzoic acid ( $\text{pK}_{\text{a}1}=4.6$ ,  $\text{pK}_{\text{a}2}=9.5$ )<sup>20</sup> can also be used as a neutral pH eluent.<sup>9</sup> Figure 4.4 shows the separations of seven inorganic anions on the 0.5 and 1 cm columns using a 5 mM 4-hydroxybenzoic acid (pH 5.6) eluent. Under these conditions, separations are complete in 1.5 and 2.5 min at 2.0 mL/min on the 0.5 and 1 cm columns, respectively. Thus 4-hydroxybenzoic acid is a



more effective eluent than 4-cyanophenol in terms of resolution and separation time. However, as can be noticed by comparing the scales of Figures 4.3 and 4.4, sensitivities can be up to 60% inferior with 4-hydroxybenzoic acid, since this eluent conductivity cannot completely be suppressed by the suppressor (Section 1.2.4.1).<sup>1,23</sup> The residual background conductivity with 4-hydroxybenzoic acid is evident in the large water dip at the dead time in Figure 4.4.

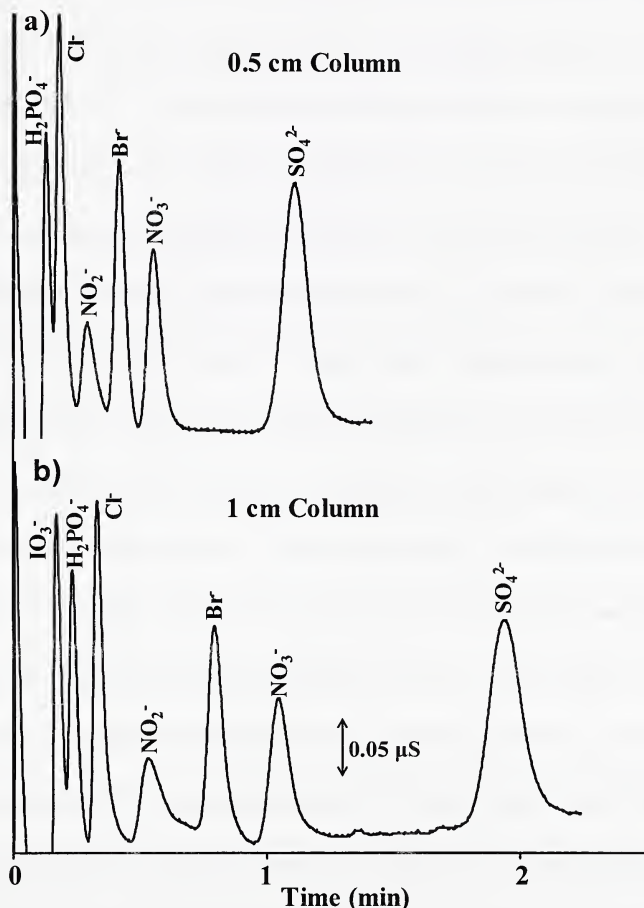


**Figure 4.4** Suppressed anion separations with 4-hydroxybenzoic acid eluent. Experimental conditions: flow rate is 2.0 mL/min, injection is 0.5  $\mu$ L, analyte concentration is 250  $\mu$ M, eluent is 4-hydroxybenzoic acid 5 mM pH 5.6, coating solution is DDAB 1 mM in 1%ACN. **a)** 0.5 cm column, column capacity is 12  $\mu$ eq/column, suppression at 70 mA. **b)** 1 cm column, Column capacity is 25  $\mu$ eq/column, suppression at 80 mA.



#### 4.3.1.2 Coating conditions

In this system, the capacity of the columns is adjusted upon coating and depends on the concentration of ACN in the coating solution.<sup>15,18</sup> The eluent concentration, pH and the column capacity are adjusted together to provide fast but resolved chromatograms. In Figure 4.3 a, the 0.5 cm column was coated with 1 mM DDAB in 1% ACN. The use of a low ACN content resulted in a column capacity of 24  $\mu\text{eq}/\text{cm}$  (12  $\mu\text{eq}/\text{column}$ , see Table 4.2), which allowed sufficient retention to separate chloride from the water dip at the dead time. The 1 cm columns were coated with 1 mM DDAB in 5% ACN (Figure 4.3 b and c), generating capacities of  $\sim$ 20  $\mu\text{eq}/\text{cm}$  (20 and 21  $\mu\text{eq}/\text{column}$ ), which was sufficient to resolve iodate from the water dip. Doubly charged analytes are more affected by the column capacity than singly charged anions (equation 1.18 in Section 1.2.3.2). Thus, the lower capacities obtained by increasing the ACN in the coating solution reduced the retention of phosphate and sulphate by 10% while not significantly affecting the retention of the other anions. In Figure 4.4, columns were coated with 1 mM DDAB in 1% ACN to resolve the early eluting peaks and to provide sufficient retention to move them away from the water dip. Capacities of 24  $\mu\text{eq}/\text{cm}$  were obtained (12 and 25  $\mu\text{eq}/\text{column}$  for the 0.5 and 1 cm long columns, respectively).

The capacities of  $20 \pm 1 \mu\text{eq}/\text{cm}$  obtained for the coatings with DDAB in 5% ACN (Table 4.2) are in agreement with previous work with 5 cm columns which had capacities of 20  $\mu\text{eq}/\text{cm}$ .<sup>15</sup> Coatings with DDAB in 1% ACN were not reported in this earlier work but are interpolated to be 22  $\mu\text{eq}/\text{cm}$  which is comparable to the capacities of 24  $\pm 2 \mu\text{eq}/\text{cm}$  obtained here (Table 4.2).



**Table 4.2 Column capacities according to coating solution.**

Figure		Column Length	DDAB in 1% ACN	DDAB in 5% ACN
4.3	a	0.5 cm	24 $\pm$ 2 $\mu$ eq/cm	na
	b	1 cm	na	20 $\pm$ 1 $\mu$ eq/cm
	c	1 cm	na	20 $\pm$ 1 $\mu$ eq/cm
4.4	a	0.5 cm	24 $\pm$ 2 $\mu$ eq/cm	na
	b	1 cm	24 $\pm$ 2 $\mu$ eq/cm	na

#### 4.3.1.3 Band broadening from extra-column effects

Section 1.2.2 explained the effects of extra-column band broadening on a separation. For the IC system used herein the variance caused by the suppressor ( $\sigma_{\text{sup}}^2$ ) is added to the overall variance equation. Equation 1.14 becomes:

$$\sigma^2 = \sigma_{\text{col}}^2 + \sigma_{\text{inj}}^2 + \sigma_{\text{tu}}^2 + \sigma_{\text{sup}}^2 + \sigma_{\text{fc}}^2 + \sigma_{\text{rt}}^2 \quad (4.2)$$

The 0.5 and 1 cm columns used for this work are much smaller than conventional columns ( $V_o \leq 0.1$  mL compared to  $\sim 1.5$  mL for a 15 cm long column). Thus the impact of each extra-column effect on band spreading can be substantial and must be minimized.

The effect of the injection volume on the overall efficiency was estimated by calculating  $V_s/V_c$ , where  $V_s$  is the volume of the sample loop and  $V_c$  is the volume of the peak (i.e. baseline width =  $4\sigma$ ).<sup>24</sup> No negative effect on the separation is observed when  $V_s/V_c$  is less than 0.1, and the loss in resolution is less than 10% when  $V_s/V_c$  is below 0.4.<sup>24</sup> Typically an injection volume of 20  $\mu$ L is used in IC. However peak volumes as small as 100  $\mu$ L are achieved with the 1 cm monolith used herein (Table 4.3). Thus for a



20  $\mu\text{L}$  injection,  $V_s/V_c$  is about 0.2 and the injection would contribute to the overall peak width. For the 0.5 cm column, a 20  $\mu\text{L}$  injection would contribute about 10% to the peak width. To insure that injection does not affect the peak efficiencies, a conservative injection volume of 0.5  $\mu\text{L}$  was used ( $V_s/V_c \leq 0.004$ ). Similarly, the detector contribution to broadening ( $\sigma_{fc}^2 + \sigma_{nt}^2$ ) was minimized by using a small flow cell (1  $\mu\text{L}$ ) and a fast rise time (0.05 s). Short (<5 cm total injector-to-suppressor) and narrow connecting tubing (0.005" I.D.) were used to minimize the connecting tubing contribution ( $\sigma_{tu}^2$ ). The diameter of the connecting tubing could have been smaller, but as it will be explained in Section 4.3.2, it was desirable to keep the backpressure of the system low.

The top section of Table 4.3 presents the efficiencies obtained in the low-volume IC system described above (non-suppressed). The efficiencies (as H or N/m) for the non-suppressed IC system are essentially independent of retention, indicating that the above adjustments were successful in eliminating extra-column band broadening. Nonetheless, the plate heights in Table 4.3 ( $H \sim 40 \mu\text{m}$ ) are substantially poorer than expected for monoliths possessing 2  $\mu\text{m}$  macropores. Typically, such monoliths behave comparably to columns packed with 3  $\mu\text{m}$  particles (Section 1.2.5.2) and, as was observed by Hatsis et al., values of H should be around 15  $\mu\text{m}$ .<sup>15</sup> Unexpectedly, an additional source of extra-column band broadening was discovered - the column holder (Figure 4.2). One end of the holder consists of a 2 cm long connector with an I.D. of ~0.02". This is very wide compared to the connecting tubing I.D. of 0.005" used, consequently increasing the overall band broadening in the system. However, as discussed below, the suppressor dominated extra-column band broadening. Therefore, no further efforts were made to reduce the extra void volume of the holder.



Detection limits for non-suppressed IC are usually only ~100 ppb. Suppression in IC increases detection sensitivity by reducing the eluent background and increasing the analyte's conductivity signal (Section 1.2.4.1).<sup>1,23</sup> Two small internal volume (~35  $\mu$ L) suppressors (Dionex AAES and Metrohm MSM) were tried. The MSM suppressor consists of 3 small packed beds positioned in a 3-position rotary valve.<sup>25</sup> During operation, one bed suppresses the eluent while the second is regenerated with sulphuric acid and the third rinsed with water. The valve is rotated prior to each separation which provides a fully regenerated suppressor bed each time. The AAES produced less broadening and was used hereafter. Table 4.3 shows the efficiencies (N/m) deteriorating by more than 2-fold for  $\text{IO}_3^-$  in suppressed mode. Also, in the suppressed separation, the efficiencies worsen by 2-fold from  $\text{Cl}^-$  to  $\text{IO}_3^-$  (Table 4.3). These are clear indications that the suppressor is the major source of extra-column band broadening.<sup>26</sup> Nevertheless, baseline resolution between  $\text{IO}_3^-$  and  $\text{Cl}^-$  is still achieved ( $R_s=1.4$ ). In addition, since the suppressor contributes to up to 50% of the total extra-column band broadening, it was possible to increase the size of the injection loop to 1  $\mu$ L to furthermore improve sensitivity without compromising efficiency. A 5  $\mu$ L loop was tried, but not used, since it doubled the plate height for iodate.



**Table 4.3 Peak efficiency in non-suppressed and suppressed modes.**

	$\text{IO}_3^-$	$\text{Cl}^-$	$\text{NO}_2^-$	$\text{Br}^-$	$\text{NO}_3^-$
<b>Non-Suppressed</b>					
$k'$	1.5	2.4	3.4	4.6	5.0
$N/m$	25,000	28,000	23,000	26,000	28,000
$H (\mu\text{m})$	40	36	43	38	36
$\sigma^2 (\mu\text{L}^2)$	520	860	1,640	2,470	2,700
<b>Suppressed</b>					
$k'$	1.6	2.6	na	na	5.3
$N/m$	11,000	23,000	na	na	18,000
$H (\mu\text{m})$	91	43	na	na	56
$\sigma^2 (\mu\text{L}^2)$	1,160	1,150	na	na	4,610

a. Experimental conditions: 1 cm column, flow rate is 1 mL/min, injection is 0.5  $\mu\text{L}$ , eluent is 4-cyanophenol 9 mM pH 7.3, coating solution is DDAB 1 mM in 5%ACN, column capacity is 20  $\mu\text{eq}/\text{column}$ , suppression at 60 mA, pre-column is 2.5 cm column coated with DDAB 1 mM in 5%ACN. For non-suppressed conductivity studies the analyte concentration is 2.5 mM, except for  $\text{IO}_3^-$  which was 10 mM. With suppressed conductivity, the analyte concentration is 250  $\mu\text{M}$ .

#### 4.3.1.4 Improved stability and the removal of the DDAB coating

With surfactant coated columns, the ion exchange capacity gradually decreases due to the slow leaching of the surfactant off of the analytical column. Reproducible retention times can be achieved either by addition of a small amount of surfactant to the eluent<sup>27</sup> or by periodically recoating the column.<sup>15</sup> The long-term stability of the DDAB coatings was studied by pumping an 8 mM 4-cyanophenol pH 7.3 eluent through a 1 cm monolith coated with 1 mM DDAB in 5% ACN. After pumping about 2900 column



volumes through the column, the retention times had decreased by 7% (Figure 4.5). If a 10% loss in retention was considered acceptable, a fresh coating would last for 11 hours of operation (roughly two days) at 1 mL/min.

The stability of the retention times was improved by placing a 2.5 cm DDAB coated monolithic pre-column prior to the injector (Figure 4.1 a). This pre-column was coated with DDAB using the same coating procedure as the analytical column. DDAB leaching from this pre-column replaces any surfactant lost from the analytical column. In this manner, the coating of the analytical column is continuously regenerated. With a DDAB coated pre-column in place, the retention times decreased by less than 1% after flushing with eluent through 6300 column volumes (Figure 4.5). About 150 hours (roughly 19 days) would then be necessary to reduce the column performance by 10%. This is nearly a 15-fold improvement compared to the stability of a coating without pre-column and signifies that a column would only need to be recoated every 3 weeks when doing routine analysis. In both the stability studies (with and without the pre-column), the pressure of the system increased by 5% after pumping for 8 or 15 hours, but was recovered using the recoating procedure described below.



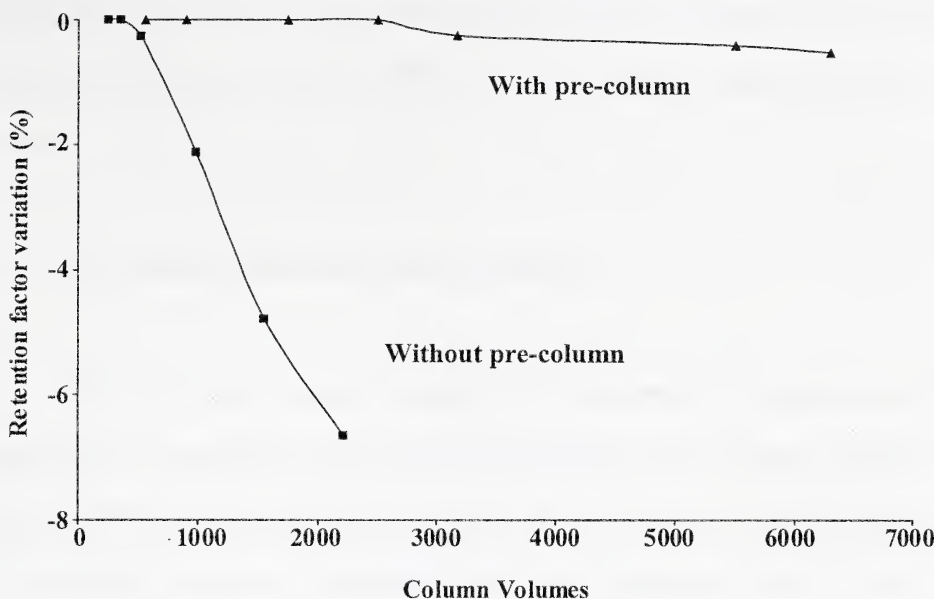


**Figure 4.5 Variation of retention time of sulphate with column volumes.**  
 Experimental conditions: Separation column is 1 cm, pre-column is 2.5 cm, coating solution is DDAB 1 mM in 5% ACN, column capacity is 21  $\mu$ eq/column, eluent is 4-cyanophenol 8 mM pH 7.3, flow rate is 1.0 mL/min, injection is 0.5  $\mu$ L, analyte concentration is 250  $\mu$ M. The curves are simply a guide to the eye.

To remove the DDAB coatings from a column, Hatsis and Lucy flushed the columns with 100% ACN (Figure 1.16).<sup>15</sup> Unfortunately, DDAB is only slightly soluble in pure ACN. Using the procedure described in Section 4.2.3, it was determined that the solubility of DDAB in ACN is only 0.1 g/ml. Thus DDAB precipitates in the column when mixed with 100% ACN. The precipitation of DDAB in the columns upon repeated removal of coatings caused pressure build ups and reproducibility problems. These difficulties were solved by using a 50% ACN/water solution to remove the DDAB coatings. The solubility of DDAB is 0.7 g/ml in 50% ACN. Using this procedure, the %RSD of the capacity obtained from successive coating/uncoating cycles ( $n=5$ ) were



below 2%, and retention time variability was less than 3%. Significantly, the column pressure also remained constant (%RSD < 3%) over multiple coating/uncoating cycles (n=4).

#### **4.3.2 Multicomponent flow injection analysis**

The use of low pressure pumps such as peristaltic or syringe pumps for separations on monolithic columns has been attempted by the groups of Satinsky and Paull.<sup>9,11,12</sup> The most important challenge when using low pressure pumps for separations on monolithic columns is to reduce the system back pressure. Using 2.5 and 5 cm monolithic columns, Satinsky and co-workers replumbed their system with very wide tubing (0.030" I.D.) which reduced the back pressure but contributed substantially to the extra-column band broadening. Despite this effort to reduce the pressure, the maximum flow rate they attained was ~0.6 mL/min with a syringe pump. As a result separations took 6-8 min.<sup>11,12</sup> Paull and co-workers, on the other hand, used shorter columns (1 cm) and peristaltic pumps. They could not exceed flow rates of 0.38 mL/min even when simultaneously using two peristaltic pumps and increasing the column temperature to 45 °C to reduce viscosity (and therefore back pressure).<sup>9</sup> The low flow rates obviously resulted in very long separations dominated by band broadening from longitudinal diffusion effects (Section 1.2.1).<sup>28,29</sup>

My work with a syringe pump (glass syringe), illustrated in Figure 4.6, shows that it is possible to overcome these difficulties. By using columns no longer than 1 cm and very short 0.005" I.D. tubing, flow rates of 0.9 mL/min were achieved. The total back



pressure of the system (i.e. syringe to detector) was about 70 psi at this flow rate, with 40 psi arising from the suppressor. Analytes (nitrate and sulphate) that were eluted in 18 and 30 minutes in Paull's system (using a gradient elution of 4-hydroxybenzoic acid from 2 to 5 mM) were resolved here in less than 2 and 4 min, respectively. Figure 4.6 demonstrates that the flow rate of the syringe pump is constant during the analysis since the chromatograms obtained with an HPLC pump matched the ones obtained with the syringe pump. Baseline fluctuations occurred because the pump's mechanisms and motor were operating at maximum speed. Fluctuations were reduced by the addition of pulse dampers.



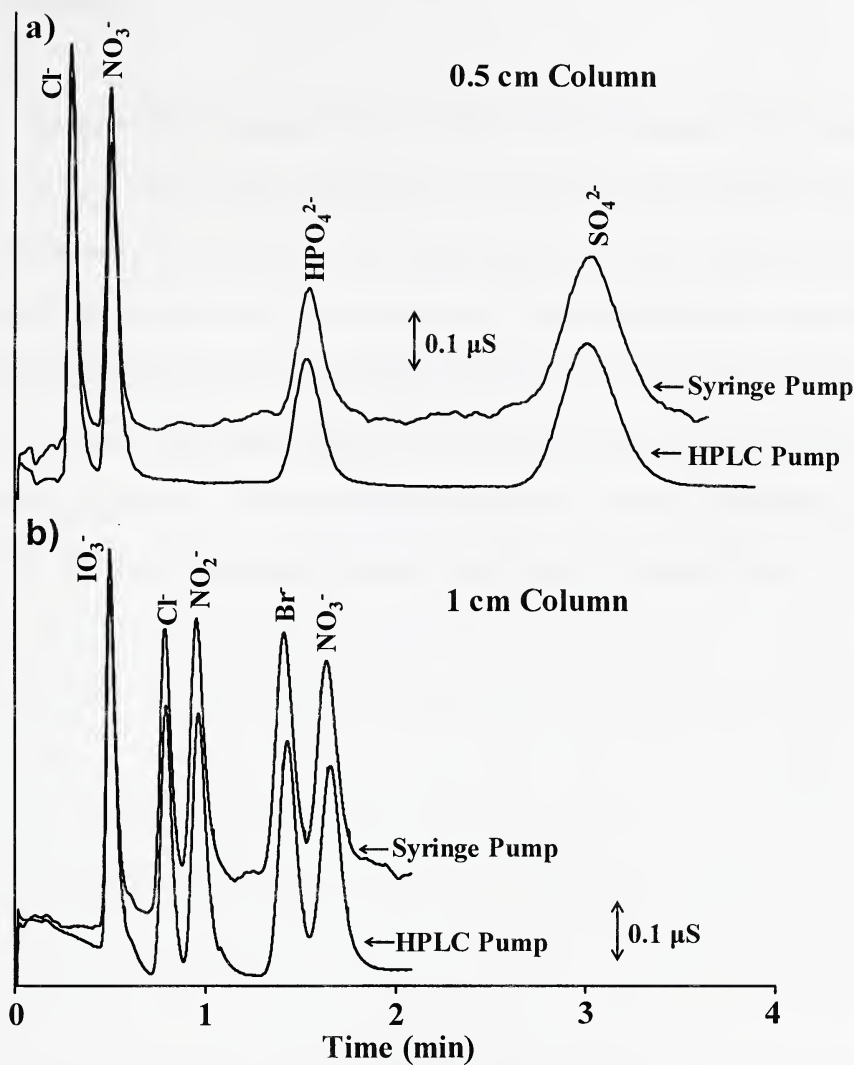


**Figure 4.6 Low pressure separations with syringe pump.** Experimental conditions: injection is 0.5  $\mu$ L, analyte concentration is 250  $\mu$ M, suppression at 40 mA. **a)** 0.5 cm column, eluent is 4-cyanophenol 9 mM pH 7.3, coating solution is DDAB 1 mM in 1% ACN, column capacity is 13  $\mu$ eq/column, flow rate is 0.9 mL/min. **b)** 1 cm column, eluent is 4-cyanophenol 6 mM pH 7.3, coating solution is DDAB 1 mM in 5% ACN, column capacity is 21  $\mu$ eq/column, flow rate is 0.9 mL/min, with HPLC pump only: pre-column is 2.5 cm column coated with DDAB 1 mM in 5% ACN.



#### 4.4. Conclusions

The separations presented in this chapter clearly demonstrate that columns as short as 0.5 cm can be used to obtain fast IC separations using reasonable flow rates. When compared to traditional IC<sup>1</sup>, our separations resolve most important inorganic anions with elution times up to five times faster. These fast separations come with the advantages of reduced solvent consumption compared to previous fast IC work<sup>15</sup>. To achieve efficient separations, sources of extra-column band broadening have to be considered and reduced. The low pressures generated from the monolithic columns enable the use of an inexpensive and simple syringe pump for eluent delivery.



#### 4.5 References

- (1) Weiss, J. *Handbook of Ion Chromatography*, 3rd ed.; Wiley-VCH: Darmstadt, 2004.
- (2) Swartz, M. E. *J. Liq. Chromatogr. Relat. Technol.* **2005**, *28*, 1253-1263.
- (3) Jiang, X.; Zhang, X.; Lui, M. *J. Chromatogr. A* **1999**, *857*, 175-181.
- (4) Zolotov, Y. A.; Maksimova, I. M.; Morosanova, E. I.; Velikorodny, A. A. *Anal. Chim. Acta* **1995**, *308*, 378-385.
- (5) Yalcin, S.; Le, X. C. *Talanta* **1998**, *47*, 787-796.
- (6) Hart, J. P.; Jordan, P. H. *Analyst* **1989**, *114*, 1633-1635.
- (7) Cabrera, K. *J. Sep. Sci.* **2004**, *27*, 843-852.
- (8) Mistry, K.; Grinberg, N. *J. Liq. Chromatogr. Relat. Technol.* **2005**, *28*, 1055-1074.
- (9) Victory, D.; Nesterenko, P.; Paull, B. *Analyst* **2004**, *129*, 700-701.
- (10) Connolly, D.; Victory, D.; Paull, B. *J. Sep. Sci.* **2004**, *27*, 912-920.
- (11) Satinsky, D.; Solich, P.; Chocholous, P.; Karliceck, R. *Anal. Chim. Acta* **2003**, *499*, 205-214.
- (12) Satinsky, D.; Neto, I.; Solich, P.; Sklenarova, H.; Conceicao, M.; Montenegro, B. M. S.; Araujo, A. N. *J. Sep. Sci.* **2004**, *27*, 529-536.
- (13) Ruzicka, J.; Hansen, E. H. *Flow Injection Analysis*, 2nd ed.; Wiley Interscience: New York, 1988.
- (14) [www.merck.de/servlet/PB/menu/1209750/](http://www.merck.de/servlet/PB/menu/1209750/).
- (15) Hatsis, P.; Lucy, C. A. *Anal. Chem.* **2003**, *75*, 995-1001.



(16) Conder, J. R.; Young, C. L. *Physicochemical Measurement by Gas Chromatography*; John Wiley & Sons: Toronto, 1979.

(17) Connolly, D.; Paull, B. *J. Chromatogr. A* **2002**, *953*, 299-303.

(18) Cassidy, R. M.; Elchuk, S. *J. Chromatogr. Sci.* **1983**, *21*, 454-459.

(19) *Metrohm-Peak, Personal Communication, September 2004*.

(20) Smith, R. M.; Martell, A. E. *Critical stability constants, Vol. 3*; Plenum Press: New York, 1975.

(21) Grant, C. L.; Hewitt, A. D.; Jenkins, T. F. *Am. Lab. (Shelton, Conn.)* **1991**, *23*, 15-32.

(22) Haddad, P. R.; Jackson, P. E.; Shaw, M. J. *J. Chromatogr. A* **2003**, *1000*, 725-742.

(23) Haddad, P. R.; Jackson, P. E. *Ion Chromatography: Principles and Applications*; Elsevier: New York, 1990.

(24) Snyder, L. R.; Kirkland, J. J.; Glajch, J. L. *Practical HPLC method development*, 2nd ed.; Wiley Interscience: Hoboken, 1997.

(25) Lucy, C. A.; Hatsis, P. In *Chromatography, part A: fundamentals and techniques*, 6<sup>th</sup> ed.; Heftmann, E., Ed.; Elsevier B.V.: Amsterdam, 2004; Vol. 69A, Journal of Chromatography Library.

(26) Dolan, J. W. *LCGC* **2004**, *22*, 26-30.

(27) Hu, W.; Tanaka, K.; Hasebe, K. *Analyst* **2000**, *125*, 447-451.

(28) Miller, J. M. *Chromatography, Concepts and Contrasts*, 2nd ed.; Wiley Interscience: Hoboken, 2005.

(29) Gritti, F.; Piatkowski, W.; Guiochon, G. *J. Chromatogr., A* **2003**, *983*, 51-71.



## CHAPTER FIVE. Small particle IC separations at high pH on a silica stationary phase

### 5.1 Introduction

The ion chromatography method described in the previous chapter is limited to a maximum eluent pH of 8 due to the poor chemical stability of silica-based stationary phases in alkaline solutions (Section 1.2.5.1). 4-Cyanophenol and 4-hydroxybenzoic acid were used as an alternate to the traditional IC eluents such as sodium hydroxide and carbonate/bicarbonate, which require pH>10. However, since alkaline eluents are suppressed more effectively because of their high  $pK_a$  and provide better sensitivity (Section 1.2.4.1), it is desirable to adapt our method to high pH eluents. In addition, high pH enables the use of more highly charged eluents, which give better control of selectivity.

Bidentate silica-based Zorbax Extend C18 columns (Section 1.2.3.1) are stable from pH 2-11.5. They are used in this work with 4-hydroxybenzoic acid and carbonate/bicarbonate eluents from pH 5.6 to 10.5.

As was explained in Section 1.2.1, the size of the particles has a great impact on the efficiency and speed of analysis. By combining the use of short columns (2.0 cm) with small particle diameter (1.8  $\mu\text{m}$ ), fast (<2 min) and efficient ( $N/\text{m} \approx 100,000$ ) separations are achieved in this work. However, the high efficiencies and low peak volumes generated by these small particle columns make even greater demands on the efficiency of the extra-column components (Sections 1.2.2 and 4.3.1.3). Thus, a



significant aspect of these studies was the reduction of the extra-column band broadening due to other system components, particularly the suppressor.

IC separations are performed using DDAB coatings as in Chapter 4. However, the removal procedure (Section 4.2.4) has been improved to eliminate the pressure build-up caused by precipitation of the surfactant in the column during uncoating.

## 5.2 Experimental

### 5.2.1 Apparatus

The ion chromatography system was essentially as discussed in Section 4.2.1 and illustrated in Figure 4.1a. A 0.5  $\mu\text{m}$  stainless steel frit (Upchurch, Oak Harbor, WA, USA) was added before the pre-column. The pre-column (Zorbax Extend-C18, 1.25 cm long x 0.46 cm I.D., 5  $\mu\text{m}$  particle diameter, Agilent Technologies, Palo Alto, CA, USA) was positioned before the injector and coated with didodecyldimethylammonium bromide (DDAB) as described in Section 5.2.3. A Rheodyne (Berkeley, CA, USA) injection valve (model 7520) fitted with a 1  $\mu\text{L}$  loop, injected samples onto a Zorbax Extend-C18 1.8  $\mu\text{m}$  particle diameter columns (2 cm long x 0.46 cm I.D., Agilent Technologies) also coated with DDAB. The column was connected directly to the injection valve through a column coupler (Merck KGaA, Darmstadt, Germany) fitted with 3 cm of 0.004" I.D. PEEK tubing (Upchurch). A Dionex (Sunnyvale, CA, USA) Anion Atlas Electrolytic Suppressor (AAES) or a Dionex Anion Self Regenerating Suppressor (ASRS ULTRA II) was connected to the column with 5 cm of PEEK tubing (0.004" I.D., Upchurch). The suppressor operated in external water mode with a regenerant flow rate of  $\sim$ 2 mL/min.



(The suppressor was removed during coating or uncoating the columns and during the stability study with carbonates.) A Dionex ED-50A electrochemical detector and a DS3 Detection Stabilizer (Dionex, model DS3-1) were used for detection. A 10 cm 0.004" I.D. PEEK tubing (Upchurch) connected the column or suppressor directly to the cell, which was within the DS3-1 stabilizer. The conductivity cell was 1  $\mu$ L, the rise time 0.05 sec and data was collected with the PeakNet 5.2 software (Dionex) at 20 Hz. A Dionex Variable Wavelength Detector-II was used at 254 nm to perform RPLC column tests.

A Corning 445 pH-meter (Corning, New York, NY, USA) with a Corning electrode (3 in 1 Combo P/N 476436) was used for pH measurements.

### **5.2.2 Reagents and solution preparation**

The reagents used and their preparation were as in Section 4.2.2. In addition, sodium bromide (Anachemia) solution was used in these experiments to rinse the columns prior to removing the DDAB coating (Section 5.2.3).

IC eluents were freshly prepared by dissolving the appropriate amount of 4-hydroxybenzoic acid (99%, Aldrich, St-Louis, MI, USA) in water, adjusting the pH with a 2.5 M and 1.0 M sodium hydroxide (Fisher) solution and diluting with water to the desired volume. The solutions were filtered through 0.22  $\mu$ m Magna nylon membrane filters (GE Osmonic, Trevose, PA, USA) prior to use. To avoid chloride contamination from the pH electrode, the pH of an aliquot of the final solutions was measured. Eluents based on carbonates were prepared by dissolving the appropriate amounts of sodium



carbonate and sodium bicarbonate (EM Science, Gibbstown, NJ, USA) in water. The solution was filtered through 0.22  $\mu$ m nylon membrane filters (GE Osmonic).

Periodically, the RPLC performance of the columns was checked to ensure that the column was still intact. A solution of 0.01 g/L uracil (98%, Aldrich, St-Louis, MI, USA), 0.3 g/L phenol (ACP Chemicals Inc.), 0.06 g/L 1-chloro-4-nitrobenzene (Aldrich) and 0.07 g/L naphthalene (Fisher) in 40/60% water/ACN was injected and monitored with UV detection at 254 nm. The eluent was 40/60% water/ACN eluent (2 mL/min).

### **5.2.3 Column coating and removal of coating**

The Extend-C18 columns were coated with 1 mM DDAB in either 35% or 40% ACN solution, and then equilibrated with 4-hydroxybenzoic acid or carbonate/bicarbonate eluents as in Section 4.2.4. Breakthrough of DDAB was observed at  $\leq$  15 mL. The ion exchange capacity of the coated columns (Q in  $\mu$ eq/column) was estimated according to equation 4.1.

To insure reproducible retention behaviour, the columns were typically recoated every 3-5 days using the following procedure (Figure 5.5). The column was first flushed with water at 1 mL/min for 10 min to remove the eluent. Then the column was flushed with aqueous 1 mM NaBr for 20 min and rinsed again with water for 10 min at 1 mL/min. The %ACN was gradually increased from 0 to 50% over 3 min and the column was flushed for 5 min with 50% ACN to remove the DDAB. Finally the %ACN was reduced to 35% or 40% over 2 min and held for 2 min to equilibrate the column prior to the next coating.



## 5.3 Results and discussion

### 5.3.1 High pH eluent on a silica-based column

#### 5.3.1.1 4-Hydroxybenzoic acid eluents

Section 1.2.5.1 states that carbonate buffers should not be used with silica-based stationary phases as this type of buffer accelerates the silica dissolution at high pH. Therefore, the initial experiments with the Zorbax Extend phase columns were performed using less aggressive 4-hydroxybenzoic acid eluents. In Chapter 4, 4-hydroxybenzoic acid ( $pK_{a1}=4.6$ ,  $pK_{a2}=9.5$ )<sup>1</sup> was shown to be an effective eluent for DDAB coated monolith columns at pH 7-7.5. However, at such neutral pH, 4-hydroxybenzoic acid carries only a -1 charge, and so is a weak eluent with respect to multiply charged ions such as sulphate (Section 1.2.3.2). Consequently, as can be seen in Figure 4.3, singly charged ions are rapidly eluted by 4-hydroxybenzoic acid at pH 5.6 while sulphate is strongly retained.

Figure 5.1 shows the variation in retention for a number of common anions using 4-hydroxybenzoic acid eluent from pH 5.6-10.5. The retention factor of all analytes decreases as the pH increases since the eluent becomes more ionized, and therefore stronger. The effect is particularly important as the second  $pK_a$  of 4-hydroxybenzoic acid (4-hb) is approached (at pH>8.5). The increased presence of 4-hb<sup>2-</sup> is very significant for the doubly charged analytes phosphate and sulfate which reduces their retention factors considerably (Section 1.2.3.2). Because phosphate and sulfate are more affected than the singly charged analytes, the later are still resolved at high pH while the gap between the singly and doubly charged analytes is considerably reduced, improving the speed of



analysis. The ideal pH for a 4-hydroxybenzoic acid eluent used with a high pH stable phase is about 10. The retention of phosphate increases between pH 7-8 because the ion ( $\text{H}_2\text{PO}_4^-$ ) reaches its second  $\text{pK}_a$  (7.2)<sup>2</sup> and becomes doubly charged ( $\text{HPO}_4^{2-}$ ) and thus, is more retained. However, by pH 8.5 phosphate is essentially fully in the -2 form, and the eluent is now approaching its second  $\text{pK}_a$  ( $\text{pK}_{a2}=9.5$ )<sup>1</sup>. Thus above pH 8.5, the retention of phosphate behaves (decreases) similarly to sulphate ( $\text{SO}_4^{2-}$ ).

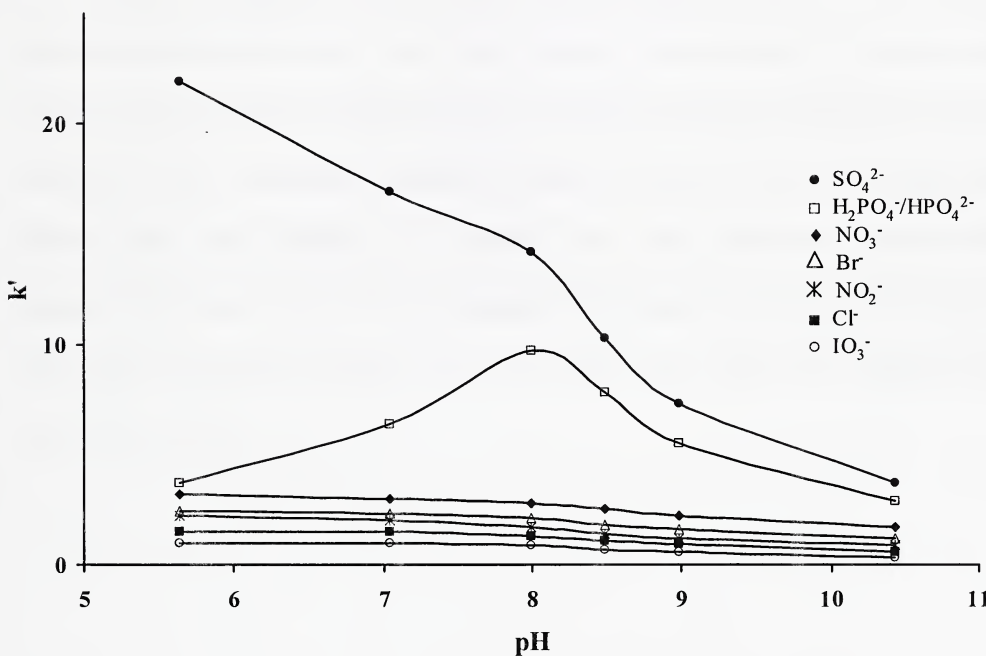


**Figure 5.1 Variation of the retention factors with pH for a 4-hydroxybenzoic acid eluent.** Experimental conditions: eluent is 4-hydroxybenzoic acid 2.0 mM, 1.0 mL/min, coating solution for pre-column and separation column is 1 mM DDAB in 40% ACN, separation column capacity is 5  $\mu\text{eq}/\text{column}$ , AAES suppressor at 20 mA, analyte concentration is 250  $\mu\text{M}$ . Standard deviation is smaller than symbols,  $n=3$ .



RPLC-UV separations were performed to study the stability of the silica when using 4-hydroxybenzoic acid at high pH. Separations were performed upon receipt of the column and after 30-35 hours of usage with 4-hydroxybenzoic acid at pH 8 to 10 with a coated pre-column (Section 5.2.1). On average peak efficiency and retention factors were reduced by 6%. The column permeability was unchanged. These results indicate that 4-hydroxybenzoic acid at high pH does degrade the silica but at a slow rate.

Figure 5.2 illustrates the separation of seven common anions with a 2.5 mM 4-hydroxybenzoic acid eluent at pH 10.0. The peaks are separated in 2 minutes and baseline resolved with peak efficiency up to 180,000 plates/meter (see second section of Table 5.1). The separations obtained in Chapter 4 (Figures 4.3 and 4.4) would have resolved the same analytes in 4 minutes with peak efficiencies 20,000-40,000 plates/meter if performed on a 2 cm long monolithic column at 1 mL/min. The impact of the small 1.8  $\mu$ m particle diameter size on efficiency is thus significant compared to the monolithic columns.



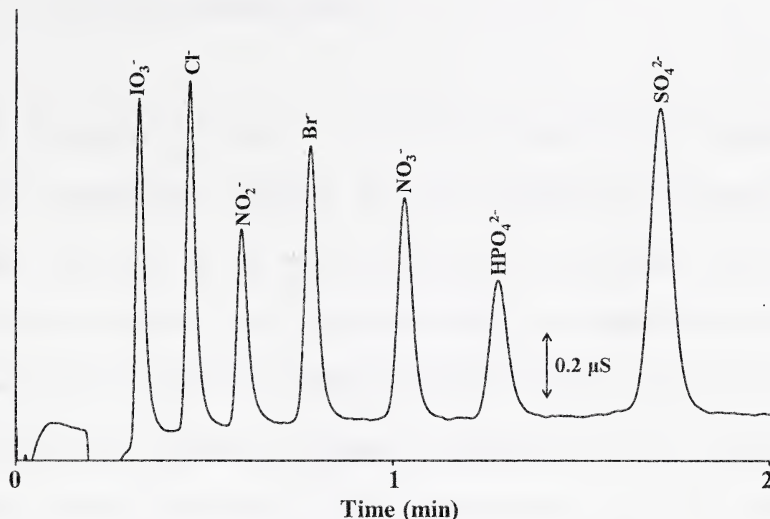


**Figure 5.2** Suppressed anion separation with 4-hydroxybenzoic acid eluent at pH 10.0. Experimental conditions: eluent is 4-hydroxybenzoic acid 2.5 mM, 1.0 mL/min, coating solution for pre-column and separation column is DDAB 1 mM in 35% ACN, separation column capacity is 12  $\mu\text{eq}/\text{column}$ , ASRS-II suppressor at 40 mA, analyte concentration is 150  $\mu\text{M}$ .

Coating of the column with a DDAB in 35% ACN solution resulted in an ion exchange capacity of 12  $\mu\text{eq}/\text{column}$  (6  $\mu\text{eq}/\text{cm}$ ). On a monolithic columns, coating with a DDAB in 35% ACN solution results in column capacity of 4  $\mu\text{eq}/\text{cm}$  (from interpolation of previous results<sup>3</sup>). Because monolithic columns have large throughpores, the density of silica/cm is less than for a particulate column. The amount of DDAB coated/cm of column is thus smaller for monolithic columns.



### 5.3.1.2 Carbonate eluents

As mentioned in Section 5.1, the use of conventional IC eluents such as carbonates provides better sensitivity since their conductivity background is better suppressed. However, the use of carbonates is not recommended with silica-based stationary phases because of their poor stability with such eluents (Section 1.2.5.1). It was shown that the Extend phase (bidentate chemistry, Section 1.2.3.1) was much more stable (>90%) than standard C<sub>18</sub> phases in carbonate/bicarbonate eluents.<sup>4</sup> Upon completion of the experiments with the 4-hydroxybenzoic acid eluent, the column stability was tested by flushing a classic IC eluent solution of carbonate/bicarbonate (3.4 and 2.7 mM respectively, pH 10.5) through the column at 1.0 mL/min. Initially (t=0 on Figure 5.3), high efficiency (up to 160,000 N/m) were obtained. After 24 hours efficiencies had decreased by about 10%. The Extend column failed after only 36 hours of operation with the carbonate eluent. Between the separations of t=0 and t=36 hours, the efficiencies decreased by 20 to 60% and the resolution between nitrate and phosphate decreased from 1.8 to 1.1 (Figure 5.3). At the same time, the pressure increased by 10%. A life time of 36 hours is not long enough to be considered usable for routine analysis. Ideally a column should be stable enough to perform 1000-2000 sample analyses<sup>5</sup> (about 50-100 hours in this case). Impairment of the silica backbone and the bonded stationary phase due to high pH eluent result in reduced plate number and column clogging.<sup>4,6,7</sup> The bottom chromatogram on Figure 5.3 was obtained after removing DDAB and replacing it by a fresh coating on the column. This chromatogram demonstrates the dramatic effect



of the carbonates on the column. In addition, the RPLC-UV tests performed before and after testing also demonstrate the degradation caused by the carbonate eluent (Figure 5.4).

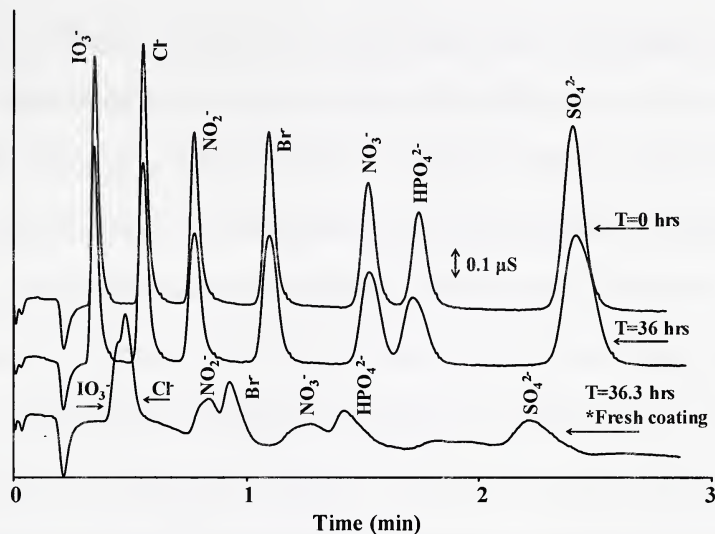


**Figure 5.3 Anion separations with carbonate/bicarbonate eluent at t = 0, 36 and 36.3 hours.** Experimental conditions: eluent is carbonate ( $\text{CO}_3^{2-}$ ) 3.4 mM, bicarbonate ( $\text{HCO}_3^-$ ) 2.7 mM, pH 10.5, 1.0 mL/min, coating solution for pre-column and separation column is DDAB 1 mM in 35% ACN, separation column capacity is 12  $\mu\text{eq}/\text{column}$ , ASRS-II suppressor at 50 mA, analyte concentration is 150  $\mu\text{M}$ .

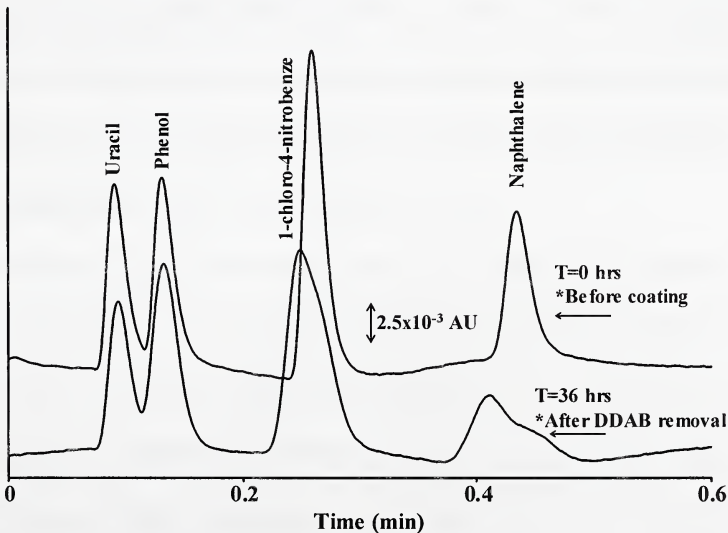


**Figure 5.4 RPLC-UV chromatograms at 0 and 36 hours.** Experimental conditions: eluent is 40/60% water/ACN, 2.0 mL/min, for analyte concentration see Section 5.2.2.



### 5.3.2 Band broadening from extra-column effects

If not carefully minimized, the extra-column band broadening effects can be substantial when using short columns packed with small particles (Sections 1.2.2 and 4.3.1.3). However, as presented in the top section of Table 5.1, these effects were virtually eliminated in the non-suppressed mode. The reduced plate heights ( $h$ ) obtained under non-suppressed conditions are within the optimal range of 1.5-3 (Section 1.2.1) and indicate that the column is performing properly and that additional broadening is eliminated. This data was obtained by removing the conductivity cell from the DS-3 detection stabilizer and connecting it directly to the column using a column coupler (from Merck, see Section 5.2.1). This prevented any broadening from the 10 cm long tube used for connection with the cell. For normal operation, in suppressed mode, the cell was put back in the DS-3 to reduce noise due to temperature fluctuations. As explained in the next paragraph, the suppressor is the prevailing broadening factor in suppressed mode, therefore the 10 cm tubing does not contribute to band broadening in that mode and can be used with the cell. A 1  $\mu$ L injection loop was used and did not significantly contribute to band broadening since  $V_s/V_c = 0.03$  (Section 4.3.1.3).

Suppression of the eluent background in IC improves the detection limits but increases the extra-column void volume and therefore the extra-column band broadening (Section 4.3.1.3). However, if the void volume of the suppressor is reduced, the detrimental effects are diminished.<sup>8</sup> Reducing the void volume of the suppressor from 35 to 15  $\mu$ L by using a different suppressor considerably decreased the extra-column effects, as shown in the second and last sections of Table 5.1. When using the low void volume



ASRS-II suppressor, the number of plates/meter can be up to ten times higher than with the AAES suppressor. However, the ASRS-II can only handle a maximum flow rate of 1 mL/min before leakage from the seals occurs within this suppressor. The AAES suppressor must be used at flow rates higher than 1 mL/min.

Detection limits were not studied, but would be the same as in Chapter 4 with the 4-hydroxybenzoic eluents. They would, however, be lower with the carbonate eluents since suppression is more efficient.

**Table 5.1 Peak efficiency in non-suppressed and suppressed modes.**

	$\text{IO}_3^-$	$\text{Cl}^-$	$\text{NO}_2^-$	$\text{Br}^-$	$\text{NO}_3^-$	$\text{HPO}_4^{2-}$	$\text{SO}_4^{2-}$
<b>Non-Suppressed</b>							
$k'$	na <sup>a</sup>	1.1	1.8	2.8	4.1	5.4	na
$N/m$	na	161,000	170,000	230,000	174,000	186,000	na
$H (\mu\text{m})$	na	6	6	4	6	6	na
$h$	na	3	3	2	3	3	na
$\sigma^2 (\mu\text{L}^2)$	na	50	90	120	300	440	na
<b>Suppressed with ASRS ULTRA II (15 <math>\mu\text{L}</math> void volume)</b>							
$k'$	0.7	1.5	2.2	3.2	4.5	5.9	8.2
$N/m$	31,000	49,000	63,000	100,000	138,000	137,000	180,000
$H (\mu\text{m})$	32	20	16	10	7	7	6
$h$	18	11	9	6	4	4	3
$\sigma^2 (\mu\text{L}^2)$	170	210	280	300	380	600	810
<b>Suppressed with AAES (35 <math>\mu\text{L}</math> void volume)</b>							
$k'$	0.9	1.7	2.5	3.6	5.1	6.5	9.0
$N/m$	3,000	12,000	12,000	22,000	39,000	53,000	79,000
$H (\mu\text{m})$	381	86	81	46	26	19	13
$h$	212	48	45	25	14	11	7
$\sigma^2 (\mu\text{L}^2)$	1950	890	1420	1400	1390	1560	1860

<sup>a</sup> In non-suppressed mode,  $\text{IO}_3^-$  co-elutes with the large water dip at the dead time.

b. Experimental conditions: Eluent is 4-hydroxybenzoic acid 2.5 mM pH 10, 1.0 mL/min, coating solution for pre-column and separation column is DDAB 1 mM in 35% ACN, separation column capacity is 12  $\mu\text{eq}/\text{column}$ , ASRS-II suppression at 40 mA, AAES suppression at 20 mA, analyte concentration in non-suppressed mode is 0.5 mM except for  $\text{IO}_3^-$  (5mM),  $\text{Cl}^-$  (0.2 mM), and  $\text{HPO}_4^{2-}$  (1mM), analyte concentration in suppressed mode is 150  $\mu\text{M}$ .



### 5.3.3 DDAB removal

In Chapter 4, it was found that a 50% ACN/water solution removed DDAB from the monolithic columns without causing a significant increase in back pressure. However, after only five coating/uncoating cycles on a column packed with 1.8  $\mu\text{m}$  particles, the pressure almost doubled ( $B_0$  halved) and the column became plugged. It was hypothesized that the plugging resulted from the formation of an insoluble ion pair within the ACN rinse solution. Just prior to cleaning the columns with 50% ACN, the DDAB molecules within the column are in the  $\text{DDA}^+/\text{Eluent}^-$  form ( $\text{DDA}^+/4\text{-hb}^-$  or  $(\text{DDA}^+)_2/4\text{-hb}^{2-}$ ) (See section 4.2.4 and Figure 1.16). This form of the surfactant is likely less soluble in 50% ACN than the  $\text{DDA}^+/\text{Br}^-$  form and probably precipitates in the column. The uncoating procedure was modified by flushing the column with a 1 mM NaBr solution for 20 min at 1 mL/min (Figure 5.5). In this manner,  $\text{DDA}^+$  was converted to the more soluble bromide form and hopefully would not precipitate in the column upon uncoating. The surfactant was then washed from the column using 50% ACN.

Using the NaBr pre-rinse before uncoating the Extend column resulted in essentially no change in column backpressure. The %RSD after eight coating/uncoating cycles was 3.9%. In addition, after uncoating the column seven times, the pressures at 50% ACN (when all the DDAB is removed) had a %RSD of only 3.2%. Because of the lower constriction within the monolithic column, the precipitation of  $\text{DDA}^+/4\text{-hb}^-$  did not have such a strong effect on the monolithic columns in Chapter 4.



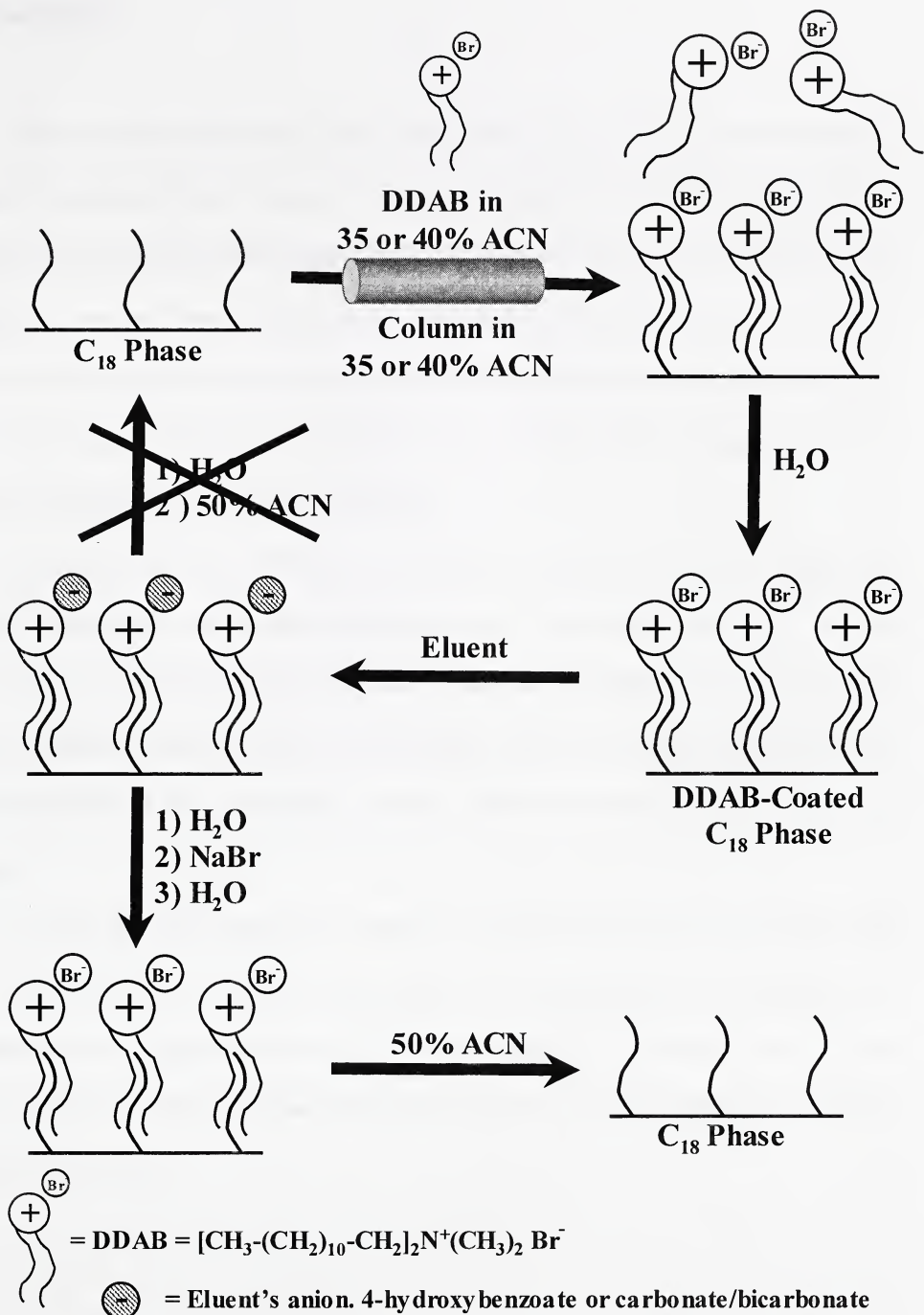


Figure 5.5 Removal of DDAB using NaBr and 50% ACN.



## 5.4 Conclusions

The work presented in this chapter demonstrates the possibility of performing IC separations on silica-based columns at pH higher than 8 with 4-hydroxybenzoic acid as an eluent. Elevated pH enables faster separations as this eluent becomes doubly charged at  $\text{pH} \geq 8.5$ . As well, the combination of small particle ( $1.8 \mu\text{m}$ ) packings with short columns (2 cm) results in high peak efficiency and reasonable backpressures. The eluent can easily be pumped through the column using a standard HPLC pump. An UPLC apparatus (Section 1.2.2) is hence not required.

It has been shown that adding a bare silica pre-column to the flow line effectively protects the analytical column from dissolution of silica and extends the column life by about 4-fold.<sup>7</sup> With the carbonate/bicarbonate eluent used in Section 5.3.1.2, the Extend column would then potentially last for  $\sim 140$  hours. However, Chapter 6 will show how the column life can be considerably extended without the need for a bare silica pre-column.

As with the work presented in Chapter 4, it is observed in the present chapter that the control and reduction of extra-column band broadening generated by the suppressor is essential to increase peak efficiency. To avoid precipitation of surfactant in the column upon its removal, NaBr is flushed through the column to convert DDAB in its more soluble bromide form.



## 5.5 References

- (1) Smith, R. M.; Martell, A. E. *Critical stability constants, Vol. 3*; Plenum Press: New York, 1975.
- (2) *CRC Handbook of Chemistry and Physics*, 80<sup>th</sup> ed.; CRC Press: New York, 1999-2000.
- (3) Hatsis, P.; Lucy, C. A. *Anal. Chem.* **2003**, *75*, 995-1001.
- (4) Claessens, H. A.; van Straten, M. A. *J. Chromatogr. A* **2004**, *1060*, 23-41.
- (5) Snyder, L. R.; Kirkland, J. J.; Glajch, J. L. *Practical HPLC method development*, 2nd ed.; Wiley Interscience: Hoboken, 1997.
- (6) Kirkland, J. J.; van Straten, M. A.; Claessens, H. A. *J. Chromatogr. A* **1995**, *691*, 3-19.
- (7) Kirkland, J. J.; van Straten, M. A.; Claessens, H. A. *J. Chromatogr. A* **1998**, *797*, 111-120.
- (8) Weiss, J. *Handbook of Ion Chromatography*, 3rd ed.; Wiley-VCH: Darmstadt, 2004.



## CHAPTER SIX. Conclusions and future work

### 6.1 Conclusions and significance

This thesis explored means of reducing analysis time and complexity in analytical separation methods. The studies in Chapters 2 and 3 involving thiols and disulfides focused on eliminating sample preparation steps which add considerably to the labor and time necessary for these analyses. The work with ion chromatography in Chapters 4 and 5 explored alternatives in column dimensions and stationary phase structure and chemistry to enable short separation times using reasonable flow rates. An important aspect of the overall work was to design techniques that would be usable in laboratories equipped with standard separation systems and detectors.

The work with thiols and disulfides demonstrated that the elimination of off-line sample derivatisation steps can significantly reduce analysis time - by 3 to 100-fold. Conventional long and complex sample derivatisations processes (from 1-24 hours) were replaced by a simple 20 minute separation that did not require any pre-derivatisation steps. It is arguable that even if the analyses are faster, the system using two post-column reagents is relatively complex. However, once the instrumental setup is in place, the method can easily be used routinely.

Laboratories are today under constant pressure to improve throughput and productivity while keeping their methods environmentally friendly. To improve separation time, one can think of increasing the flow rate through the columns. The commercialization of high permeability monolithic columns for LC separations enabled



the use of exceptionally fast flow rates (up to 16 mL/min) for separations.<sup>1</sup> However, solvent consumption becomes excessive and a specific pump capable of high flow rates is essential. My work using short monolithic columns (Chapter 4) demonstrates that IC analysis can be performed in as little as 2 minutes using conventional flow rates of 1-2 mL/min. This reduces solvent use and can be carried out using standard HPLC instrumentation. The separations are far quicker than established IC separations which usually resolve the same analytes in 10 minutes on 15 cm long columns.<sup>2</sup> Separations of multiple compounds on short columns are only possible if extra-column band broadening effects are minimized. These effects become very significant as the columns are shortened and particle size reduced. It was demonstrated that the contribution to band broadening of the injection loop, the tubing and detector is minor in a well optimized system. However, it was also shown that the suppressor in IC is the principal cause of band broadening.

The short length and trivial pressure drops of the monolithic columns enabled the use of a syringe pump to circulate the eluent at constant flow rates. This is an important step towards an eventual development of portable LC systems.

The work with the small particle columns in Chapter 5 not only demonstrates the ability to perform efficient separations on short columns, but is also of significance in the field of IC. Selectivity in IC is mainly based on column chemistry, resulting in the manufacture of a variety of different columns adapted to diverse needs. The capacity of DDAB coated columns is easily modified and regenerated. This flexibility reduces the need for an array of costly columns required for different applications. Moreover, with the advent of high pH stable silica phases, DDAB coated columns could potentially be



used with the most common IC eluents. Interest for commercialization of DDAB coated columns and implantation in research labs has been expressed by two companies. Since most laboratories possess RPLC columns, IC becomes a very accessible technique. In addition, it is shown in Chapter 4 that when used with a coated pre-column, DDAB coated columns can be stable for weeks.

The improvement of column technology unites robustness, stability, performance and alas elevated prices. Columns are precious and must be used with care. My work using short columns brings a new dimension to this general vision on column usage. Short columns, often commercialized as guard columns, are available at a fraction of the cost of standard columns and can be easily replaced. In this manner, separation columns may become a general consumable product.

## 6.2 Future work

### 6.2.1 Improvements in fast ion chromatography with small particles

#### 6.2.1.1 Hybrid stationary phases

In HPLC separations, an ideal support material would unite the best properties from both the silica and the polymer-based packings: high efficiency and mechanical strength, wide pH stability range and no silanol interactions. Columns made of a hybrid organic-inorganic material combining these properties have recently been developed.<sup>3-5</sup> To slow down degradation of the silica in alkaline conditions, organic ethyl groups are bridged within the silica particle (Figure 6.1). The organic groups sterically protect the silica surface from the hydroxide attack while reducing the amount of free silanols on the surface. In addition, these materials are more difficult to hydrolyze since up to five



siloxane bonds have to be broken to free one ethylene-bridge unit. These phases are stable from pH 1-14, mechanically strong and are as efficient as silica. They are now commercialized by Waters as the XBridge columns.<sup>6</sup> These columns are available packed with 1.7  $\mu\text{m}$  particles and can be as short as 2 cm. Waters claims that under alkaline conditions the XBridge columns are more than 20 times more stable than the Extend phase used in Chapter 5.<sup>6</sup> With XBridge columns it would therefore be possible to use carbonate/bicarbonate eluent for IC with DDAB coatings for more than 2 or 3 months without degrading the stationary phase.

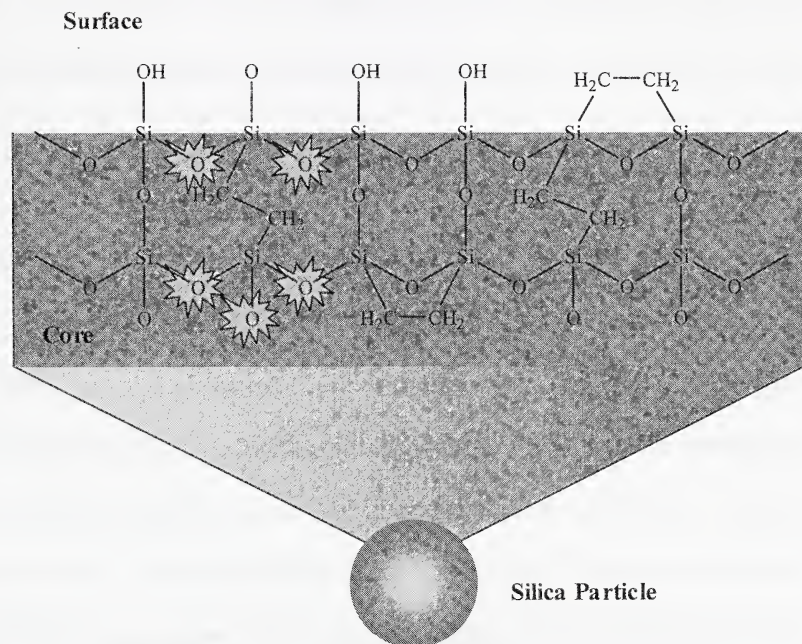


**Figure 6.1 Structure of an ethylene bridged hybrid organic-inorganic particle.**  
Adapted from reference 6, courtesy of Waters Corporation.



### **6.2.1.2 Improved suppressors**

To perform anion analysis in less than 1 minute with short columns and small particles, a flow rate of 2 mL/min is necessary. However, as explained in Section 5.3.2, the low volume ASRS-II suppressor which minimizes band broadening operates at a maximum flow of 1 mL/min. The AAES suppressor is the other option for operation at 2 mL/min but it generates more broadening. Dionex has expressed interest in building a low volume suppressor (comparable to the ASRS-II) that would sustain flows of 2 mL/min. By combining this enhanced suppressor with the XBridge columns, IC analysis based on DDAB coatings can become a robust alternate or complement to traditional IC analysis.

### **6.2.2 Increasing retention of weakly retained compounds in RPLC**

HPLC column technology is always improving and evolving. The work in this thesis involved the use of a few specialized RPLC columns such as monolithic, wide pH stable, aqueous compatible or small particulate phases. For RPLC analysis of polar compounds such as thiols and disulfides (Chapters 2 and 3) an array of different columns are available for separations under acidic and highly aqueous conditions (Section 1.2.3.1). The actual trend is to produce RP columns with added hydrophilicity and bulky group protection. This chemistry enhances wettability of the stationary phase in 100% water and the compatibility at low pH. I had the opportunity to beta test a new low pH stable polar embedded column (Dionex, Acclaim PolarAdvantage II, PA2)<sup>7</sup> and compare it with



the Zorbax SB-Aq used in Chapter 3. The increased polarity of the PA2 column resulted in an average retention factor increase of 45%. However peak shape was poor compared to the SB-Aq. This demonstrates that this area of column development is still growing and will improve separation of polar analytes.

As seen in Chapters 2 and 3, the separation of weakly retained polar compounds in RPLC is still a challenge. Elevated column temperature has traditionally been used to reduce analysis time since retention factors decrease at higher temperature.<sup>8,9</sup> Conversely, reduced temperatures can be used to increase retention times. Working with Jen Cook, a WISEST (Women in Scholarship, Engineering, Science and Technology) student, we observed up to a 20% increase in retention factors and some selectivity changes were observed when separating organic acids on a Zorbax SB-Aq column at 30 °C and 6 °C.<sup>10</sup> In addition, it has been observed that the loss in retention in highly aqueous conditions attributed to phase collapse is reduced at low temperatures.<sup>11</sup> Resolution of polar compounds in RPLC could be improved by combining below room temperature separations with aqueous and low pH compatible phases. This could become a powerful analytical tool for polar compounds in RPLC.



### 6.3 References

- (1) Hatsis, P.; Lucy, C. A. *Anal. Chem.* **2003**, *75*, 995-1001.
- (2) Weiss, J. *Handbook of Ion Chromatography*, 3rd ed.; Wiley-VCH: Darmstadt, 2004.
- (3) Cheng, Y.-F.; Walter, T. H.; Lu, Z.; Iraneta, P.; Alden, B. A.; Gendreau, C.; Neue, U. D.; Grassi, J. M.; Carmody, J. L.; O'Gara, J. E.; Fisk, R. P. *LCGC* **2000**, *18*, 1163-1172.
- (4) Wyndham, K. D.; O'Gara, J. E.; Watlter, T. H.; Glose, K. H.; Lawrence, N. L.; Alden, B. A.; Izzo, G. S.; Hudalla, C. J.; Iraneta, P. C. *Anal. Chem.* **2003**, *75*, 6781-6788.
- (5) Claessens, H. A.; van Straten, M. A. *J. Chromatogr. A* **2004**, *1060*, 23-41.
- (6) *XBridge<sup>TM</sup> HPLC Columns*; Waters Corporation, 2005.
- (7) Pelletier, S.; Lucy, C. A.; For Dionex Corporation: Acclaim Polar Advantage II Beta Test Plan, Column Development Report, 2005, pp 8.
- (8) Castells, C. B.; Gagliardi, L. G.; Rafols, C.; Roses, M.; Bosch, E. *J. Chromatogr. A* **2004**, *1042*, 12-35.
- (9) Hatsis, P.; Lucy, C. A. *J. Chromatogr. A* **2001**, *920*, 3-11.
- (10) Cook, J. L.; Pelletier, S.; Lucy, C. A. *The effects of temperature and pH on the separation of carboxylic acids by high performance chromatography* Women in Scholarship, Engineering, Science and Technology (WISEST) research poster presentation day, Edmonton 2004.
- (11) Bidlingmeyer, B. A.; Broske, A. D. *J. Chromatogr. Sci.* **2004**, *42*, 100-106.













